U.PORTO
INSTITUTO DE CIÊNCIAS BIOMÉDICAS ABEL SALAZAR
UNIVERSIDADE DO PORTO

ECOLOGICAL MODELLING OF THE DOURO ESTUARY: INFLUENCE OF RIVER FLOW VARIABILITY ON ESTUARINE WATER QUALITY AND PRIMARY PRODUCTION

Maria Isabel da Silva Costa Azevedo

Dissertação de Doutoramento em Ciências do Meio Aquático

2008

Maria Isabel da Silva Costa Azevedo

ECOLOGICAL MODELLING OF THE DOURO ESTUARY: INFLUENCE OF RIVER FLOW VARIABILITY ON ESTUARINE WATER QUALITY AND PRIMARY PRODUCTION

Dissertação de Candidatura ao grau de Doutor em Ciências do Meio Aquático, submetida ao Instituto de Ciências Biomédicas de Abel Salazar da Universidade do Porto.

Orientador – Professor Doutor Adriano Bordalo e Sá

Categoria – Professor Associado com Agregação

Afiliação – Instituto de Ciências Biomédicas Abel Salazar da Universidade do Porto.

Co-orientador – Professor Doutor Pedro Manuel da Silva Duarte

Categoria – Professor Associado

Afiliação – Universidade Fernando Pessoa

Ao Pedro, à Joana e ao Raúl

Aos meus pais

Agradecimentos

Ao meu orientador, Prof. Bordalo, por me ter recebido no seu laboratório e me ter proposto o desafio que foi este trabalho. Pela forma interessada com que acolheu os meus entusiasmos e desabafos e por se ter sempre empenhado em me dar todo o apoio necessário para que conseguisse levar este trabalho até ao fim.

Ao meu co-orientador, Prof. Pedro Duarte, pela dedicação e empenho com que me ajudou, em todas as etapas do trabalho, e pela paciência e interesse com que sempre respondeu às minhas dúvidas. E por me ter ensinado muito do que aprendi durante este trabalho.

À Fundação para a Ciência e Tecnologia, pelo apoio financeiro disponibilizado através da concessão da bolsa de doutoramento (SFRH/BD/4660/2001), que tornou possível a realização deste trabalho.

Ao Instituto de Ciências Biomédicas Abel Salazar, pela disponibilização das instalações e equipamentos.

Ao Prof. Rui Cortes, pela disponibilidade e amabilidade com que esclareceu às minhas dúvidas de estatística.

Aos SMAS do Porto pelo apoio prestado, em termos da disponibilização da embarcação, e respectiva tripulação, dos Sapadores Bombeiros do Porto, para a realização das amostragens.

Aos Mergulhadores dos Sapadores Bombeiros do Porto, pela boa disposição e pela disponibilidade que sempre demonstraram em ajudar na recolha das amostras, tornando assim as amostragens mais fáceis.

À Capitania do Porto, pela disponibilização das instalações dos Socorros a Náufragos, para a realização das amostragens dos ciclos de maré.

Ao Sr. Quim e ao Sr. João, pela simpatia com que me receberam na sua “casa” dos Pilotos, e zelaram para que tivesse todas as condições para a realização dos ciclos de maré. E por se terem disponibilizado a ajudar na montagem e desmontagem dos equipamentos, mesmo nas suas horas de descanso.

A todas as colegas e amigas do Lab, que de uma forma ou de outra, participaram nesta aventura. À Ana, Ana Paula, Catarina Magalhães, Catarina Teixeira, Liliana, Sandra e Rita, obrigada por se terem disponibilizado sempre para ajudar e pelo ambiente acolhedor e bem-disposto que me proporcionaram no Lab. Quero agradecer em especial à Liliana pela constante ajuda nas análises microbiológicas e à Rita por me ter acompanhado nas amostragens e tratamento das amostras. Não posso também deixar de agradecer à D. Deolinda, pelo carinho com que me ajudou com o material no laboratório, e também à D. Lurdes, por estar sempre disposta a ajudar no que for preciso.

Aos meus pais, por tudo o que fizeram por mim, pelo apoio incondicional e incentivo que sempre me deram para seguir as minhas escolhas. E pela dedicação e paciência com que me ajudaram, no dia-a-dia, a terminar esta etapa. Aos meus irmãos, pelas conversas bem-dispostas com que desanuviam os dias menos bons, e por saber que posso contar com eles quando precisar.

À D. Elisa e ao Sr. João, por toda a ajuda e carinho que me deram.

Aos meus filhos e ao Raúl, pelo carinho e momentos felizes que me dão, e que foram tão importantes para me ajudar nesta etapa.

FCT Fundação para a Ciência e a Tecnologia
MINISTÉRIO DA CIÊNCIA, TECNOLOGIA E ENSINO SUPERIOR Portugal

Ciência.Inovação 2010 Programa Operacional Ciência e Inovação 2010
MINISTÉRIO DA CIÊNCIA, TECNOLOGIA E ENSINO SUPERIOR

UNIÃO EUROPEIA
FUNDOS ESTRUTURAIS

GOVERNO DA REPÚBLICA PORTUGUESA

U.PORTO
INSTITUTO DE CIÊNCIAS BIOMÉDICAS ABEL SALAZAR
UNIVERSIDADE DO PORTO

Resumo

Os estuários são ecossistemas caracterizados por um elevado dinamismo onde as condições ambientais variam grandemente em diferentes escalas temporais e espaciais. Por outro lado, estes ecossistemas estão também sujeitos a profundas pressões antropogénicas traduzidas numa crescente urbanização e emparedamento das margens, recepção de água residuais, construção de barragens, entre outras. O fluxo de água doce nos estuários é uma característica fundamental destes ecossistemas, cuja quantidade e qualidade pode sofrer alterações à medida que os seus usos se intensificam, nomeadamente irrigação e produção de electricidade. A alteração do regime do caudal de água doce afluente aos estuários influencia o padrão de circulação, a estratificação e o tempo de residência da água, bem como o aporte de substâncias dissolvidas e particuladas, com consequências sobre a estrutura e função das comunidades estuarinas.

O estuário do Douro é a parte terminal da maior bacia hidrográfica da Península Ibérica, com um caudal médio anual de 505 m^3s^{-1}. O seu limite montante foi imposto pela construção de uma barragem a 21.6 km da foz, em 1985. O regime de caudais afluentes ao estuário é caracterizado por uma grande variabilidade horária, especialmente durante o Verão, em que o aporte de água doce está dependente das necessidades de produção de hidroelectricidade. Assim, em vez de um fluxo contínuo de água doce, sazonalmente variável, ocorrem "pulsos" de descarga, especialmente durante o período de menor caudal, quando este pode, numa questão de horas, variar de 0 a 1 000 m^3s^{-1}.

A hipótese testada neste trabalho foi a de que este regime artificial de descargas de água doce influencia a hidrodinâmica, qualidade da água e produção primária (PP) do estuário. Com base em dados recolhidos através de campanhas de amostragem dedicadas, efectuadas em enchente e vazante, foi desenhado um modelo conceptual da biogeoquímica do estuário. O rio constitui a maior fonte de nutrientes, clorofila *a* e matéria em suspensão, embora fontes adicionais estejam presentes no estuário médio e inferior, associadas à descarga de águas residuais e pequenos afluentes. A distribuição vertical da salinidade e o seu padrão ao longo do estuário revelaram-se fortemente dependentes do caudal e, como tal, caracterizados por uma sazonalidade

apreciável. No Douro, ocorre uma notória estratificação vertical da coluna de água para caudais inferiores a 800 m^3s^{-1}. Na Primavera, com a progressiva diminuição do caudal e aumento da temperatura, assim como da disponibilidade de luz na coluna de água, a biomassa do fitoplâncton e a PP atingem o seu máximo no estuário. Durante o Verão, em que se verifica uma forte redução do caudal e consequente aumento do tempo de residência, ocorre uma diminuição da biomassa de fitoplâncton e PP. Esta diminuição pode ser explicada pela diminuição do aporte de biomassa oriunda de montante, bem como pela incapacidade de desenvolvimento do fitoplâncton (de origem fluvial) nas condições de salinidades elevadas dominantes no estuário durante esse período. O estuário revelou-se predominantemente heterotrófico, excepto no estuário superior durante o Verão, observando-se um aumento da heterotrofia em direcção à foz, devido ao aumento da respiração. O principal factor de controlo da produção primária foi a temperatura, com um contributo positivo da taxa fotossintética máxima (P_{max}) e da biomassa do fitoplâncton. A temperatura, a luz e a salinidade foram os factores que mais influenciaram a variabilidade dos parâmetros fotossintéticos.

O conhecimento adquirido sobre as tendências temporais e espaciais, bem como sobre as relações entre as diferentes variáveis que caracterizam o sistema, foi usado na implementação de um modelo tridimensional acoplado hidrodinâmico – biogeoquímico, adaptado às condições do Douro, o qual, após calibração e validação, foi usado para testar diferentes cenários de magnitude e variabilidade do caudal afluente ao estuário. Numa primeira fase, foi implementado, calibrado e validado o modelo hidrodinâmico, o qual foi posteriormente usado para analisar a influência da magnitude e regime do caudal na circulação da água do estuário. Foi também avaliada a dispersão de contaminantes através do uso de um traçador conservativo. Verificou-se que, para além da magnitude, também o regime do caudal tem influência na hidrodinâmica do sistema: para caudais mais uniformes (com menor variabilidade), a salinidade média foi menor e a dispersão de contaminantes, maior. Numa segunda fase, foi acoplado um modelo biogeoquímico ao referido modelo hidrodinâmico, com o objectivo de analisar a influência da magnitude e regime do caudal na qualidade da água e PP do estuário. Verificou-se que, enquanto a concentração de nutrientes variou positivamente com o caudal, a clorofila *a* apresentou uma relação parabólica com o caudal, com a obtenção de valores mais elevados de biomassa para um caudal intermédio. Esta relação pode ser explicada pela diminuição do tempo de residência, para caudais mais elevados, e um menor aporte de nutrientes e biomassa, para caudais reduzidos. Em relação à variabilidade do caudal, verificou-se que, para

caudais mais uniformes, a concentração de clorofila *a*, bem como os níveis de PP, foram mais elevados.

Estes resultados permitem concluir que a gestão do caudal de água doce afluente ao estuário pode ter efeitos importantes na qualidade da água e PP. Considerando que um regime de caudal mais uniforme pode ser considerado como “proxy” da situação existente antes da barragem em períodos de menor caudal, os resultados obtidos parecem indicar que a barragem, com o actual regime de descargas, conduz a um aumento da salinidade média e uma diminuição do potencial de diluição de contaminantes, bem como a uma diminuição da biomassa e produção fitoplanctónicas.

Abstract

Estuaries are highly dynamic ecosystems, where changes in environmental conditions occur at different temporal and spatial scales. These ecosystems are under heavy anthropogenic pressures such as land reclamation for construction and flood protection, wastewater disposal and damming. Freshwater inflow to estuaries is a fundamental feature of these ecosystems, which may be profoundly altered by river damming as human needs for water consumption, irrigation or energy production increase. Changes in freshwater inflow cause alterations in water circulation, stratification and residence time, as well as in dissolved and particulate materials delivered to estuaries by river runoff, such as nutrients and sediments, with consequences on estuarine community function and structure.

The Douro estuary is part of the largest watershed in the Iberian Peninsula, receiving an average river flow of 505 m^3s^{-1}. The upper limit of the Douro estuary is represented by a hydroelectric power dam, built in 1985, which confined the estuary to the last 21.6 km of the river. Freshwater flow regime is characterised by a high hourly variability, depending on electricity needs. Thus, instead of a continuous flow of freshwater, seasonally variable, there are pulse discharges, especially during the summer months when, in a mater of hours, flow can rise from 0 to over 1,000 m^3s^{-1}.

The hypothesis tested in the present study was that the highly variable freshwater inflow regime imposed by the dam will have important consequences on the hydrodynamics, water quality and primary production of the Douro estuary. A conceptual model of the estuarine biogeochemistry was designed, based on data collected within the framework of a dedicated sampling program that covered ebb and flood tides, along the entire estuary. The river emerges as the major source of nutrients, chlorophyll *a* and total particulate matter (TPM), although additional anthropogenic sources are noticeable, especially at the middle and lower estuary. Vertical and horizontal salinity distributions are strongly dependent on river flow, and characterised by a considerable seasonal variability. In the Douro, water column salinity stratification occurs when river flows are lower than 800 m^3s^{-1}. Phytoplankton biomass and primary production (PP) reaches their maxima during spring, when flow decreases and light availability and temperature increase. In summer, when river flow

is the lowest, and temperature and water transparency are the highest (as well as salinity), chlorophyll *a* and PP decline. This decline may be partly explained by the lower phytoplankton input and the inability of freshwater phytoplankton to thrive in high salinity water that dominates the estuary during this period. The estuary was found to be predominantly heterotrophic, except for the upper reaches in summer, with heterotrophy increasing in the lower estuary, mostly related to increases in community respiration. PP was mostly controlled by temperature with positive feedbacks from maximum production rate (Pmax) and phytoplankton biomass. Light, temperature and salinity were the most influential factors on photosynthesis-irradiance (P-E) parameters variability.

These findings on the spatial and temporal trends, as well as relationships between the different variables that drive estuarine dynamics, were used in the adaptation, calibration and validation of a 3D coupled hydrodynamic-biogeochemical model for the Douro estuary. The model was then used to study the impact of the dam and its highly variable discharge regime on estuarine water quality and PP. In a first step, the hydrodynamic model was implemented, calibrated, validated and used for analysing the influence of river flow magnitude and variability on estuarine water circulation. Contaminant dispersion was also analysed by means of a conservative tracer. It was found that, apart from river flow magnitude, its variability also plays an important role in estuarine hydrodynamics; stable flows led to lower average salinity and to higher contaminant dispersion. In a second step, coupling of the hydrodynamic and the biogeochemical models was performed, followed by calibration and validation of the latter, in order to study the influence of river flow magnitude and variability on estuarine water quality and PP. Model predictions suggest a direct relationship between flow magnitude and nutrient concentration, whereas a parabolic relationship between phytoplankton biomass and flow magnitude was found, with biomass decreasing for both increases and decreases in river flow. A pattern probably related to lower residence time and lower nutrient and biomass input, for increased and decreased flow, respectively, since nitrate and primary production per unit mass increased with flow magnitude. Considering the different discharge regimes, stable flows yielded higher mean phytoplankton biomass and production than the more variable flows.

Results indicate that flow management may have important effects on estuarine hydrodynamics, water quality and PP. Considering that stable summer freshwater inputs are a proxy for estuarine behaviour before the dam was built, when those inputs depended mostly on Douro base flow, results obtained suggest that flow regulation

through the dam may be responsible for increasing estuarine mean salinity during summer months and reducing its dilution potential for contaminant dispersion, as well as for decreasing phytoplankton biomass and production in the estuary.

Résumé

Les estuaires sont des écosystèmes caractérisés par un grand dynamisme où les conditions environnementales varient beaucoup à différentes échelles temporelle et spatiale. D'autre part, ces écosystèmes sont aussi soumis à de profondes pressions anthropiques se traduisant par une croissante urbanisation et aménagement, une affluence des eaux résiduelles, des constructions de barrages. Le flux d'eau douce dans les estuaires est une caractéristique fondamentale de ces écosystèmes, dont la quantité et la qualité peuvent être modifiées au fur et à mesure que les utilisations s'intensifient, notamment l'irrigation et la production d'électricité. La modification du régime d'eau douce affluant vers les estuaires influence la circulation, la stratification et le temps de résidence de l'eau, ainsi que l'entrée de substances dissoutes et en suspension. Ceci, ayant des conséquences sur la structure et la fonction des communautés estuariennes.

L'estuaire du Douro est la partie terminale du plus grand bassin versant de la Péninsule Ibérique, avec un débit moyen annuel de 505 m^3s^{-1}. Sa limite amont a été imposée par la construction d'un barrage à 21,6 km de l'embouchure, en 1985. Le débit d'eau affluant vers l'estuaire est caractérisé par une grande variabilité dans le temps, spécialement pendant l'Eté où le flux d'eau douce varie en fonction des nécessités pour l'hydro-électricité. Ainsi, au lieu d'un flux continu d'eau douce, normalement variable saisonnièrement, se produisent des «pouls» de déchargement, spécialement pendant la période de moindre débit. En effet, le flux peut varier drastiquement de 0 à 1 000 m^3s^{-1} en une heure.

Ce travail tente à vérifier l'hypothèse selon laquelle le régime artificiel de déchargement d'eau douce influencerait l'hydrodynamisme, la qualité de l'eau et la production primaire (PP) de l'estuaire. Des campagnes d'échantillonnage ont été effectuées pendant le flot et le jusant et la base de données obtenue a permis de dessiner un modèle conceptuel de la biogéochimie de l'estuaire. Le fleuve constitue la plus grande source de nutriments, de chlorophylle a et de matière en suspension, bien que des sources supplémentaires de ces derniers soient présentes dans l'estuaire moyen et inférieur, associées au déchargement d'eaux résiduelles et de petits affluents. La distribution verticale et longitudinale de la salinité s'est révélée fortement

dépendante du débit et, de fait, caractérisée par une grande saisonnalité. Au Douro, une importante stratification verticale de la colonne d'eau se produit pour des débits inférieurs à 800 m^3s^{-1}. Au printemps, avec la progressive diminution du débit et l'augmentation de la température et de la lumière, la biomasse de phytoplancton et la PP atteignent leur maximum dans l'estuaire. Pendant l'Eté, où le débit est fortement réduit et le temps de résidence élevé, la biomasse de phytoplancton et PP décroissent. Ce décroissement peut être expliqué par une diminution de l'apport de biomasse originaire de l'amont, ainsi qu'à l'incapacité de développement du phytoplancton (d'origine fluviale) dans des conditions de salinités élevées dominantes dans l'estuaire pendant cette période. L'estuaire s'est révélé majoritairement hétérotrophe, avec quelques exceptions au niveau de l'estuaire supérieur durant la période Printemps/Eté. La production primaire a été principalement contrôlée par la température, avec une contribution positive du taux photosynthétique maximum (P_{max}) et de la biomasse du phytoplancton. La température, la lumière et la salinité ont été les facteurs qui ont le plus influencé la variabilité des paramètres photosynthétiques.

Les connaissances acquises sur les tendances temporelle et spatiale, ainsi que sur les rapports entre les variables caractérisant le système, ont été utilisées pour l'application d'un modèle tridimensionnel reliant hydrodynamisme – biogéochimie, adapté aux conditions du Douro. Ce modèle, après calibrage et validation, a été utilisé pour tester différents scenarii de magnitude et de variabilité du débit affluant vers l'estuaire. Dans une première phase, le modèle hydrodynamique a été mis en oeuvre, calibré et validé, et utilisé pour analyser l'influence de la magnitude et du régime du débit dans la circulation de l'eau de l'estuaire. La dispersion des contaminants a aussi été évaluée a travers l'utilisation d'un traceur conservatif. Les résultats ont démontré que, outre la grandeur, le régime du débit a également influencé l'hydrodynamisme du système: pour des débits plus uniformes (avec une moindre variabilité), la salinité moyenne a été réduite et la dispersion des contaminants a augmenté. Dans une seconde phase, un modèle biogéochimique a été relié au modèle hydrodynamique, avec l'objectif d'analyser l'influence de la magnitude et du régime du débit sur la qualité de l'eau et sur la production primaire de l'estuaire. La concentration des nutriments a varié positivement avec le débit, alors que la chlorophylle a a présenté une relation parabolique avec le débit, avec l'obtention de valeurs plus élevées de biomasse pour un débit intermédiaire. Cette relation peut être expliquée par la diminution du temps de résidence pour des débits plus élevés, et un moindre apport de nutriments et de biomasse, pour des débits réduits. Concernant la variabilité du débit, pour des volumes

plus uniformes, la concentration de chlorophylle a ainsi que les niveaux de production primaire, ont été plus élevés.

Ces résultats permettent de conclure que la gestion du débit d'eau douce affluant vers l'estuaire peut avoir des effets importants sur la qualité de l'eau et sur la production primaire. Supposant qu'un régime de débit plus uniforme est équivalent à celui avant le barrage, pour des périodes de moindre débit, les résultats obtenus indiquent que le barrage, avec l'actuel régime de déchargement, conduit à l'augmentation de la salinité moyenne et à la diminution du potentiel de dilution des contaminants ainsi qu'à une diminution de la biomasse et de la production phytoplanctonique.

Nota Prévia

Na elaboração desta dissertação foi efectuado o aproveitamento total dos resultados de trabalhos já publicados ou submetidos, os quais integram alguns capítulos da presente tese. Em todos estes trabalhos, a candidata participou na obtenção, análise e discussão dos resultados, bem como na elaboração da sua forma publicada.

List of papers

This thesis is based on the following papers:

1. Azevedo I, Duarte P, Bordalo A (2006). Pelagic metabolism of the Douro estuary (Portugal) - Factors controlling primary production. Estuarine Coastal and Shelf Science 69:133-146.

2. Azevedo I, Duarte P, Bordalo A (2008). Understanding spatial and temporal dynamics of key environmental characteristics in a mesotidal Atlantic estuary (Douro, NW Portugal). Estuarine Coastal and Shelf Science 76:620.

3. Azevedo I, Duarte P, Bordalo A. Temporal and spatial variability of phytoplankton photosynthetic characteristics in a southern European estuary (Douro, Portugal). Submitted to Marine Ecology Progress Series.

4. Azevedo I, Duarte P, Bordalo A. Influence of river discharge patterns on the hydrodynamics and contaminant dispersion in the Douro estuary (Portugal). Submitted to Water Research.

5. Azevedo I, Duarte P, Bordalo A. Influence of freshwater inflow variability on the Douro estuary biogeochemistry: a modelling study. In prep.

Contents

Agradecimentos iii

Resumo vii

Abstract xi

Résumé xv

Nota Prévia xviii

List of papers xix

Contents xxi

List of Figures xxv

List of Tables xxix

CHAPTER 1 1

General introduction 1

1.1 Estuarine ecosystems 1

1.2 The Douro estuary 7

1.3 Motivation 9

1.4 Objectives 10

CHAPTER 2 13

Understanding spatial and temporal dynamics of key environmental characteristics in a mesotidal Atlantic estuary (Douro, NW Portugal) 13

2. 1 Introduction 13

2. 2 Material and Methods 16

2.2.1 Study area 16

2.2.2 Sampling 17

2.2.3 Analytical procedures 18

2.2.4 Data analysis 19

2.3 Results **20**

2.3.1 Estuarine level properties 20
2.3.2 Temporal and spatial trends 25

2.4 Discussion **28**

2.5 Conclusions **34**

CHAPTER 3 **35**

Pelagic metabolism of the Douro estuary (Portugal) – factors controlling primary production **35**

3.1 Introduction **35**

3.2 Material and Methods **37**

3.2.1 Study area 37
3.2.2 Sampling 38
3.2.3 Experimental and analytical procedures 39
3.2.4 Data analysis 40

3.3. Results **43**

3.3.1 Environmental conditions 43
3.3.2 Chlorophyll *a* and photosynthetic parameters 46
3.3.3 Estuarine metabolism 49
3.3.4 Effect of time, tide and stations 50
3.3.5 Patterns of similarity between samples 51

3.4 Discussion **52**

3.5 Conclusions **58**

CHAPTER 4 **59**

Temporal and spatial variability of phytoplankton photosynthetic characteristics in a southern European estuary (Douro, Portugal) **59**

4.1 Introduction **59**

4.2 Material and Methods **61**

4.2.1 Study area 61
4.2.2 Data collection 62
4.2.3 Analytical and experimental procedures 63

4.2.4 Data analyses 64

4.3 Results **66**

4.3.1 Environmental variables 66
4.3.2 Photosynthetic parameters 68
4.3.3 Temperature and phosphate integration in the Steele's P-E equation 73

4.4 Discussion **74**

4.4.1 Environmental variability 74
4.4.2 Photosynthetic variability 75

4.5 Conclusions **80**

CHAPTER 5 **81**

Influence of river discharge patterns on the hydrodynamics and contaminant dispersion in the Douro estuary (Portugal) **81**

5.1 Introduction **81**

5.2 Methodology **83**

5.2.1 Study site 83
5.2.2 Model description 84
5.2.3 Model calibration and validation 87
5.2.4 Simulation Scenarios 88

5.3 Results **91**

5.3.1 Model calibration and validation 91
5.3.2 Scenario analysis 95

5.4 Discussion **97**

5.4.1 Model calibration and validation 97
5.4.1 Scenario analysis 98

5.5 Conclusions **101**

CHAPTER 6 **103**

Influence of freshwater inflow variability on the Douro estuary biogeochemistry: a modelling study **103**

6.1 Introduction **103**

6.2 Methodology **105**

6.2.1 Study site 105
6.2.2 Model description 106
6.2.3 Model setup 108
6.2.4 Model calibration and validation 109
6.2.5 Sensitivity analysis 110
6.2.6 Simulation Scenarios 111

6.3 Results **111**

6.3.1 Model calibration and validation 111
6.3.2 Sensitivity analysis 118
6.3.3 Scenario analysis 118

6.4 Discussion **122**

6.4.1 Model calibration and validation 122
6.4.2 Sensitivity analysis 124
6.4.3 Scenario analysis 124

6.5 Conclusions **125**

CHAPTER 7 **127**

General conclusions and future directions **127**

References **132**

List of Figures

Figure 1.1. Satellite image of the Douro estuary. 7

Figure 2.1. Location of sampling stations (●), wastewater treatment plants (▲) and small rivers (⇧) discharging into the estuary. Limits of estuarine stretches (upper, middle and lower) according to Vieira e Bordalo (2000). Samples for primary production analyses were collected at stations 1, 5 and 10. 17

Figure 2.2. Estuary number (Ne) as a function of river flow. Ne values lower than 0.1 are indicative of stratified conditions. 22

Figure 2.3. Relationships between nutrients, TPM, chlorophyll *a*, DO, FC bacteria, and salinity. Data shown were collected during July surveys and are representative of the observed patterns, except F and H (from September and August surveys, respectively), corresponding to deviations from those patterns (see text). 23

Figure 2.4. N:P obtained for all samples collected. The line indicates the Redfield ratio. 24

Figure 2.5. Seasonal variability of TPM, nutrients, chlorophyll *a*, PP, FC bacteria and CR. Each value corresponds to monthly averages±SE, integrating data from all sampling stations. 26

Figure. 2.6. Water column salinity structure, observed during flood sampling surveys, under different river flow magnitude. A – 875 $m^3 s^{-1}$ (March); B – 500 $m^3 s^{-1}$ (October); C - 292 $m^3 s^{-1}$ (July); D - 36 $m^3 s^{-1}$ (June). 27

Figure 2.7. Salt wedge position (water with salinity equal or higher than 30) as a function of river flow. Dashed line indicates distance from the mouth of the salt wedge under a river flow of 300 $m^3 s^{-1}$ (*cf* - Section 2.3.2). 28

Figure 2.8. Spatial variability of TPM, nutrients, chlorophyll *a*, primary production, CR and FC bacteria. Each value corresponds to time-averaged data collected at each sampling station, integrating the entire sampling period. 29

Figure 2.9. Variability of TPM, nitrate and PP with river discharge (A) and with distance from the mouth (B), observed during this study. A - Quantitative relationships were derived using averaged values

integrating all stations for each sampling survey; B - Quantitative relationships were derived using time and tide-averaged values for each sampling station. 31

Figure 2.10. Conceptual model of the Douro estuarine biogeochemistry. Nutrient loads and uptake by phytoplankton at each stretch, calculated from data obtained during the present study, are represented in the upper part of the diagram. Dark horizontal arrows correspond to loads whereas curved vertical arrows correspond to uptake. Values are in Kg day $^{-1}$. Key environmental characteristics seasonal variability is presented in the lower part of the diagram. Shaded areas indicate seawater intrusion. Horizontal arrows width is proportional to river flow magnitude. ⬀ - increase; ⇧ - high; ⬂ - decrease; ⇩ - low. 33

Figure 3.1. The river Douro estuary and location of sampling stations (L – lower, M – middle and U – upper estuary, WTP – Wastewater Treatment Plant). 38

Figure 3.2. River flow (m^3s^{-1}) during sampling surveys (vertical bars) and monthly averages (dotted line), from December 2002 to December 2003. 44

Figure 3.3. Water column salinity levels at the upper (U), middle (M) and lower (L) estuarine stations during the ebb and flood surveys from December 2002 to December 2003. 45

Figure 3.4. Water column chlorophyll *a* values at the lower (L), middle (M) and upper (U) estuarine stations, during the ebb and flood surveys, from December 2002 to December 2003. 47

Figure 3.5. Daily integrated phytoplanktonic PP and water column CR in the lower (L), middle (M) and upper (U) estuarine stations, during the ebb and flood surveys, from December 2002 to December 2003. 50

Figure 3.6. Projection of samples in two dimensions, defined by the first two principal components, labelled by season - winter (△); spring (▼); summer (□); fall (○). 54

Figure 3.7. Projection of samples in two dimensions, defined by the first two principal components, labelled by station - Lower (▲); Middle (▽); Upper (□). 56

Figure 3.8. Projection of samples in two dimensions defined by the two first principal components. Bubble size is related to the magnitude of the variable represented. A – depth integrated hourly PP; B – extinction coefficient (k). Samples are labelled by season: winter (W); spring (Sp); summer (S); fall (F). 57

Figure 4.1. The river Douro estuary and location of sampling stations (L – lower, M – middle and U – upper estuary, WTP – Wastewater Treatment Plant). 62

Figure 4.2. Hourly river flow ($m^3 s^{-1}$) during the fall, winter and summer tidal cycle surveys. Data for the spring survey were not available. 67

Figure 4.3. Hourly river flow ($m^3 s^{-1}$) during the fall, winter and summer tidal cycle surveys. Data for the spring survey were not available. 69

Figure 4.4. Salinity and nutrients variability along the tidal cycle surveys. Open symbols correspond to bottom samples and block symbols correspond to surface samples. 71

Figure 4.5. Diel variation of photosynthetic parameters P_{max} (in mg C mg $Chla^{-1}$ h^{-1}), α (in mg C mg $Chla^{-1}$ h^{-1} (µE $m^{-2}s^{-1})^{-1}$) and E_k (in µE $m^{-2}s^{-1}$). 77

Figure 4.6. Projection of samples in the space defined by the first two principal components. A – samples labelled by season; B – samples labelled by time of day. 78

Figure 4.7. Relationship between P_{max} and Chl *a* obtained during spring, fall and winter tidal surveys. ● - Spring; ■ - Fall and ▲ - Winter. 79

Figure 5.1. Study site, showing the 3 estuarine stretches and the upstream limit. Arrows represent location of main small rivers discharging into the estuary. 84

Figure 5.2. River flow regimes tested: 1) the observed, highly variable flow; 2) daily averaged flow, and 3) constant flow throughout the simulation period, corresponding to the averaged value of the flow measured for the entire simulation period (*cf.* – Methodology – simulation scenarios). 89

Figure 5.3. Tidal heights predicted by the model versus observed values (obtained from Admiralty Tables) at the estuary mouth. 91

Figure 5.4. Tidal height predicted by the model at 2 extreme locations: station 1, near the mouth and station 10 near the dam, the estuary upstream limit (*cf.* – Figure 5.1). Squares correspond to river flow hourly values. 92

Figure 5.5. Current velocities predicted by the model and observed values, from seasonal tidal cycles conducted at the estuary mouth. 93

Figure 5.6. Observed versus predicted values for salinity and temperature at 10 stations along the estuary (*cf.* – Figure 5.1) and at 3 depths for June simulation 94

Figure 5.7. Observed versus predicted values for salinity and temperature at 10 stations along the estuary (*cf.* – Figure 5.1) and at 3 depths for August simulation. 96

Figure 5.8. Observed versus predicted values for salinity and temperature at 10 stations along the estuary (*cf.* – Figure 5.1) and at 3 depths for October simulation. 97

Figure 5.9. Spatial distribution of tracer concentration during flood and ebb periods, for the, 9 scenarios of flow variability and magnitude: A) standard flow magnitude; B) halved river flow; C) doubled river flow. 99

Figure 6.1. Study site, showing the 3 estuarine stretches and the upstream limit. Arrows represent location of main small rivers discharging into the estuary. 106

Figure 6.2. Observed and predicted chlorophyll *a* values for the June, August and October periods, in mg m^{-3}. 114

Figure 6.3. Observed and predicted nitrate values for the June, August and October periods, in µM. .. 114

Figure 6.4. Observed and predicted phosphate values for the June, August and October periods, in µM. 115

Figure 6.5. Observed and predicted ammonium values for the June, August and October periods, in µM. 115

Figure 6.6. Observed and predicted TPM values for the June, August and October periods, in mg L^{-1}... 116

Figure 6.7. Observed and predicted POM values for the June, August and October periods, in mg L^{-1}. . 117

Figure 6.8. Time series of surface nitrate (in µM) and phytoplankton biomass (chlorophyll *a*, in mg m^{-3}) predictions for June at different locations: A – near the mouth; B – at the middle estuary (5.3 km from the mouth) and C – near the dam. S1, S2 and S3 correspond to the different river flow regimes. River flow is in m^3s^{-1}. 120

Figure 6.9. Chlorophyll *a* and salinity, predicted in simulations S1, S2 and S3 (*c.f.* Table 5.2) along the estuary, during the ebb and the flood 121

List of Tables

Table 2.1. Equations, parameters and references used in calculation estuarine wide indices tidal prism, freshwater residence time and estuary number. 19

Table 2.2. Freshwater residence time (Tr) and estuary number calculated for each sampling survey from December 2002 to December 2003. River flow values are daily averages of each survey. Ne values represented in bold type are lower than 0.1, indicative of stratified conditions. 21

Table 2.3. Ranges, averages and standard errors for selected variables obtained in this study for the entire estuary. River flow range was derived from recorded values during each survey. 22

Table 3.1. Averages and standard errors for selected variables at each location during flood and ebb surveys for the December 2002 – December 2003 period. 43

Table 3.2. Monthly photosynthetic parameters obtained for the PI curves for the 3 sampling stations along the year during the ebb and flood surveys. P_{max} in mg C mg $Chla^{-1}$ h^{-1}; E_{opt} in µE m^{-2} s^{-1}; Initial slope of the P/E curve in mg C mg $Chla^{-1}$ h^{-1} (µE m^{-2} $s^{-1})^{-1}$ 48

Table 3.3. Compensation depths calculated for the 3 sampling stations along the year during the ebb and flood surveys. Compensation depth values represented in bold type are close to or higher than water column depth. 49

Table 3.4. Eigenvalues, percent variation and cumulative percent variation of the first 5 principal components. 51

Table 3.5. Eigenvectors or Coefficients in the linear combinations of variables making up PC's. 52

Table 3.6. Summary of pelagic primary production (PP) measurements (mean values or ranges) in temperate estuaries. 53

Table 4.1. Descriptive statistics of environmental variables measured during seasonal tidal cycles; s.d. – standard deviation; C. V. – coefficient of variation (%). 70

Table 4.2. Descriptive statistics of photosynthetic parameters obtained during seasonal tidal cycles. s.d. – standard deviation; C. V. – coefficient of variation (%); P_{max} in mg C mg Chla^{-1} h^{-1}; α in mg C mg Chla^{-1} h^{-1} (μE m^{-2}s^{-1})$^{-1}$; E_{opt}, E_o and E_k in μE m^{-2}s^{-1}; chlorophyll *a* in mg m^{-3}. 71

Table 4.3. Eigenvectors or Coefficients in the linear combinations of variables making up PC's (see Figure 4.6); P_{max} in mg C mg Chla^{-1} h^{-1}; α in mg C mg Chla^{-1} h^{-1} (μE m^{-2}s^{-1})$^{-1}$; E_{opt} and E_o in μE m^{-2}s^{-1}; chlorophyll *a* in mg m^{-3}; PP in mgCmg Chl^{-1}.h^{-1}; nutrients in μM; temperature in ºC and ODsat in % saturation. 73

Table 4.4. Descriptive statistics of photosynthetic parameters obtained during annual surveys at the 3 stations along the estuary. s.d. – standard deviation; C. V. – coefficient of variation (%); P_{max} in mg C mg Chla^{-1} h^{-1}; α in mg C mg Chla^{-1} h^{-1} (μE m^{-2}s^{-1})$^{-1}$; E_{opt}, E_o and E_k in μE m^{-2}s^{-1}; chlorophyll *a* in mg m^{-3}. 75

Table 4.5. Parameters obtained by integration of temperature and phosphate limiting functions with Steele equation; T – temperature; Ph – phosphate; Kp – phosphate half-saturation constant; k_T – temperature augmentation rate (ºC)$^{-1}$. 76

Table 5.1. EcoDynamo objects implemented for the Douro estuary. 85

Table 5.2. Scenarios representing different river flow variability and magnitude (see text). 88

Table 5.3. Average salinity, Ne, freshwater residence time and tracer concentration for the different river flow magnitudes and regimes tested. Ne < 0.1 indicative of stratified conditions; Rt – freshwater residence time (days); Tracer in μM. 95

Table 6.1. EcoDynamo objects implemented for the Douro estuary. 107

Table 6.2. Calibrated parameters and respective values. 112

Table 6.3. Model performance after calibration, in simulated key variables, using September data. 112

Table 6.4. Goodness of fit and error measures obtained for model performance, in key variables simulation. 113

Table 6.5. Measured primary production and model results for net (NPP) and gross primary production (GPP) in mg C (mg C)$^{-1}$ h^{-1}, obtained in June, August September and October. 118

Table 6.6. Sensitivity analysis results for parameters P_{max} and E_{opt}. 118

Table 6.7. Scenario analysis - Averages obtained for key variables, in each simulation performed. Phytoplankton biomass is in mg m^{-3}, nutrients in µM, TPM and POM in mg L^{-1} and NPP and GPP in mg C (mg C)$^{-1}$ h^{-1}. 119

CHAPTER 1

General introduction

1.1 Estuarine ecosystems

Estuaries are ecosystems characterized by a high environmental variability, mainly driven by salinity changes due to tidal and river flow dynamics. Although there are several definitions of “estuary” in the literature (Dyer 1997), most of them include the mixture of saline and freshwater, as a fundamental feature of estuarine systems. The degree and pattern of this mixture depends on morphology, tidal characteristics and freshwater flows. Seawater intrusion produces a longitudinal density gradient (higher water densities at the mouth and lower at the head), resulting in increased flood velocities near the bed and increased ebb velocities at the surface. For tide averaged conditions, this behaviour leads to residual flows, which consist of saline water flowing upstream along the bottom and fresher water flowing seawards near the surface. Because this is a density driven circulation, caused by gravity acting on horizontal density differences, it is called gravitational circulation (Dyer 1997).

The relative importance of tidal amplitude and river flow determines estuarine circulation and salinity distribution, criteria used for estuarine classification. Estuaries may be classified in three main types, according to those criteria: salt wedge or highly stratified, partially mixed and homogeneous or well mixed. Distinction between those types is based

on the ratio of river to tidal flow. In salt wedge estuaries, a surface layer of freshwater flows seaward on top of an inflowing seawater layer. Entrainment (mixing) is observed at the interface between the two layers. Generally, this type of estuarine circulation occurs when river flow is larger than tidal flow. In a partially mixed estuary, tidal flow is greater or similar to river flow and a smooth salinity gradient is found over the water column. Well mixed estuaries are characterised by a homogeneous water column, and are usually wide and shallow estuaries.

The above described classification of estuaries is based on tidally and spatially averaged conditions. Nevertheless, temporal and spatial variability of estuarine salinity and water circulation patterns are usually high, dependent on freshwater flow variability and tidal dynamics. With increased freshwater flow, or during neap tides, the extent of tidal intrusion of seawater diminishes, while during spring tides, or decreased freshwater flow, the tidal intrusion increases. The rise and fall of the tide produces horizontal flows, the tidal currents. These currents may reach considerable values, depending on tidal range, depth and estuary mouth characteristics. Intensity of flood and ebb tide current velocities varies daily and during the spring-neap cycle, coupled with water levels variation (Dyer 1997, Uncles & Lewis 2001).

The steep gradients characteristic of most estuaries implies that organisms must be adapted to highly variable conditions, thus estuaries are areas of low diversity. On the other hand, they are among the most productive ecosystems, and the most valuable, per unit area (Costanza et al. 1997). In fact, estuaries provide many services and functions to humankind, from recreational and cultural services to food production and refuge for many resident and transient species. Also, estuaries are preferred places for human settlement and many large cities are located in their banks, increasing human pressure.

Increasing anthropogenic pressure is reflected in the many different and sometimes conflicting uses to which estuaries are subjected, which significantly modify these ecosystems (Nichols et al. 1986). Examples are land reclamation for agriculture and building, sand and gravel abstraction for construction, navigation, with consequent channel dredging, wastewater disposal, and damming for flood control, electricity production or water abstraction (McLusky & Elliot 2004).

Importance of freshwater inflow

One of the most drastic estuarine modifications is dam construction, since it introduces severe changes on the timing, quantity and quality of freshwater delivered to estuaries and adjacent coastal zones (Hopkinson & Vallino 1995). The alteration of freshwater flow regime is one of the most important factors affecting estuarine community function and structure (Sklar & Browder 1998). The effects of freshwater flow variability on estuarine dynamics are, at a first level, physical and chemical. Physical effects include alteration of circulation patterns, stratification and residence time, whereas chemical effects are related with changes in particulate and dissolved matter, such as sediments and nutrients. These effects, in turn, affect biotic communities through changes in species composition, abundance and distribution of organisms, with consequences on primary and secondary production (Sklar & Browder 1998, Alber 2002).

There are a number of pathways through which freshwater flow influences estuarine organisms at the different trophic levels. Biological responses to changes in freshwater flow are very variable, site-specific and dependent on overall estuarine characteristics, often preventing generalizations among different estuaries (Kimmerer 2002a).

In estuaries with small intertidal areas, estuarine primary production is mostly dependent on phytoplankton. Phytoplankton production is dependent on physical (light and temperature), chemical (nutrients) and biological factors, such as phytoplankton biomass, species composition, size structure and grazing (Stearns et al. 1987, Cloern 1991, Landry et al. 1995, Gallegos & Jordan 1997, Calbet & Landry 2004, Cermeno et al. 2006), as well as viral control (Proctor & Fuhrman 1991). All these factors are directly or indirectly affected by changes in freshwater inflow.

Therefore, phytoplankton may respond to flow in different ways, according to the mechanism involved. If nutrient limitation occurs, then the response to flow is positive (e.g. Malone et al. 1988, Mallin et al. 1993), whereas if light limitation by high suspended matter or low residence time are experienced, the response to flow is negative. In some estuaries, the relationship to flow is not linear, due to the contribution of different mechanisms at different temporal or spatial scales, resulting in opposite responses to flow in different estuarine reaches (Cloern & Nichols 1985, Sin et al. 1999), or in a parabolic relationship between river discharge and phytoplankton biomass (Snow et al. 2000). Another indirect mechanism, by which river flow reduction may cause a negative effect on phytoplankton biomass, is immigration of benthic grazers due to higher salinity levels, leading to increased grazing pressure (Cloern & Nichols 1985, Alpine & Cloern 1992).

As a consequence of changes in phytoplankton biomass and production, altered freshwater flow regimes will also affect estuarine metabolic balance, which is dependent on its primary production and community respiration. Estuaries are considered heterotrophic systems, in which consumption exceeds production, although seasonal shifts from auto- to heterotrophy according to river flow variations have been reported (Ram et al. 2003). The autotrophic-heterotrophic nature of an estuary is determined by three primary factors: the ratio of inorganic to organic matter inputs, water residence time and the overall degradability of allochthonous organic matter inputs (Hopkinson & Vallino 1995). Thus, discharge of treated or untreated wastewater into estuaries also affects metabolism by increasing allochthonous nutrient or organic matter inputs, respectively. The former may increase production and the latter bacterial respiration. If bacterial respiration exceeds net primary production due to utilization of external sources of organic matter, heterotrophy dominates (delGiorgio et al. 1997).

Freshwater inflow also determines estuary flushing time. Flushing time is defined as the time required to replace the freshwater volume in the estuary at a given river flow. It is also called freshwater residence time and it is a valuable concept in estuarine management for predicting pollutant discharge impacts or allowable effluent disposal (Dyer 1997).

Thus, effects of changing freshwater flow to estuaries are manifold, which makes knowledge of ecosystem functioning important to anticipate the result of changes induced by human action. The European Community approved in 2000 the Water Framework Directive (WFD, EC 2000), which sets a framework for water resources management in Europe. It is based on management at the river basin level and its overall goal is to achieve a good ecological status for all surface water bodies by the year 2015. Measures to maintain or achieve a good ecological status need to be set within River Basin Management Plans. Ecological models may be used as tools to increase understanding of ecosystem behaviour under variable forcing conditions, natural or not, as well as to predict its response to pressures or to improvement measures.

Modelling estuarine ecosystems

The use of mathematical models to address environmental and ecological problems is increasing. They have been used as scientific tools, to synthesize knowledge of ecosystems functioning, on one hand, and to increase understanding of ecosystems properties, through, for example, scientific hypotheses testing, on the other hand. They

have also been used as management tools to predict the results of human actions affecting the environment (Jørgensen & Bendoricchio 2001).

Models used in estuarine research and management vary widely in their complexity, depending on the mathematical equations used for modelling the different processes or on the number of spatial dimensions considered. In estuaries, there are a number of processes, from physical to biogeochemical, which may be modelled by means of more or less complex mathematical formulations, in order to understand or predict ecosystem behaviour. An example is modelling of estuarine primary production in order to obtain estimates or to study its variability as a function of environmental characteristics. Primary production estimates may be retrieved using simple empirical models, for example, based on chlorophyll concentration, photic depth and surface irradiance, described as a composite parameter, BZpIo (Cole & Cloern 1987), or more complex equations, based on the physiology of organisms, known as mechanistic models. These are based on the relationship between photosynthesis and light (P/E relationship), and may be static (e.g. Eilers & Peeters 1988), where parameters describing this relationship are constant in time or dynamic models when their temporal variability is included (Duarte & Ferreira 1997).

Considering the high temporal and spatial variability inherent to most estuaries, modelling physical processes underlying the transport and dispersion of all suspended and dissolved materials, such as nutrients and contaminants, is of uttermost importance. Physical processes affect all biological activity, including the transport of larvae and bacteria, the growth of phytoplankton and the behaviour of fish (James 2002). Thus, hydrodynamic models have been implemented in estuaries to study physical characteristics, such as residence time, salinity stratification, and salt wedge dynamics, among others (Kurup et al. 1998, Huang & Spaulding 2002, Wang et al. 2004, Liu et al. 2007, Yuan et al. 2007). Hydrodynamic modelling has also been performed as a basis for water quality studies, to predict contaminant transport, distribution and fate in estuaries and coastal zones (Falconer & Lin 1997, Thouvenin et al. 1997, Passone et al. 2003), which are important issues, particularly in urbanized estuaries, or to predict bathing water compliance (Kashefipour et al. 2002).

Model type selection, as well as its complexity, should be based on the objectives of the work. If a time-integrated description of estuarine properties is intended, then a simple mass-balance budget model may be sufficient, in most cases, whereas if the aim is to study temporal and spatial behaviour of estuarine properties, more complex, high dimensional models are needed. Selection of model complexity should also take into

account the knowledge of processes and state variables, as well as the data set available in order to avoid high uncertainty levels (Jørgensen & Bendoricchio 2001).

Modelling estuarine systems has undergone a great development in the last decades, namely due to improved computer power. The development of coupled, high resolution, physical and ecological models has been increasing, thanks to parallel processing, allowing real-time predictions of water quality (James 2002). Examples of this advances are recently developed, three-dimensional coupled hydrodynamic-biogeochemical models that have been applied in several systems for studying the relationship between physical-chemical processes and estuarine primary production (Robson & Hamilton 2004, Huret et al. 2005, Trancoso et al. 2005, Xu & Hood 2006), or to predict phytoplankton responses to nutrient reduction management measures (Lacroix et al. 2007, Saraiva et al. 2007).

1.2 The Douro estuary

The Douro estuary is part of the largest watershed in the Iberian Peninsula (98,000 km^2). More than 50 large dams have been built in the watershed for irrigation and electric power generation, resulting in flow regulation. The construction of the most downstream dam, at 21.6 Km from the mouth, in 1985, reduced estuarine length by 60% (Bordalo, unpublished data). The Douro drains into the Atlantic Ocean, at the west coast of Portugal, near the city of Porto (41.14ºN and 8.66ºW; Figure 1.1). It is a drowned valley estuary, narrow in the middle and upper reaches, widening towards the mouth. It has been divided in 3 stretches by Vieira and Bordalo (2000), as a function of seawater intrusion, with average width and depth of respectively, 333 m and 7.8 m for the upper estuary; 271 m and 10 m for the middle estuary and 645 m and 7 m for the lower estuary. Tides are semi-diurnal with average tidal range of 2.8 m at the mouth and 2.6 m at the head. During the flood and under low river flow, sea water creates a salt wedge that eventually reaches the head of the estuary, where the tidal excursion is halted by the dam, and remains within the estuary during the next ebb. In this situation, residence time can reach 14 days, whereas during high discharge events, the estuary is flushed completely during one tidal cycle and seawater intrusion is prevented during the flood (Vieira & Bordalo 2000).

Figure 1.1. Satellite image of the Douro estuary.

The mouth is partially obstructed by a concrete stabilized sand bar, with ongoing hard work alterations for navigation accessibility improvement. Bathymetry is characterized by a regularly dredged 6-m deep navigation channel and a V-shaped cross-section, with asymmetric slopes. Daily freshwater discharge by the Douro River ranges from 0 to more than 13,000 m^3s^{-1}, with an average of 505 m^3s^{-1}, since the construction of the upstream dam, in 1985. Other sources of freshwater are present along the estuary, originated from 13 small rivers, with average flows in the range 0.1 - 5 m^3s^{-1}, several of which are channelized over most of their course, especially those located in the lower highly urbanized stretch.

The lower estuary is heavily polluted by sewage discharge (Bordalo 1993, Bordalo & Vieira 2005), and heavy metals contamination (Zn, Cu, Pb, Cd and Cr) is present, with effects on macrobenthic community structure, namely, low diversity and presence of opportunistic species (Mucha et al. 2003, 2004, 2005). Furthermore, major endocrinologic disturbances were found in pelagic and benthic fish – mullet (*Mugil cephalus*) and flounder (*Platichthys flesus*) - indicating the presence of xeno-estrogenic pollution in the Douro estuary (Ferreira et al. 2004). Benthic intertidal areas, including hard-surface substrates, were found to be highly autotrophic, actively removing inorganic nutrients from the water column (Magalhaes et al. 2003). Over the last 15 years, an increase in nitrate concentration in the upstream reservoir has been reported (Magalhaes et al. 2005), leading to increased loads to the estuary, with potential consequences on estuarine productivity.

1.3 Motivation

The upper limit of the Douro estuary is separated from the river by a hydroelectric power dam. This is an unusual characteristic that has immediate consequences: the tidal wave is halted by the dam wall and the freshwater inflow regime is profoundly altered. Previous studies in the Douro (Vieira & Bordalo 2000) presented evidence that the presence of the dam wall is responsible by the dominant standing wave behaviour of the tide. As a result, the longitudinal energy transport is low, preventing water column mixing and enhancing stratification. This phenomenon may explain, at least partly, why the Douro, a mesotidal estuary, presents often a salt wedge behaviour. On the other hand, consequences of changing the freshwater flow regime on the estuarine hydrodynamic and biogeochemical characteristics were not yet studied.

Presently, the discharge of freshwater by the dam is strongly dependent on electric power demand, especially during the summer low river flow period. As a consequence, river inflow to the estuary is characterised by high short-term variability, between zero flow and over 1,000 m^3s^{-1}, in a matter of hours (Bordalo, unpublished data).

Considering the mechanisms involved in river flow influence on estuarine characteristics, discussed above, it seems reasonable to hypothesise that the highly variable freshwater inflow regime imposed by the dam will have important consequences on hydrodynamics, water quality and primary production in the Douro estuary. Considering the impossibility to test experimentally this hypothesis, a modelling approach was necessary. However, the implementation, calibration and validation of an ecological model require a significant amount of data and knowledge about the system being modelled. Therefore, testing the above mentioned hypothesis – the main motivation for this work - involved a large amount of field and laboratory work, followed by model implementation and application.

1.4 Objectives

The main goal of the present work was to assess the effects of changes in freshwater inflow magnitude and variability on estuarine hydrodynamics, water quality and primary production. In order to accomplish this goal, the following specific objectives were defined:

- Establish quantitative relationships and trends, towards a better understanding of estuarine behaviour as a function of time and space by: (i) analysing estuarine level properties;(ii) describing the Douro estuary, by means of chemical and biological properties, as well as rates; (iii) designing a conceptual model of river flow influence on the Douro estuary biogeochemistry.
- Analyse estuarine environmental conditions and photosynthetic parameters in relation to its metabolism, in order to determine which factors control primary production on a spatial and temporal basis.
- Analyse the temporal and spatial variability of estuarine phytoplankton photosynthetic characteristics.
- Implement and apply a hydrodynamic model to the estuary, in order to improve understanding of its hydrodynamic characteristics and the effects of river flow magnitude and variability on estuarine water circulation and quality.
- Calibrate and validate a biogeochemical model coupled to the previously implemented hydrodynamic model for the Douro estuary in order to understand how phytoplankton biomass and production, nutrient and suspended matter temporal and spatial dynamics are influenced by freshwater flow variability and magnitude.

The methodology followed to accomplish these objectives started with a sampling program that covered the entire estuary. Samples were taken under ebb and flood tide situations along the estuarine length and depth. These sampling surveys were conducted twice a month, at 10 stations, with sample collection at three depths. Primary production measurements were performed at three stations, one at each estuarine stretch. Additionally, seasonal tidal cycle surveys were conducted at an anchor station located near the river mouth. In these surveys, samples were collected every two hours at near surface and near bottom depths together with quasi-continuous CTD measurements. Primary production was measured every 3 hours. Statistical analysis of field data was carried out and quantitative relationships between key variables, as well as their spatial

and temporal trends, were obtained. Both raw data and the knowledge gained from data analysis were used in the implementation of a 3D-coupled hydrodynamic-biogeochemical model for the Douro estuary. This model was then used to analyse different scenarios of river discharge magnitude and variability on estuarine hydrodynamic behaviour, water quality and primary production. The study of contaminant dispersion under the different scenarios was based on a virtual experience, which consisted in considering the discharge of a conservative tracer through the estuarine tributaries, and analysing its behaviour.

The present dissertation is organised in seven chapters, including the present one, where a general introduction to the thesis theme is presented and the objectives identified. Chapter two is concerned with a spatial and temporal characterization of key environmental variables, as well as relationships between them, through the design of a conceptual model of the Douro estuary biogeochemistry. Chapter three presents an analysis of the pelagic metabolism of the Douro estuary and the factors influencing primary production and community respiration. Chapter four analyses temporal and spatial scales of variability in phytoplankton photosynthetic parameters as well as the factors responsible for that variability. Chapter five presents a hydrodynamic model, implemented for the Douro estuary, and analyses several scenarios of river flow magnitude and variability in order to study the influence of those variables in estuarine hydrodynamic behaviour and contaminant dispersion. Chapter six presents the coupling of a biogeochemical module to the previous hydrodynamic model in order to analyse the influence of river flow variability and magnitude on estuarine biogeochemistry. Model calibration and validation were based on data from chapters two, three and four. Some model parameters were also derived from data obtained in previous chapters.

CHAPTER 2

Understanding spatial and temporal dynamics of key environmental characteristics in a mesotidal Atlantic estuary (Douro, NW Portugal)

2. 1 Introduction

Estuaries are areas under high anthropogenic pressure and subject to many different and sometimes conflicting uses, which significantly modify these ecosystems (Nichols et al. 1986). The alteration of freshwater flow regime is one of the most important factors affecting estuarine community function and structure (Sklar & Browder 1998).

The effects of freshwater flow variability are, at a first level, physical and chemical. Physical effects include alteration of circulation patterns, stratification and residence time,

---

The contents of this chapter were originally published in Azevedo IC, Duarte PM, Bordalo AA (2008). Understanding spatial and temporal dynamics of key environmental characteristics in a mesotidal Atlantic estuary (Douro, NW Portugal). Estuarine Coastal and Shelf Science 76:620.

whereas chemical effects are related with changes in particulate and dissolved matter. These effects, in turn, affect biological characteristics such as species composition, abundance and distribution of organisms, as well as primary and secondary production (Sklar & Browder 1998, Alber 2002). There are a number of pathways through which freshwater flow influences estuarine organisms at the different trophic levels. For a review of the possible mechanisms underlying flow effects on estuarine biota see Kimmerer (2002b).

Biological responses to changes in freshwater flow emerge as very variable, site-specific and dependent on overall estuarine characteristics, often preventing generalizations among different estuaries (Kimmerer 2002a). For example, in San Francisco Bay, phytoplankton biomass, community composition and productivity response to variability in river flow differs between the river-dominated northern reach and the South Bay, a lagoon-type estuary. In the former case, blooms occur when river flow falls within a narrow range (100 – 400 m^3s^{-1}) and are related to accumulation of suspended material in shallow, more productive areas, whereas, in the latter case, biomass increases with river flow, related to water column stabilization due to stratification (Cloern et al. 1985). A similar pattern was reported by Sin et al (1999) in the York River estuary, where a negative correlation between chlorophyll *a* and river discharge was observed in the upper estuary whereas in the lower estuary a positive correlation existed for mean and high discharge rates. Snow (2000) reported an optimum river discharge for phytoplankton biomass increase (around 1 m^3s^{-1}), in Gamtoos estuary. In this system, the mechanisms preventing biomass increase are nutrient limitation at lower inflow and low residence time at higher inflow. Increased nutrient availability during river flow pulses has been often described as a mechanism influencing estuarine primary productivity (Mallin et al. 1993). In Cheasapeak Bay, freshwater flow and nitrate input during spring freshets governs the timing and magnitude of the spring phytoplankton biomass maximum, which in turn determines the amount of nitrogen available for recycling during the following summer, when a productivity maximum occurs (Malone et al. 1988, Mallin et al. 1993). Another mechanism by which river flow reduction, indirectly, may cause a negative effect on phytoplankton biomass, is immigration of benthic grazers due to higher salinity levels, leading to increased grazing pressure (Cloern & Nichols 1985, Alpine & Cloern 1992). Food web regulation by freshwater discharge volume, timing and duration has been observed by Chicharo et al (Chicharo et al. 2006b) in Guadiana estuary. In this system, a short freshwater pulse increased phytoplanktonic diversity with consequent increase in zooplankton diversity. This higher grazing pressure acted as a positive feed back on phytoplankton diversity, preventing harmful algal blooms. At higher trophic levels,

influence of freshwater flow reduction has been described as a shift in habitat (Catalano et al. 2006) or even decline in some populations (Jassby et al. 1995), related to salinity changes, or changes in gravitational circulation (Kimmerer 2002a). Considering fish populations, decrease in the abundance of planktivorous and omnivorous species, caused by salinity changes, may have effects on algal blooms development, by preventing top-down control on those planktonic populations (Chicharo et al. 2006b).This diversity of responses to flow implies that ecosystem-specific quantitative models are needed as essential tools for the management of freshwater inflow to each estuary.

One of the most drastic man-induced alterations on river flow regime results from dam building, changing not only the quantity but also the timing and quality of freshwater delivered to estuaries (Hopkinson & Vallino 1995). River Douro has been heavily dammed for the last 50 years. Since 1985, the upper limit of the Douro estuary is separated from the river by a hydroelectric power dam that confined the estuary to the last 21.6 km of the river (Vieira & Bordalo 2000, Bordalo & Vieira 2005). Instead of a continuous flow of freshwater, there are pulse discharges, especially during summer months when, in a mater of minutes, flow can rise from 0 to >1,000 m^3s^{-1} (Bordalo, unpublished). The release of freshwater is controlled by commercial strategies rather than by environmental needs.

The Douro estuary is mostly heterotrophic, with exceptions of the upper stretch during spring (Azevedo et al. 2006). The lower estuary, heavily polluted by sewage discharge (Bordalo 1993, Bordalo & Vieira 2005), presents heterotrophic conditions all year round (Azevedo et al. 2006). On the other hand, benthic intertidal areas, including hard-surface substrates, are highly autotrophic and actively remove inorganic nutrients from the water column (Magalhaes et al. 2005). The lower estuary is contaminated by heavy metals (Zn, Cu, Pb, Cd and Cr) with effects on macrobenthic community structure, namely low diversity and presence of opportunistic species (Mucha et al. 2003, 2004, 2005). Furthermore, major endocrinologic disturbances were found in pelagic and benthic fish – mullet (*Mugil cephalus*) and flounder (*Platichthys flesus*), respectively indicating the presence of xeno-estrogenic pollution in the Douro estuary (Ferreira et al. 2004).

Over the last 15 years, an increase in nitrate concentration in the upstream reservoir has been reported (Magalhaes et al. 2005), leading to increased loads to the estuary, with potential consequences on estuarine productivity. The knowledge of ecosystem functioning is important to anticipate the result of different water management strategies for the Douro estuary. The achievement of a good ecological status, as required by the Water Framework Directive (WFD; EC, 2000), implies that the response of the system to

pressures or to improvement measures can be predicted. The use of a conceptual model, which allows knowledge organization through representation of the relationships between variables, may facilitate ecosystem functioning understanding, as well as management decision making (Alber 2002).

This study is part of a larger project, where one of the main objectives is to get quantitative understanding of Douro estuarine ecosystem functioning in order to be used for management purposes. Therefore, it is important to apprehend the time and spatial variability of several key descriptors, as well as the relationships forged between them. Accordingly, the main objective of this study is to establish quantitative relationships and trends, towards a better understanding of estuarine behaviour as a function of time and space by (i) analysing estuarine level properties, such as the estuary number, as a function of river flow; (ii) describing the Douro estuary, by means of chemical and biological properties such as temperature, salinity, nutrients, suspended matter, and chlorophyll concentrations, as well as rates, such as primary production and community respiration; (iii) designing a conceptual model of river flow influence on the Douro estuary biogeochemistry.

2. 2 Material and Methods

2.2.1 Study area

The Douro is an international river, giving birth to the largest watershed in the Iberian Peninsula (98,000 km^2). Flowing E-W, drains to the north-western shore of Portugal, near the city of Porto at 41.14ºN and 8.66ºW (Figure 2.1). All over its course, more than 50 large dams have been built for irrigation and electric power generation. The last dam, located at 21.6 Km from the mouth, constitutes the upstream limit of the Douro estuary, since its construction in 1985. The estuary has been divided in 3 stretches by (Vieira & Bordalo 2000), as a function of seawater intrusion, with average width and depth of respectively, 645 and 7.8 m for the upper estuary; 271 and 10 m for the middle estuary and 333 and 7 m for the lower estuary (Figure 2.1). The last 8 Km are heavily urbanized, with more than 700,000 inhabitants living in the vicinity of the estuary (Azevedo et al. 2006). Effluents of 8 wastewater treatment plants (WTP) drain into the estuary, without nutrient removal. The mouth is partially obstructed by a sand bar currently subjected to

hard stabilization works. Tides are semi-diurnal and average tidal range is 2.8 m at the mouth and 2.6 m at the head (Vieira & Bordalo 2000). Residence time ranges from 8 hours to more than two weeks, depending on river flow (Vieira & Bordalo 2000). These authors classified the Douro as a salt-wedge estuary.

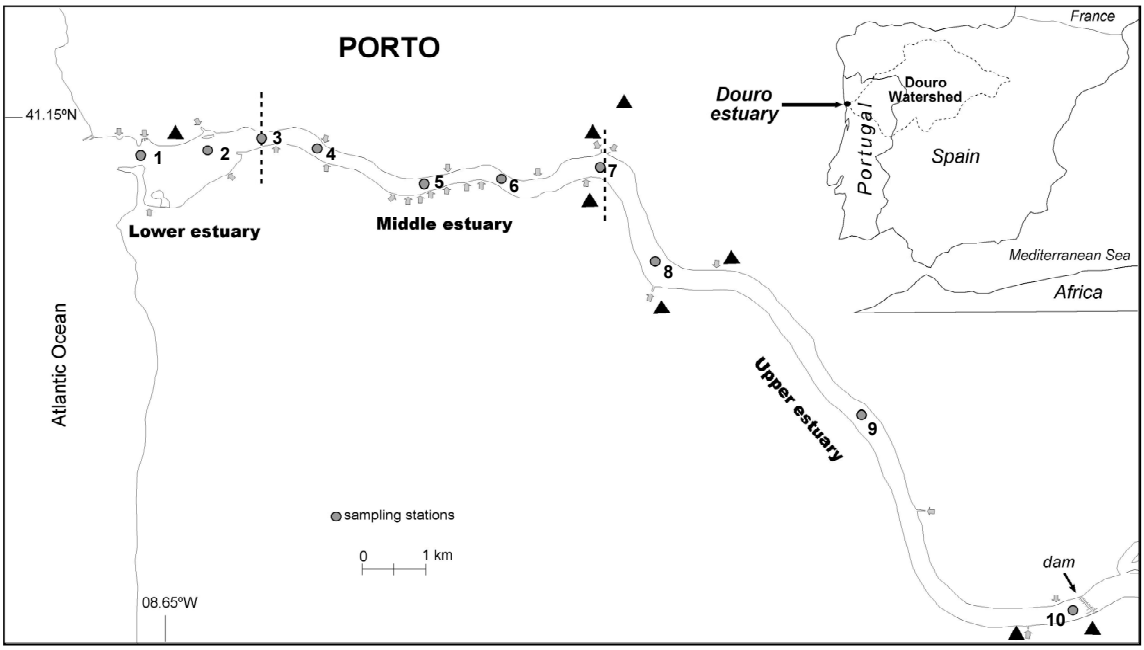

Figure 2.1. Location of sampling stations (●), wastewater treatment plants (▲) and small rivers (⇧) discharging into the estuary. Limits of estuarine stretches (upper, middle and lower) according to Vieira e Bordalo (2000). Samples for primary production analyses were collected at stations 1, 5 and 10.

2.2.2 Sampling

Data presented in this study were obtained under a contract with Oporto Water Authority, designed to evaluate the spatial and temporal water quality variability in the estuary. Sampling surveys were conducted twice a month, during ebb and flood spring tides, in order to sample the most extreme situations, namely concerning seawater intrusion.

Water column was sampled at 10 stations along the estuary (Figure 2.1) at 3 levels - surface, middle depth and near bottom, from December 2002 to December 2003. Sampling time varied between 1.5 and 2 hours, depending on flow conditions.

Vertical profiles of temperature, conductivity, salinity, dissolved oxygen (DO), pH and turbidity were performed with a CTD (YSI, 6600). Salinity was measured using the Practical Salinity Scale.

Water samples were collected with a Van Dorn bottle for chlorophyll *a*, nutrients (nitrate, nitrite, ammonium, phosphate and silicate), total particulate matter (TPM), particulate organic matter (POM), faecal coliform (FC) bacteria and community respiration (CR) analyses. Water samples were transported to the laboratory in refrigerated ice chests and processed within one hour from the collection of the last sample.

Samples for primary production (PP) measurements were collected at three stations, in the lower, middle and upper estuary, at approximately 0.7, 5.0 and 21.6 Km respectively, from the river mouth (stations 1, 5 and 10; Figure 2.1).

2.2.3 Analytical procedures

Chlorophyll *a* was assayed spectrophotometrically after extraction with 90% acetone (Parsons et al. 1984) with cell homogenization, using the SCOR-UNESCO (1966) trichromatic equation. Dissolved orthophosphate, nitrite, ammonium and silicate were analyzed following the methods described in Grasshoff et al. (1983). Nitrate was quantified by an adaptation of the spongy cadmium reduction technique (Jones 1984), subtracting nitrite from the total. All the analyses were performed in triplicate. For TPM and POM assessment, samples were filtered through glass fibre filters which were dried at 105 ºC (TPM) and then incinerated at 500 ºC (POM), according to APHA (1992).

PP was assayed by the ^{14}C method (Steeman Neilsen 1952). Samples were placed in 125-mL Pyrex glass flasks and 2 µCi of aqueous solution of sodium bicarbonate was added (Carbon 14 Centralen). Duplicate samples were incubated at 5 light levels (100%, 75%, 50%, 25%, 1%), to mimic light attenuation of different depths within the euphotic zone, for 1 – 2 hours in a water bath, at *in situ* temperature. An artificial light source providing a PAR of 920 $\mu Em^{-2}s^{-1}$ was used. A neutral screen was used to provide for the different light levels. One additional dark bottle was also incubated. After incubation, samples were filtered through 0.45 µm membranes; washed, placed in 20-ml scintillation vials and 10-ml scintillation cocktail (Beckman Instagel Packard) was added. Countings, in disintegrations per minute (DPM), were performed in a Beckman LS3801 liquid scintillation analyser using internal standards for the automatic establishment of the quenching curve. Dark DPM values were subtracted from light DPM values and results were expressed in mg C m^{-3} h^{-1}. Depth integrated PP was calculated according to Azevedo et al (2006).

Samples for faecal coliform (FC) bacteria assessment were filtered through sterile membrane filters, plated in FC-agar (Difco) and incubated at 44.5 ºC for 24 hours.

CR was estimated as the difference in dissolved oxygen at the beginning and after 24 hours incubation of samples in the dark at *in situ* temperature. Oxygen was measured by a modification of the Winkler method (Carpenter 1965). Oxygen values were converted into carbon units using a conversion factor of 0.375 (Uthicke & Klumpp 1998).

Table 2.1. Equations, parameters and references used in calculation estuarine wide indices tidal prism, freshwater residence time and estuary number.

Index	Equation	Parameters	Reference
Tidal prism	$Tp = V_{HT} - V_{LT}$	V_{HT} - volume at high tide	e.g. Dyer (1997)
		V_{LT} - volume at low tide	
Freshwater residence time	$Tr = Vf / Q$	Vf - freshwater volume	Dyer (1997)
	$Vf = f * V$	Q - inflow	
	$f = (S_0 - S) / S_0$	f - freshwater fraction	
		S_0 - ocean salinity	
		S - salinity at any part of the estuary	
Estuary number	$Ne = (P(Fm)^2)/(TR)$	P - tidal prism volume	Dyer (1997)
	$Fm = uf/ raizq(gh(\Delta\rho/\rho))$	Fm - densimetric Froude number	
	$uf = R/(AT)$	T - tidal period	
		R - river discharge	
		uf - crosssectional average of the vertically averaged mean velocity	
		g - acceleration due to gravity	
		h - estuary depth	
		$\Delta\rho$ – density difference between surface and bottom	
		ρ - vertically averaged mean density	

2.2.4 Data analysis

Data were analysed in order to emphasize estuarine functioning at the scale of the whole estuary and at smaller spatial scales, by resolving variability of several water quality

parameters longitudinally and vertically. Regarding the former analysis, a set of estuarine wide indices were calculated: tidal prism, freshwater residence time (using the freshwater fraction method) and estuary number (Table 2.1). Furthermore, mixing diagrams were used to evaluate whether properties behave conservatively or non-conservatively, using data from surveys conducted in spring, summer and fall. Winter was not analysed, since freshwater dominated in most parts of the estuary. Regarding the latter analysis, graphs depicting the relationship between several water properties and distance from river mouth were used, with annually averaged data for each station. Best fit regressions were performed in order to derive quantitative relationships between several variables.

In order to investigate potential nutrient limitation of phytoplankton growth, two different approaches were used: (i) observed nitrogen/phosphorus ratios were compared with Redfield ratios; (ii) phytoplankton nutrient uptake was compared with nitrogen and phosphorus loads. Uptake rates were estimated from PP values in carbon units, obtained for each estuarine stretch depicted in Figure 2.1, and converted to nitrogen or phosphorus units using the Redfield ratio. Nutrient loads were estimated from river flow and nutrient concentrations in the river, for the upper estuarine stretch. For the remaining stretches, river flow and nutrient concentration at the upstream compartment were used. Biomass/Primary production (B/P) ratio was calculated as an estimate of phytoplankton turnover time, in order to analyse the probability of blooms occurrence.

Salt wedge was defined as water with salinity equal or higher than 30, corresponding to euhaline water, according to the Venice classification system ([Anon] 1958, EC 2000).
River flow data were obtained from the Portuguese Water Institute (INAG).

2.3 Results

2.3.1 Estuarine level properties

The results of daily river flow, freshwater residence time and estuary number, calculated for each sampling period, are presented in Table 2.2, whereas averages, ranges and standard errors for selected variables obtained during this study are presented in Table 2.3.

Table 2.2. Freshwater residence time (Tr) and estuary number calculated for each sampling survey from December 2002 to December 2003. River flow values are daily averages of each survey. Ne values represented in bold type are lower than 0.1, indicative of stratified conditions.

Month	Tide	Daily river flow ($m^3 s^{-1}$)	Tr (days)	Ne
D	Flood	1067	0.58	0.73
J	Flood	1343	0.43	1.11
F	Flood	1110	0.58	1.73
M	Flood	884	0.66	0.52
A	Flood	829	0.74	0.74
M	Flood	631	0.68	0.18
J	Flood	244	1.02	**0.07**
J	Flood	231	1.33	**0.05**
A	Flood	46	2.97	**0.02**
S	Flood	306	0.93	0.13
O	Flood	297	1.09	0.10
N	Flood	840	0.69	0.37
D	Flood	1176	0.57	31.07
D	Ebb	448	0.83	0.33
J	Ebb	1353	0.32	149.40
F	Ebb	1104	0.40	30.93
M	Ebb	893	0.48	25.45
A	Ebb	803	0.52	9.30
M	Ebb	654	0.61	0.93
J	Ebb	328	0.86	0.11
J	Ebb	131	1.90	**0.04**
A	Ebb	11	13.81	**0.01**
S	Ebb	495	0.67	0.51
O	Ebb	498	0.75	0.67
N	Ebb	943	0.45	19.24
D	Ebb	772	0.55	13.73

Freshwater residence time was less than 1 day for river flows higher than 300 m^3s^{-1}. Lower river flow resulted in an exponential increase of residence time, reaching 13.8 days during the August ebb survey, when the average daily river flow was just 11.3 m^3s^{-1}. Variation along the estuary was assessed through calculation of the residence time in the upper, middle and lower stretches (Figure 2.1). Similar values were found for the lower and middle estuary and higher for the upper estuary, consistently with the respective volumes.

Table 2.3. Ranges, averages and standard errors for selected variables obtained in this study for the entire estuary. River flow range was derived from recorded values during each survey.

Parameter	Units	Range	Average±SE
Salinity		0 - 35	9±0.5
Temperature	ºC	7.2 - 25.4	15±0.2
Nitrate	µM	1.3 - 498.9	81.3±1.8
Nitrite	µM	0.0 - 3.1	0.7±0
Ammonium	µM	0.3 - 158.5	8.9±0.4
Phosphate	µM	0.2 - 6.8	1.5±0
Silica	µM	0.9 - 257.2	56.3±1.4
N:P ratio		4.3 - 838.6	69.7±1.9
TPM	mg L^{-1}	2.2 - 100.8	17.2±0.5
Chlorophyll *a*	mg m^{-3}	0.3 - 15.8	3.8±0.1
PP	mg C m^{-2} h^{-1}	0.3 - 158.9	28.1±4.1
CR	mg C m^{-2} h^{-1}	3.1 - 329.1	44.8±3.1
FC bacteria	cfu $100ml^{-1}$	45 - 366000	11328±1097
River flow	m^3 s^{-1}	0 - 2704	728±116

Estuary Number suggests that strong stratified conditions (Ne <0.1) occurred in June, during the flood, and in July and August, during the ebb and the flood. An exponential relationship was found between river flow and Ne (Figure 2.2), which indicates that water column stratification could be expected under river flow values lower than 300 m^3s^{-1}.

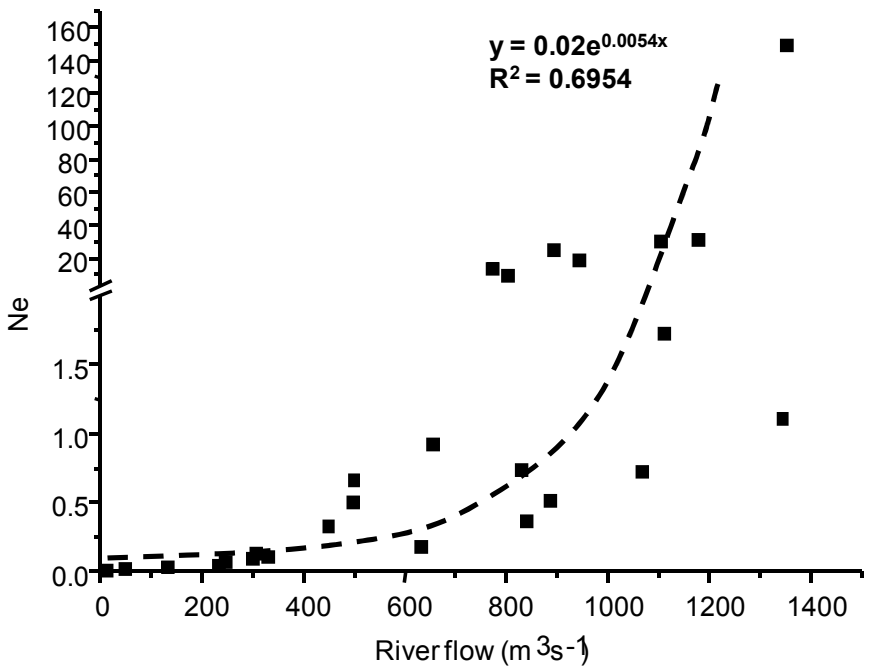

Figure 2.2. Estuary number (Ne) as a function of river flow. Ne values lower than 0.1 are indicative of stratified conditions.

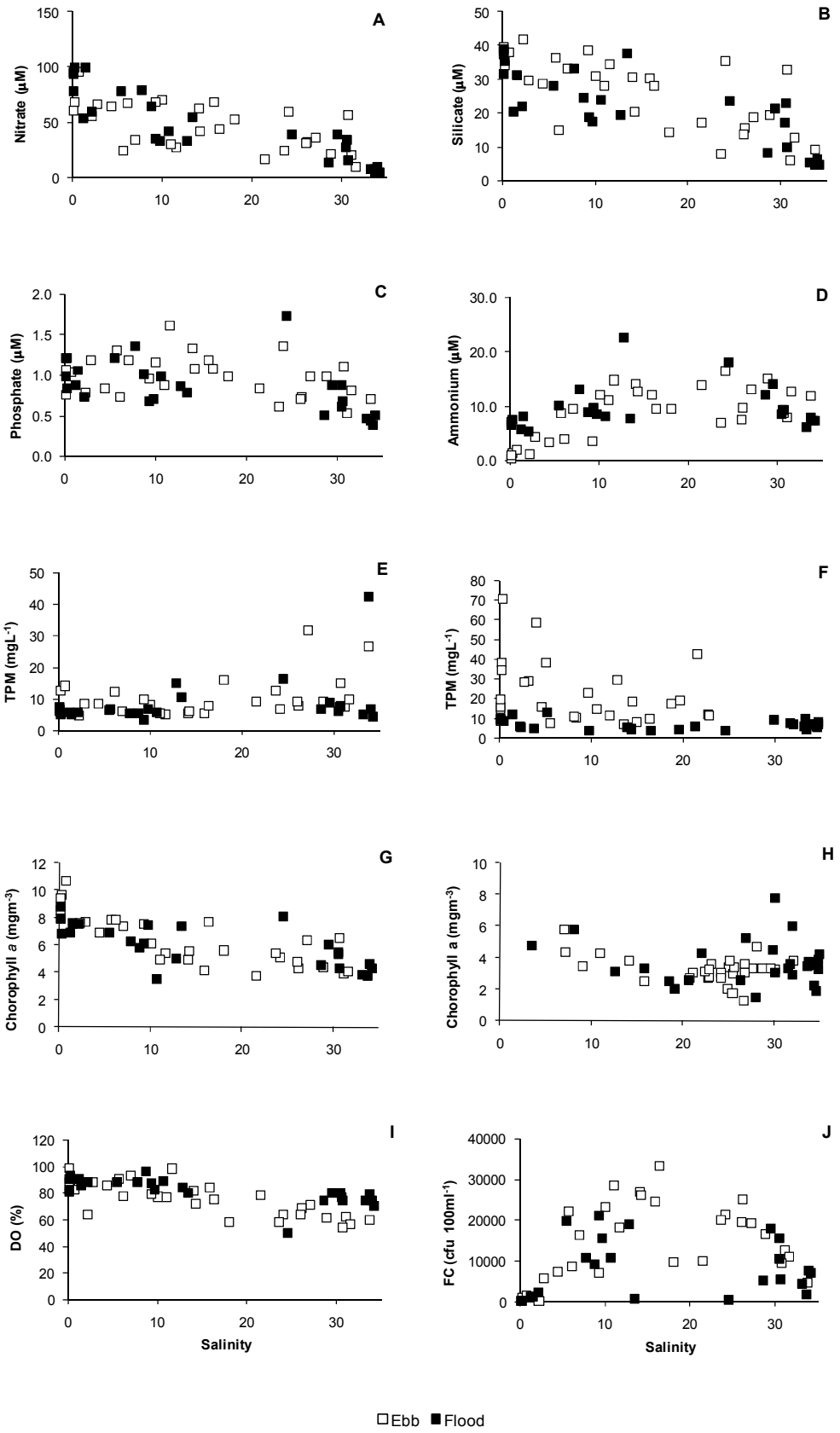

Figure 2.3. Relationships between nutrients, TPM, chlorophyll *a*, DO, FC bacteria, and salinity. Data shown were collected during July surveys and are representative of the observed patterns, except F and H (from September and August surveys, respectively), corresponding to deviations from those patterns (see text).

Mixing diagrams (Figure 2.3) displaying the relationship of nutrients, TPM, DO saturation, chlorophyll *a* and FC bacteria with salinity were analysed, in order to investigate potential sources or sinks along the estuary. Due to space limitation only July values are shown, except when deviations from "normal" behaviour observed over spring, summer and fall occurred, in the case of TPM and chlorophyll *a*. Nitrate and silicate presented consistently a conservative behaviour (Figure 2.3 A, B). Phosphate did not show a clear trend with salinity, indicating potential sources along the estuary (Figure 2.3 C). Ammonium behaviour was non-conservative, with increased values in intermediate salinity water (Figure 2.3 D). TPM also presented a non-conservative behaviour, with levels increasing in intermediate and high salinity water (Figure 2.3 E), with exception of the September ebb survey, when TPM decreased with salinity (Figure 2.3 F). Chlorophyll *a* concentration decreased with salinity, presenting a behaviour close to conservative (Figure 2.3 G), although at intermediate salinities this trend was less clear. Departure from this trend was observed during the August flood survey, when some high values were observed in water with salinity around 30 (Figure 2.3 H). DO saturation levels showed, consistently, a decreasing trend with salinity (Figure 2.3 I), except for the September flood survey, when the inverse was observed. Values are usually near the saturation level, except during August, when 40 to 60 % saturation was registered in c.a. 25 salinity water. FC bacteria behaviour was clearly non-conservative, with increased levels in intermediate salinity water (Figure 2.3 J).

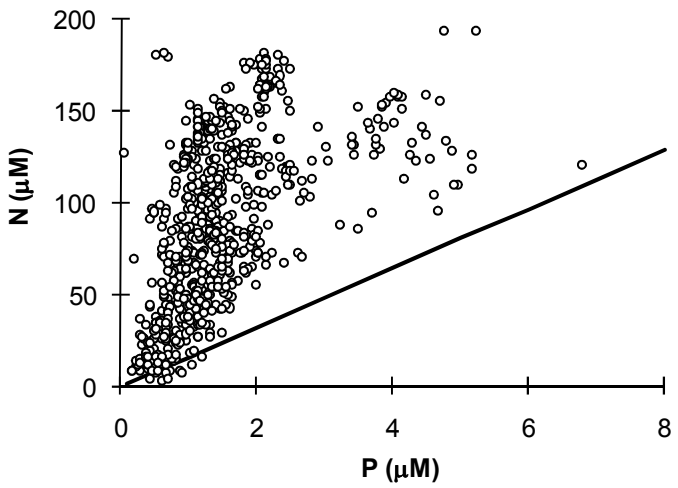

Figure 2.4. N:P obtained for all samples collected. The line indicates the Redfield ratio.

N:P ratio was generally above the Redfield ratio of 16:1 (Figure 2.4), suggesting an excess of nitrogen availability in the estuary and a potential limiting role for phosphate. Results obtained by comparing phytoplankton nutrient uptake with nutrient loads suggest

that the latter is between one and five orders of magnitude higher than the former, with the exception of the August ebb survey, at the upper estuary, when limitation by phosphate may occur – phosphorus uptake was estimated as 75 kg P day^{-1}, whereas loads were c.a. 26 kg P day^{-1}.

Considering the entire estuary, phytoplankton turnover time, estimated by B/P ratio, was always higher than residence time, except for the August ebb survey. River flow recorded during this survey was the lowest of the study period, increasing residence time above B/P ratio values.

2.3.2 Temporal and spatial trends

River flow presented a seasonal pattern, with higher values in winter and lower in summer. During this study, maximum river flow was recorded in January (2,704 m^3s^{-1}) and minimum in August (0 m^3s^{-1}) sampling surveys.

Seasonal variability of TPM, nutrients, DO saturation, chlorophyll *a* concentration, PP, CR and FC bacteria, is presented in Figure 2.5. TPM values were highest in January coinciding with the highest river flow, but no clear seasonal trend was observed. Nutrients, except ammonium, presented a clear seasonal trend with lower values in spring and summer. Ammonium highest levels were found in August, when FC also peaked, although the high standard error indicates a large variability between samples (spatial variability). Chlorophyll *a* concentration and PP showed a similar pattern, with highest values in late spring to early summer, as expected. However, a more modest peak was found for chlorophyll *a* in early fall. In what CR is concerned, the highest values were found during the warmer summer months.

As stated above, Ne was calculated for the estuary as a whole. If the estuarine water column structure is considered with further detail and a spatial analysis is performed, differences arise along the estuary, concerning water column haline stratification. For example, under river flow values of 500 m^3 s^{-1}, during the flood, stratification occurred from the mouth to about middle estuary (Figure 2.6). Also, the salt wedge position, during flood surveys, reached 8 km upstream when river flow was below 300 m^3 s^{-1} (Figure 2.7), flow corresponding to a Ne<0.1 (*c.f.* Section 2.3.1).

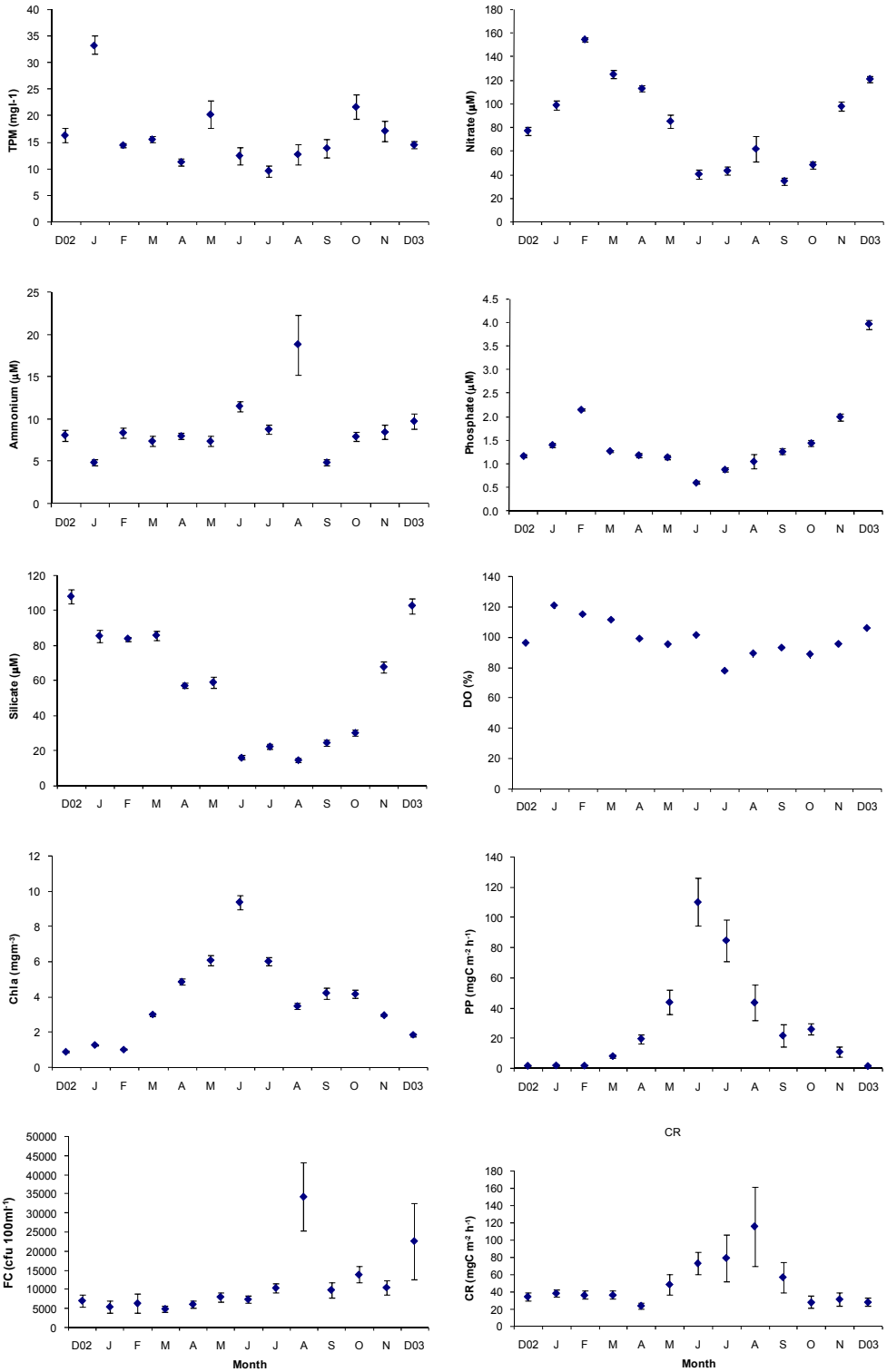

Figure 2.5. Seasonal variability of TPM, nutrients, chlorophyll *a*, PP, FC bacteria and CR. Each value corresponds to monthly averages±SE, integrating data from all sampling stations.

The variability of mean annual values (one value per sampling station) of TPM, nutrients, DO saturation, chlorophyll *a*, PP, FC bacteria and CR along the estuary is presented in Figure 2.8. In what nutrients are concerned, a decreasing trend downstream, during the

flood, was observed for nitrate and silicate, especially from middle to the lower estuary where coastal water influence was more evident. During the ebb, this pattern was not so evident although higher values were found upstream. These observations, together with the previously described increasing levels towards low salinity waters, suggest that the reservoir was the main source for nitrate and silicate to the estuary. On the other hand, phosphate peaked at c.a. middle estuary.

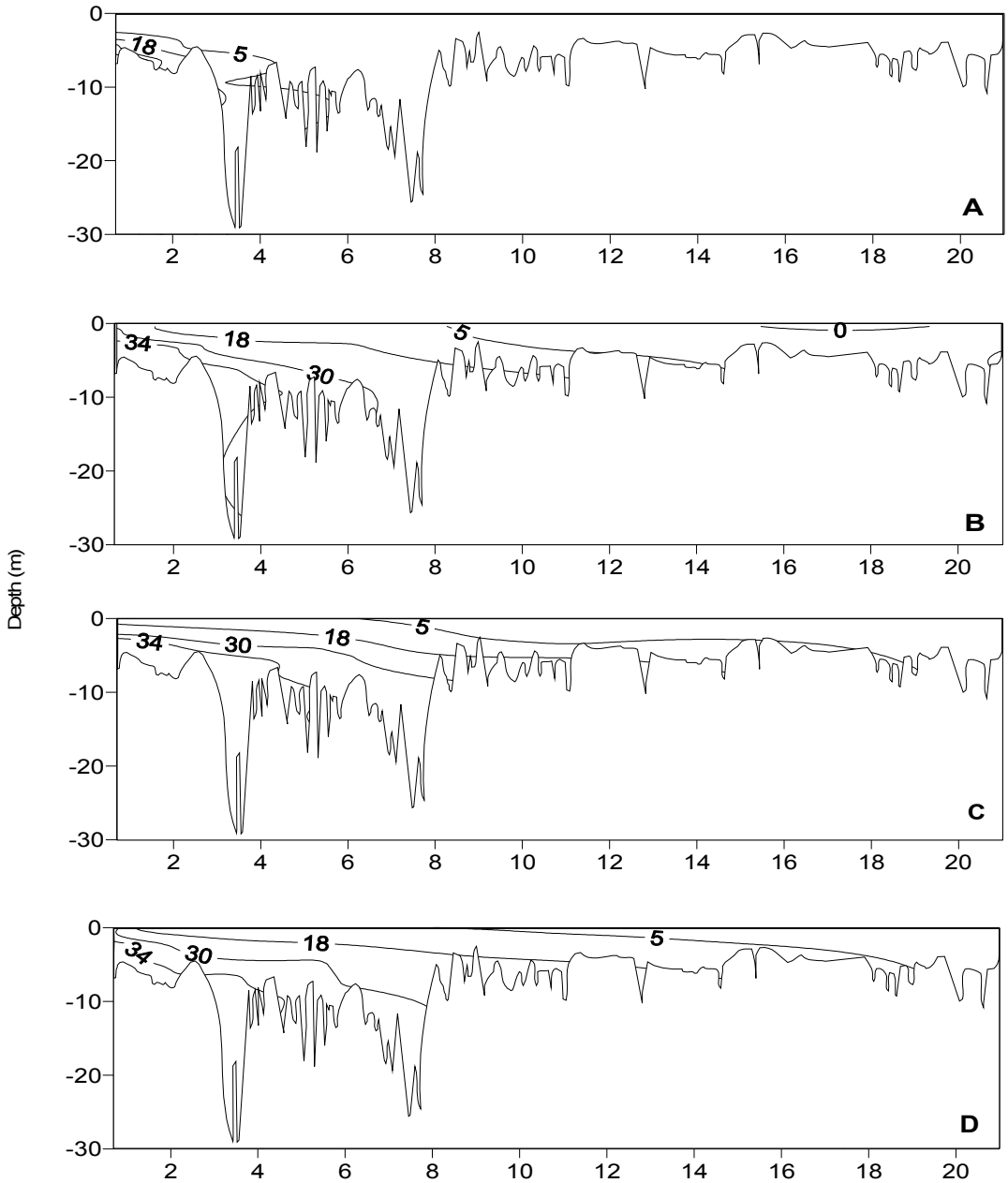

Figure. 2.6. Water column salinity structure, observed during flood sampling surveys, under different river flow magnitude. A – 875 m^3 s^{-1} (March); B – 500 m^3 s^{-1} (October); C - 292 m^3 s^{-1} (July); D - 36 m^3 s^{-1} (June).

Chlorophyll *a* values decreased downstream during the flood. During the ebb, there was an increase at c.a. middle estuary coinciding with the phosphate peak. PP decreased

downstream independently of the tide. During periods of salinity stratification, chlorophyll *a* concentration was lower in high salinity water, except during the August flood survey, when a maximum was found in bottom, high salinity water, close to the salt wedge, at around 10 Km from the mouth. Regarding ammonium and TPM, an increasing trend downstream was observed. A similar trend was observed for FC bacteria and CR levels, suggesting an allochthonous organic matter input at the lower estuary.

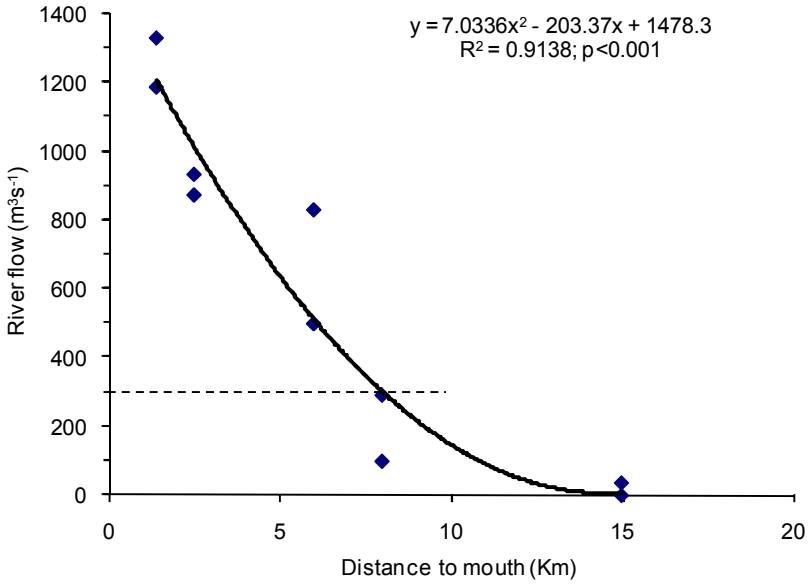

Figure 2.7. Salt wedge position (water with salinity equal or higher than 30) as a function of river flow. Dashed line indicates distance from the mouth of the salt wedge under a river flow of 300 $m^3 s^{-1}$ (*cf* - Section 2.3.2).

2.4 Discussion

Implementation of management and protection measures depend on the knowledge of ecosystem functioning and its response to pressures. There has been a growing need to organize data underlying that knowledge into ecosystem classification systems, in order to assist managers and policy makers, namely in the delimitation of management units and legislation implementation (Elliott & McLusky 2002). Data concerning morphology, salinity and circulation are necessary for the definition of a typology according to the European Water Framework Directive (EC 2000). This typology will serve as a basis for the establishment of type-specific reference conditions, which in turn will be used as a framework for the classification of the different water bodies concerning their ecological status.

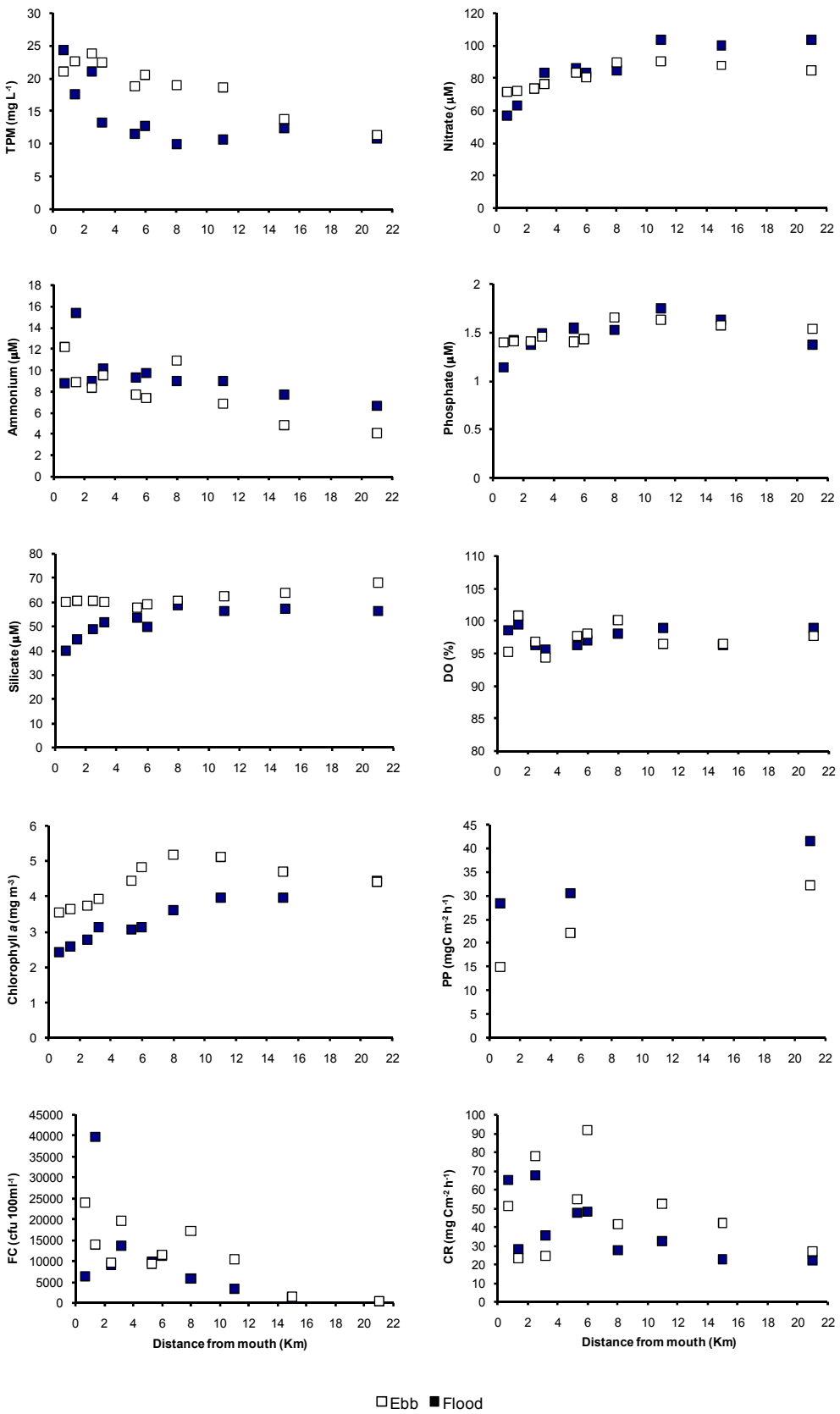

Figure 2.8. Spatial variability of TPM, nutrients, chlorophyll *a*, primary production, CR and FC bacteria. Each value corresponds to time-averaged data collected at each sampling station, integrating the entire sampling period.

The classification of the Douro estuary according to its salinity structure depends essentially on river flow variability, which has a clear seasonal pattern (Bordalo & Vieira 2005, Azevedo et al. 2006). The estuarine stratification index obtained, classifies the Douro estuary as stratified when river flow is lower than 300 m^3s^{-1}. Nevertheless, if spatial variability is considered, vertical stratification occurs in the lower to middle estuarine stretches when river flow is lower than 500 m^3s^{-1} (Figure 2.6). In previous studies, conducted during the ebb, a salt wedge was observed for river flow < 800 m^3s^{-1}; above this value, the estuary was entirely freshwater (Vieira & Bordalo 2000). These authors classified the Douro as a salt wedge estuary - an estuary in which a wedge of salt water is established under low river flows (Ibanez et al. 1997). Salt wedge estuaries are usually associated with microtidal systems, since macrotidal conditions normally lead to mixing by tidal forcing. However, stratification in the Douro estuary, a mesotidal system, is explained by the dominant standing wave behaviour of the tide, with the result that longitudinal energy transport is low, preventing water column mixing. This phenomenon is caused by the presence of the dam wall at the head, reflecting the tidal wave. The estuary acts as a quarter wave resonator, with the node of the standing wave located at the mouth and only its final portion fitting inside the estuary (Vieira & Bordalo 2000).

Mixing diagrams (Figure 2.3) show that the river Douro was the main source of nitrate and silicate to the estuary, whereas in the case of phosphate and, especially, ammonium, additional sources should be considered. Ammonium highest values were recorded in August and coincided, spatially, with increased FC bacteria and CR. Increased levels of these three major environmental variables in the middle and lower stretches, the most urbanized areas, are probably due to wastewater discharges through tributaries.

In what phytoplankton is concerned, results indicate that its main origin is the river. Chlorophyll *a* concentration tended to decrease with salinity, although the behaviour was not entirely conservative, since chlorophyll *a* accretion was seasonally found in the middle estuary, during the ebb, suggesting that some biomass accumulation may have occurred during spring and summer low river flow period. A similar behaviour was previously described in the Douro estuary (Bordalo & Vieira 2005).

River discharge may act as a positive feedback on estuarine primary production, through nutrient and phytoplankton biomass inputs, and as a negative feedback by decreasing residence time and increasing turbidity. The negative exponential relationship between river flow and chlorophyll *a* (R^2=0.37; $p<0.005$), as well as with PP (Figure 2.9A) observed in the present study reflects, basically, this negative effect. Increased light availability and

residence time, as well as higher temperature, during late spring early summer, were responsible for higher chlorophyll *a* and PP levels, obtained during this period.

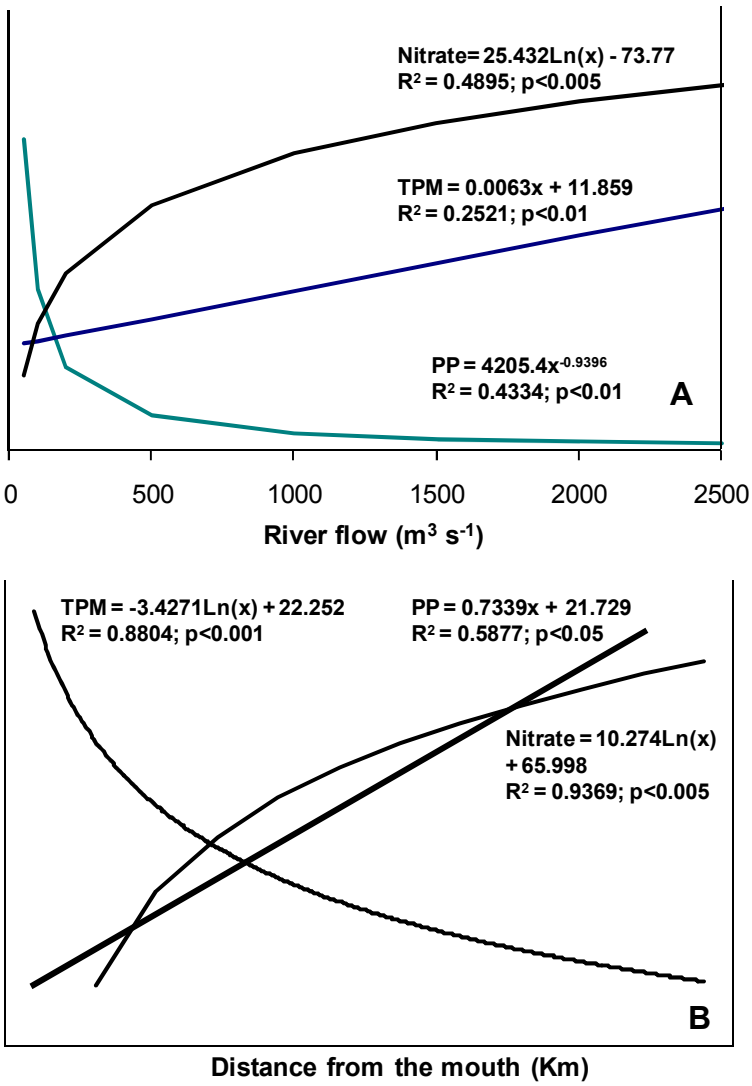

Figure 2.9. Variability of TPM, nitrate and PP with river discharge (A) and with distance from the mouth (B), observed during this study. A - Quantitative relationships were derived using averaged values integrating all stations for each sampling survey; B - Quantitative relationships were derived using time and tide-averaged values for each sampling station.

TPM dynamics in estuaries depend on sediment transport from rivers and on locally derived suspended sediments, associated with a turbidity maximum or estuarine bed sediment resuspension (Uncles & Smith 2005). TPM relationship with salinity may also be influenced by wind or spate events (Uncles et al. 2000). In the Douro estuary no clear relationship with salinity was observed, and longitudinal distribution showed a decreasing trend upstream. Possible explanations for this situation may be sediment retention by the dam upstream, which causes a low TPM concentration in this estuary, and the above

mentioned sewage disposal in the middle and lower estuary, associated with higher ressuspension rates due to larger current velocities (Azevedo et al. 2006).

Considering water quality status, nitrate levels were high, compared to other Portuguese estuaries such as the Tagus (Gameiro et al. 2004), where annual averages ranged 12-40.9 μM, or the Guadiana (Rocha et al. 2002), in the 0.56 - 110 μM range, but within values reported for other temperate eutrophic estuaries (Goosen et al. 1999). Nevertheless, nitrate values were well below the 50 mg L^{-1} (806 μM) threshold established by the nitrates directive 75/440/EEC (EEC 1975). Phytoplankton biomass concentration, on the other hand, was lower in the Douro, comparing to a 5.4 mg m^{-3} annual average in Tagus (Gameiro et al. 2004) and a 0.93 – 35.6 mg m^{-3} range in Guadiana (Rocha et al. 2002), probably related to a lower residence time. Only when river flow is drastically reduced, usually during spring and early-summer, and when temperature and light availability increase, phytoplankton blooms of fluvial origin may occur. Moreover, the traditional late summer cyanobacterial bloom was noticed (Figure 2.5), although very modest when compared to previous years (Bordalo, unpublished data). Bacterial contamination was several times higher than the maximum determined in European legislation for bathing waters (EEC 1976), especially in the lower to middle estuary, where urbanization is more intense, which is in accordance to earlier reports (Bordalo 1993, Bordalo & Vieira 2005). The contamination increase was particularly dramatic during the low flow summer months, which was accompanied by the increased of CR levels in the same estuarine stretches.

The above-discussed results are tentatively synthesized in Figure 2.9. Equations presented are a mere attempt to demonstrate statistical relationships between some of the studied variables, without the assumption of direct causal-effect mechanisms. One of the ideas beyond this analysis is to get some insight into Douro estuary dynamics, to assist on the validation of an ecological model presently under development, by comparing longitudinal gradients predicted by the model and its responses to changing river flows with patterns observed in the present study. Relationships between nitrate, TPM, PP and river flow are depicted in Figure 2.9A. Temporal dynamics arise from this analysis: higher PP occurred during the warmer months, under low river flow and when TPM and turbidity were also lower. Longitudinal behaviour of these 3 major environmental descriptors is presented in Figure 2.9B. While TPM decreased exponentially with distance from mouth, nitrate and PP showed increasing logarithmic and linear trends, respectively. Both higher nutrient levels and lower TPM (with concomitant higher water column light availability) act as positive feedbacks, leading to higher PP upstream. Increasing trends in

nitrate (Magalhaes et al. 2005), as well as in phosphate (Bordalo et al, unpublished data), have been observed in the upstream reservoir, over the last 15 years. However, this was not translated into larger phytoplankton blooms (Bordalo, unpublished data). On the other hand, *Ulva sp* and *Enteromorpha spp* late-spring and summer blooms are recurrent in the intertidal areas of the lower estuary, reaching a wet biomass of 3 kg m^{-2} (Bordalo, unpublished data). In systems where nutrient levels are high and phytoplankton growth is limited by factors such as water residence times and/or light availability, which probably occurs in Douro estuary, growth of other primary producers, such as macroalgae may be favoured (Valiela et al. 1997, Painting et al. 2007).

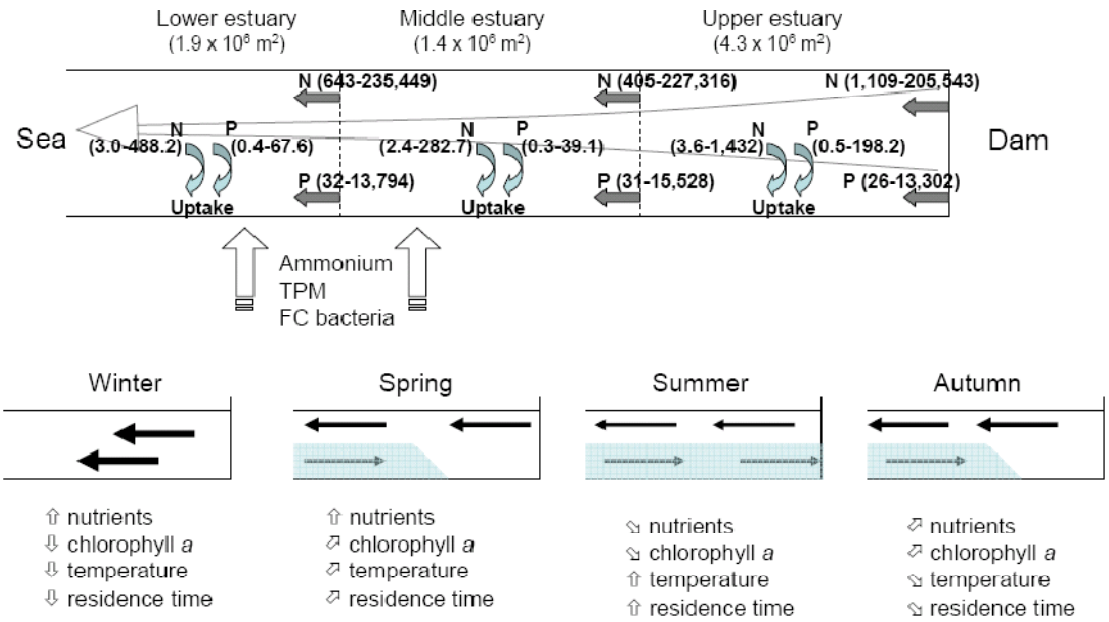

Figure 2.10. Conceptual model of the Douro estuarine biogeochemistry. Nutrient loads and uptake by phytoplankton at each stretch, calculated from data obtained during the present study, are represented in the upper part of the diagram. Dark horizontal arrows correspond to loads whereas curved vertical arrows correspond to uptake. Values are in Kg day $^{-1}$. Key environmental characteristics seasonal variability is presented in the lower part of the diagram. Shaded areas indicate seawater intrusion. Horizontal arrows width is proportional to river flow magnitude. ⬀ - increase; ⇧ - high; ⬊ - decrease; ⇩ - low.

Results discussed above were summarized in the form of a conceptual model of the Douro estuarine biogeochemistry (Figure 2.10). The river is the major source of nutrients, chlorophyll *a* and TPM, although additional nutrient and TPM anthropogenic sources are present in the middle and lower estuary. Water column salinity structure is dependent on river flow magnitude, which presents high seasonal variability. Flows above 800 m^3s^{-1} prevent seawater from entering the estuary, whereas, for flows below 300 m^3s^{-1}, the estuary is stratified (Ne<0.1). During spring, when flow decreases and light availability and

temperature increase, phytoplankton biomass and primary production reach their maxima within the estuary. In summer, when river flow is the lowest, and temperature and water transparency are the highest (as well as salinity), chlorophyll *a* and PP decline. This may be partly explained by the lower phytoplankton input and the inability of freshwater phytoplankton to thrive in polyhaline to seawater that dominates the estuary during this period. Nutrient limitation, mostly by phosphate, is another possible explanation for lower summer PP. This may be one of the reasons why phytoplankton blooms have not been observed frequently in this system: during the low river flow period, when residence time is higher than phytoplankton turnover time, nutrient limitation occurs.

2.5 Conclusions

Management problems of the Douro estuary are mostly related to nitrate inputs from upstream and high ammonium and bacterial levels caused by discharge of untreated wastewater within the lower and middle estuarine stretches.

Considering those nutrient loads and its seasonality it is predictable that PP may increase in the estuary over time. Although relatively low residence times in spring may prevent the built up of phytoplankton biomass, it seems advisable to extend monitoring to benthic algae dynamics in order to follow estuarine response to the mentioned increase in nutrient inputs from river Douro.

The quantitative relationships derived between key variables, although representative of spring tides only, provide a first approach towards the understanding of Douro estuary functioning. Together with raw field data, they will serve as a basis to assist in the calibration and validation of an ecosystem model under implementation.

CHAPTER 3

Pelagic metabolism of the Douro estuary (Portugal) – factors controlling primary production

3.1 Introduction

The metabolic balance of a given system depends upon its primary production and community respiration. Primary production is dependent on physical (light availability, temperature), chemical (nutrients) and biological factors, like phytoplankton biomass, species composition, size structure and grazing (Stearns et al. 1987, Cloern 1991, Landry et al. 1995, Gallegos & Jordan 1997, Calbet & Landry 2004, Cermeno et al. 2006), as well as viral control (Proctor & Fuhrman 1991).

In estuaries, these factors may be influenced by freshwater inflow, since it carries nutrients, phytoplankton and suspended matter, which determines light availability in the water column. River flow magnitude also controls residence time and, hence, the susceptibility of ecosystems to algal blooms, with effects propagating throughout the food web to higher trophic levels (Kimmerer 2002a). Seasonal shifts from auto- to heterotrophy according to river flow variations have also been reported. For example, heterotrophy occurs during monsoon periods in tropical estuaries, when increased allochthonous organic input leads to enhanced respiration (Ram et al. 2003).

Phytoplankton dynamics may also be influenced by tides. Episodes of biomass increase during neap tides and decline during spring tides have been reported (Cloern 1991), as well as differences between ebb and flood tide phytoplankton biomass (Roegner 1998). Aubry and Acri (2004) found higher phytoplankton abundance at flood than at ebb for most of the year in the Lagoon of Venice, due to the presence of neritic species. Tidal turbulence can also influence vertical distribution of different phytoplankton species, e.g., slack water periods enhance aggregation of dinoflagelates while diatoms rely on periods of turbulence to ensure entrainment into the upper water column and to prevent sinking from the photic zone (Lauria et al. 1999).

Another important factor affecting estuarine metabolism is human pressure, for example, through the construction of dams since they alter the timing and quantity of freshwater, sediment, inorganic and organic matter delivered to estuaries and adjacent coastal zones (Hopkinson & Vallino 1995). The discharge of treated or untreated wastewater into estuaries also affects metabolism by increasing allochthonous nutrient or organic matter inputs, respectively. The former may increase production and the latter bacterial respiration. If bacterial respiration exceeds net primary production due to utilization of external sources of organic matter, heterotrophy dominates (delGiorgio et al. 1997).

Thus, in estuaries, a transient environment, the understanding of the trophic status is crucial in order to evaluate the role of such systems as a potential source of autochthonous organic matter for the coastal environmental. The autotrophic-heterotrophic nature of an estuary is determined by three primary factors: the ratio of inorganic to organic matter inputs, water residence time and the overall degradability of allochthonous organic matter inputs (Hopkinson & Vallino 1995). Data on metabolic balance of European estuaries is scarce, namely due to a lack of studies concerning pelagic depth-integrated community respiration (Gazeau et al. 2004).

The river Douro originates from the largest watershed in the Iberian Peninsula. Its 98,000 Km^2 are unequally shared between Portugal (20%) and Spain (80%). Over 50 large dams have been constructed especially in the last 50 years for irrigation and electric power generation purposes, resulting in flow regulation.

The Douro estuary is limited upstream by the last dam, located 21.6 Km from the mouth. This dam determines the freshwater flow into the estuary, ranging from 0 to 13,000 m^3 s^{-1} (Vieira & Bordalo 2000) with an average of 501 m^3 s^{-1}. River flows present a large inter-

annual variability, with considerable differences between wet and dry years. A decrease of annual flow has been reported, due to climate phenomena (Trigo et al. 2004) but also to an increase of water storage for hydroelectric power generation, agriculture and domestic consumption (Bordalo & Vieira 2005). The fact that freshwater flowing into the estuary originates in a reservoir, a semi-lotic ecosystem, may also influence estuarine metabolism, due to specific phytoplankton characteristics. Moreover, in the case of the Douro, the last dam is the main source of phytoplankton biomass (Bordalo & Vieira 2005).

The objective of this work is to analyse estuarine environmental conditions and photosynthetic parameters in relation to its metabolism, in order to answer the following questions:

- Is the Douro estuary auto- or heterotrophic?
- Which factors control primary production (PP) on a spatial and temporal basis?
- Are there significant differences in estuarine PP and metabolism between ebb and flood tides?

3.2 Material and Methods

3.2.1 Study area

The Douro is a granitic drowned valley river, draining to the north western shore of Portugal. Its estuary is mesotidal, characterized by semidiurnal tides and a mean tidal range of 2.8 m. During the flood and under low river flow, sea water creates a salt wedge that eventually reaches the head of the estuary (at 21.6 Km from the mouth), where the tidal excursion is halted by the Crestuma dam (Figure 3.1), and remains within the estuary during the next ebb. In this situation, residence time can reach 14 days, whereas during high discharge events, the estuary is flushed completely during one tidal cycle and seawater intrusion is prevented during the flood (Vieira & Bordalo 2000).

The last 8 Km stretch of the river is heavily modified and over 700,000 inhabitants live within the estuarine area. A total of eight wastewater treatment plants (WTP) drain into the estuary, without nutrient removal.

3.2.2 Sampling

Data presented in this study were obtained within a larger sampling program under a contract with Oporto Water Authority, designed to evaluate the influence of WTPs on estuarine water quality. Sampling surveys were conducted monthly, during ebb and flood spring tides, in order to sample the most extreme situations, namely concerning seawater intrusion.

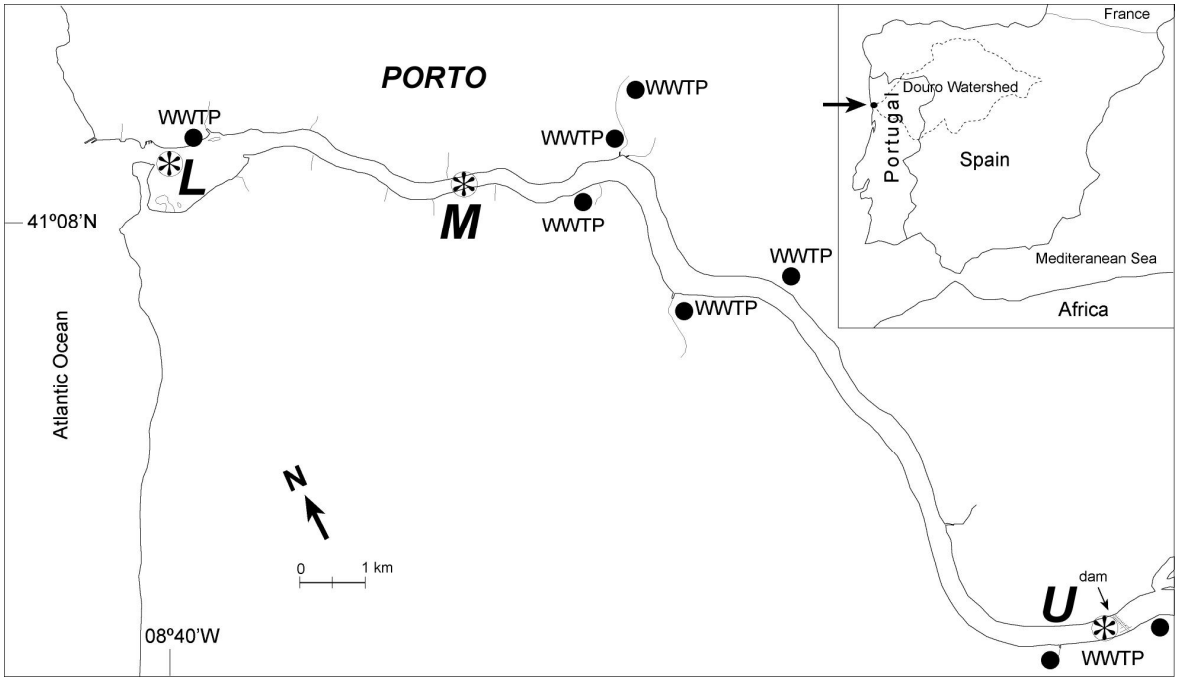

Figure 3.1. The river Douro estuary and location of sampling stations (L – lower, M – middle and U – upper estuary, WTP – Wastewater Treatment Plant).

From December 2002 to December 2003, three stations were visited, in the lower, middle and upper estuary, at approximately 0.7, 5.0 and 21.6 Km respectively, from river mouth (Figure 3.1). The boundaries of these 3 estuarine stretches have been defined based on the seasonal salt water intrusion (Vieira & Bordalo 2000). Each survey lasted between 90 and 120 minutes according to flow conditions.

Vertical profiles of temperature, conductivity, salinity, dissolved oxygen, pH and turbidity were performed with a CTD (YSI, 6600). Salinity was measured using the Practical Salinity Scale. Photosynthetic active radiation (PAR) profiles were obtained with a spherical quantum sensor light meter, at 0.5 m depth steps (LI-COR, LI-250).

Simultaneously, samples were collected at three depths (surface, middle and near bottom) with a Van Dorn bottle for chlorophyll *a*, nutrients (nitrate, nitrite, ammonium, phosphate and silicate), total particulate matter (TPM) and particulate organic matter (POM) assessments.

Mean water depth during sampling is presented in Table 3.1. During the surveyed period, tidal height ranged between 0.13 and 1.29 m, at ebb surveys, whereas at flood surveys, was within the 2.65 - 3.52 m range.

For PP assessments, subsurface samples were used, after testing their adequacy to depth integrated PP assessments in the present estuarine system (*c. f.* – Section 3.2.3 Experimental and analytical procedures). Community respiration (CR) was initially estimated from samples collected at 3 depths and from surface samples only, after confirmation that no significant ($p>0.05$) differences were found with depth.

Water samples were kept refrigerated in ice chests and processed in the laboratory within 1 hour from collection of the last sample.

3.2.3 Experimental and analytical procedures

PP was assayed by the ^{14}C method (Steeman Neilsen 1952), following the standard ICES (1996) recommendations. Briefly, water samples were placed in 125-ml Pyrex glass flasks and 2 μCi of aqueous solution of sodium bicarbonate was added (Carbon 14 Centralen). Duplicate samples were incubated for 1 – 2 hours in a water bath, at 5 light levels (100%, 75%, 50%, 25%, 1%), to mimic light attenuation of different depths within the euphotic zone, at *in situ* temperature. An artificial light source providing a PAR of 920 $\mu Em^{-2}s^{-1}$ was used. Attenuation was achieved by means of a neutral screen. One additional dark bottle was also incubated. After incubation, samples were filtered through 0.45 μm membranes, washed, placed in 20-ml scintillation vials and 10-ml scintillation cocktail (Beckman Instagel Packard) was added. Countings, in disintegrations per minute (DPM), were performed in a Beckman LS3801 liquid scintillation analyser using internal standards for the automatic establishment of the quenching curve. Dark DPM values were subtracted from light DPM values and results were expressed in mg C m^{-3} h^{-1}.

In order to validate the sampling strategy for PP assessments, simultaneous incubations, at 5 light intensity levels, of surface samples and samples collected at depths

correspondant to those light levels, were performed. These experiments yielded similar results, thus only surface water samples were used for PP measurements.

Inorganic Carbon was assayed from pH and alkalinity measurements by direct titration according to Parsons et al.(1984).

CR was estimated as the difference in dissolved oxygen at the beginning and after 24 hours incubation of samples in the dark at *in situ* temperature. Oxygen was assayed by a modification of the Winkler method (Carpenter 1965). Oxygen values were converted into carbon units using a conversion factor of 0.375 (Uthicke & Klumpp 1998).

Chlorophyll *a* was assayed spectrophotometrically after extraction with 90% acetone (Parsons et al. 1984) with cell homogenisation, using the SCOR/UNESCO (1966) trichromatic equation. Dissolved orthophosphate, nitrite, ammonium and silicate were analysed following the methods described in Grasshoff et al.(1983). Nitrate was quantified by an adaptation of the spongy cadmium reduction technique (Jones 1984), subtracting nitrite value from the total. All analyses were performed in triplicate. Samples were filtered through glass fibre filters which were dried at 105 ºC for TPM assessment and then incinerated at 500 ºC for POM assessment (APHA et al. 1992).

3.2.4 Data analysis

Bi-dimensional plots, generated by “Surfer” software, were used to represent variation with depth of measured variables along the sampling period. Data were interpolated using the “kriging” gridding method.

In order to perform statistical and multivariate analysis, data were depth averaged.

3.2.4.1 PP calculations

Steele’s production-light function (P/E) (Eq. 1) (Steele 1962) was fitted to experimental data from incubation experiments, using the Gauss-Newton non-linear regression method with Statistica software (StatSoft 2001), since photoinibition was apparent. The photosynthetic parameters obtained, maximum production rate (P_{max}) and optimal light intensity (E_{opt}), were used to fit Eq. 1. The normalisation to chlorophyll *a* was made using the values obtained for each sample analysed. Depth-integrated primary production ($\overline{P}$) was then calculated by integrating Steele equation over depth (Eq. 2).

$$P = P_{max}\left[\frac{E}{E_{opt}}\exp\left(1-\frac{E}{E_{opt}}\right)\right]^{n} \qquad \text{(Eq. 1)}$$

n=1 (n empirical integer)

$$\bar{P} = P_{max}\frac{\exp(1)}{k*z}\left[\exp\left(-\frac{E_0\exp(-kz)}{E_{opt}}\right)-\exp\left(-\frac{E_0}{E_{opt}}\right)\right] \qquad \text{(Eq. 2)}$$

where,

P_{max} – maximum production rate (mg C mg $Chla^{-1}$ h^{-1})

E_0 - surface light intensity (μE m^{-2} s^{-1})

k - light extinction coefficient (m^{-1});

z – depth (m)

Light extinction coefficients (k) were estimated from the vertical profiles of PAR measured during each sampling survey, using the Lambert-Beer equation (Eq. 3).

$$E = E_0\exp(-kz) \qquad \text{(Eq. 3)}$$

Time integrated PP estimates were obtained as follows:

(i) Hourly E_o values were estimated by means of a model implemented with Stella software using standard formulations described in Brock (1981) and Portela & Neves (1994) for periods of 24 hours and adjusted to values measured during the sampling surveys. This adjustment was made by changing cloud cover values, to make sure that predicted light intensities at the hours when sampling took place were similar to those measured.

(ii) From these surface light intensity estimates, the k values measured during the surveys and the P/E curves obtained in the incubation experiments, daily and depth-integrated PP was estimated separately for ebb and flood surveys. In these estimates, vertically averaged chlorophyll values (measured at three depths, cf. – Section 3.2.2 Sampling) were considered.

Compensation depth (z_c) - the depth at which CR equals PP (net production equal to zero) - was calculated solving equation 4 by the Lambertw function ($w.e^w=x$) using the Matlab 6.5 software.

$$P_{max}\frac{E_0\exp(-kz_c)}{E_{opt}}\exp\left(1-\frac{E_0\exp(-kz_c)}{E_{opt}}\right)-CR=0 \qquad \text{(Eq. 4)}$$

where,
CR – community respiration (mgL^{-1})

Initial slope was estimated by deriving the Steele' function in relation to E and calculating the limit of the derivative when E approaches zero.

3.2.4.2 Statistical and Multivariate Analyses

Spearman rank correlation analysis was performed to evaluate relations between environmental and biological variables and metabolic processes. Regression analysis was also carried out between some specific variables.

MANOVA was used to investigate differences between results obtained at different times, tides and stations. To analyse the factors "time" and "tides" a Two-way factorial MANOVA was carried out, using as surrogates for replicates the values measured at the three sampling stations at each month and each tide. To analyse the factor "station", a One-way MANOVA was carried out. In this case, all values (26) measured at each station over the 13-month sampling were used as surrogates for replicates. In the absence of true replicates, the assumptions here are that each of the mentioned "surrogates" was a representative sample of real conditions, although not based on a random sampling, since time, tides and stations were sampled on a systematic way. Wilks test was computed for the multivariate analysis as well as the univariate tests. Calculations were carried out with the Statistica software. MANOVA was computed with raw and log transformed data, after analysing the homogeneity of variances and the relationship between means and variances. Newman-Keuls test was applied *a posteriori*.

Principal components analysis (PCA) was performed using Primer Software in order to investigate patterns of similarity between samples (Q – mode analysis) based on the values of environmental and biological variables. The data matrix was organized with

samples as rows and observations (variables) as columns. Data was log transformed to account for non-normal distribution of variables and standardized to account for the different units in which the variables were expressed. In this work, seasons are defined as: winter (December – February); spring (March – May); summer (June – August) and fall (September – November).

3.3. Results

3.3.1 Environmental conditions

Averages and standard errors for the major environmental parameters measured at each sampling station, at ebb and flood tide, are presented in Table 3.1.

Table 3.1. Averages and standard errors for selected variables at each location during flood and ebb surveys for the December 2002 – December 2003 period.

Parameter	Units	Lower		Middle		Upper	
		Flood	Ebb	Flood	Ebb	Flood	Ebb
Salinity	-	20.4±2.6	11.0±1.6	12.1±2.3	5.8±1.3	1.7±1.1	2.0±1.1
Temperature	ºC	14.2±0.5	14.2±0.7	14.5±0.7	15.3±0.8	17.0±1.1	16.0±1.0
NO3+NO2	μM	57.1±8.9	71.5±6.7	86.2±8.9	85.5±6.6	103.9±8.0	87.3±6.2
Ammonium	μM	8.8±0.7	12.5±2.7	9.3±0.5	7.8±0.5	6.6±0.8	4.0±0.4
Phosphate	μM	1.1±0.1	1.4±0.1	1.5±0.2	1.4±0.1	1.4±0.1	1.6±0.2
Sílica	μM	39.8±6.0	59.7±6.2	53.3±6.0	58.4±5.9	56.3±5.0	68.6±6.6
N:P ratio		53.8±4.7	63.4±3.5	67.4±5.9	72.7±5.2	109.7±19.6	69.4±6.9
TPM	mgL^{-1}	24.0±3.6	19.5±1.7	11.5±1.2	16.7±1.9	10.9±1.1	11.1±1.0
POM	mgL^{-1}	4.8±0.5	4.4±0.4	3.1±0.2	3.4±0.3	2.7±0.2	2.7±0.2
Chlorophyll *a*	mgm^{-3}	2.4±0.2	3.6±0.3	3.1±0.4	4.7±0.5	4.4±0.6	4.6±0.6
PP daily	$mgC\ m^{-2}d^{-1}$	312.2±118.7	205.5±76.5	328.2±109.1	252.9±93.7	455.8±163.1	411.1±150.0
CR daily	$mgC\ m^{-2}d^{-1}$	1810.1±407.1	1355.2±587.3	1170.2±196.9	1487.2±342.0	474.2±84.2	629.7±126.3
Water column depth	m	6.8±0.2	5.5±0.3	9.7±0.4	7.7±0.3	8.1±0.5	6.0±0.4

River flow values during each survey, at sampling time, and monthly averaged values are shown in Figure 3.2. As expected, higher values were found in winter and lower values in summer, with relatively small differences between actual survey values and monthly averaged values, except for December 2002. The highest actual river discharge was registered during the January ebb survey when flow reached 2,700 m^3s^{-1}, and the lowest

in August during both surveys, when river discharge was zero. Average river flow during the sampling period was 935 m^3s^{-1}.

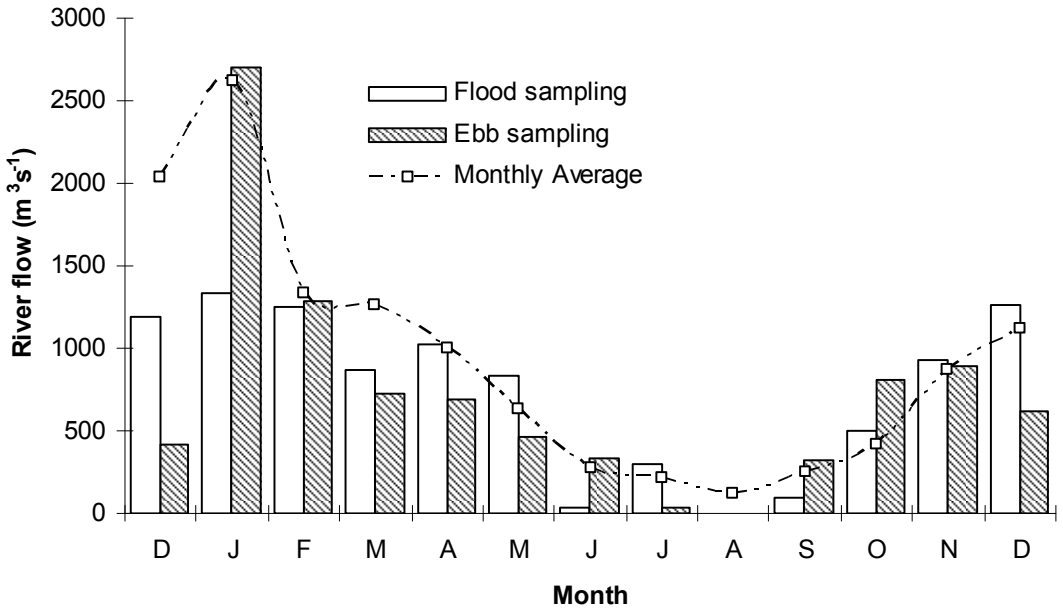

Figure 3.2. River flow (m^3s^{-1}) during sampling surveys (vertical bars) and monthly averages (dotted line), from December 2002 to December 2003.

Average estuarine salinity during the study period was 8.5 with values ranging between 0 and 35. Salinity was significantly correlated to river discharge, regardless of the tide ($p<0.01$). During high discharge periods, mostly in winter, estuarine water was completely flushed out at low tide, and even during the flood, salinity values remained low at the mouth (Figure 3.3). On the other hand, during the summer low discharge period, salinity values increased throughout the estuary and, in the upper estuary, salinity higher than 18 could be found, independently of the tide.

Noticeable stratification of the water column occurred in some occasions, and a halocline was present at the lower station in the March ebb, April flood, May flood, July ebb and November flood surveys; and at the middle station in the May flood, June ebb, July flood and November flood surveys.

Water temperature followed the expected seasonal trend from a minimum of 7.2 ºC during January and February freshet to a maximum of 25.4 ºC in the upper estuary, during the high salinity summer period.

In general, nutrient concentrations showed a seasonal pattern, increasing during the fall-winter period and decreasing during summer. Significant ($p<0.01$) correlations with salinity (negative) and river flow (positive) were observed. The exception was ammonium, which exhibited no clear seasonal trend and was positively correlated with salinity.

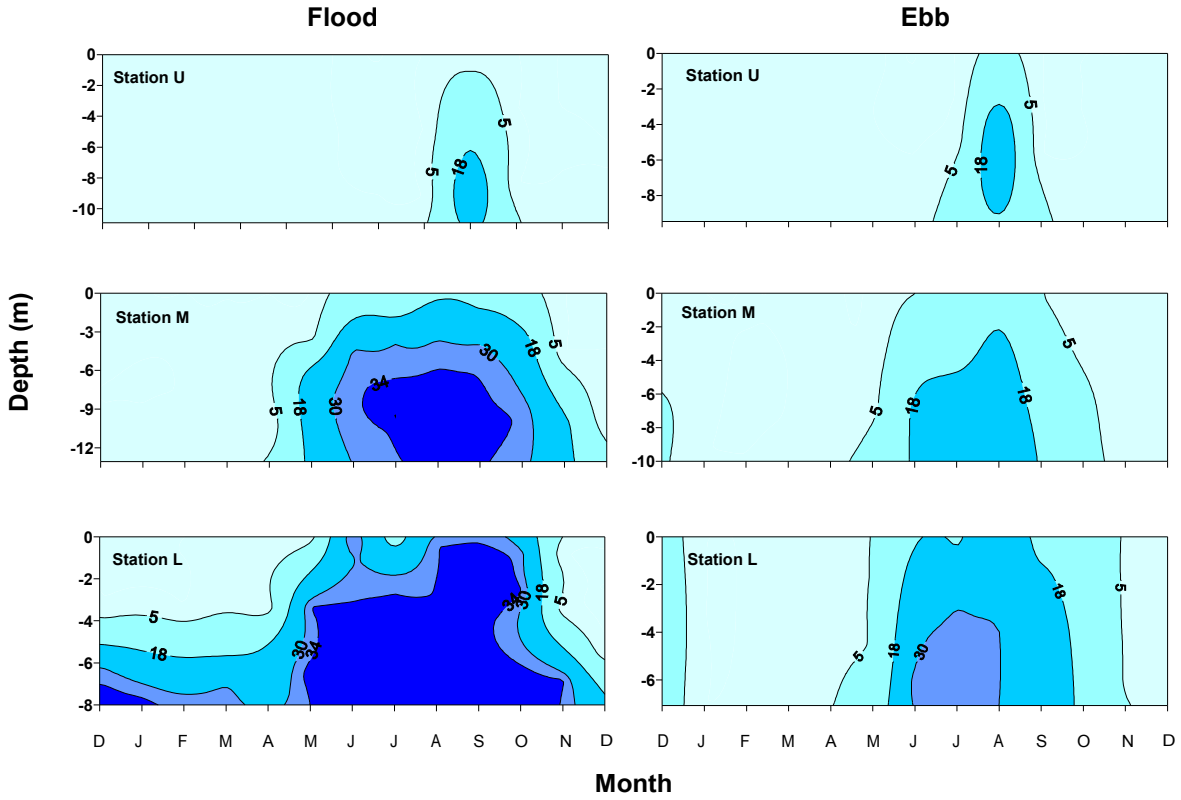

Figure 3.3. Water column salinity levels at the upper (U), middle (M) and lower (L) estuarine stations during the ebb and flood surveys from December 2002 to December 2003.

During the August flood survey, high values of NO_3+NO_2 were observed in the upper estuary along the water column and in the middle estuary only at surface. Averaged values decreased from the dam to the mouth independently of the tide (Table 3.1). Considering the study period, NO_3+NO_2 ranged between 1.4 and 227.4 μM.

Ammonium concentration ranged between 0.3 and 108.5 μM. The averaged values (Table 3.1) increased downstream during the ebb, while during the flood the middle station presented the highest value. Silicate values decreased downstream (Table 3.1) both during the ebb and the flood.

Concerning phosphate variability, values ranged from 0.2 to 4.7 μM. In general, concentration values were under 3 μM throughout the sampling period, except in December. Only at the lower station during the flood, a significant linear relationship

($p<0.001$) was found between phosphate and salinity, *i. e.* salinity did not control the dynamics of phosphate and average values throughout the estuary were rather similar.

N:P ratio ranged between 493, at the upper station during the August flood survey, and 8, at the middle station during the September flood survey. Nitrate was generally the predominant form of nitrogen. N:P values were always above the Redfield ratio of 16, except for the bottom and middle depth samples collected during the September flood survey at the lower and middle stations. A general decreasing trend downstream was observed (Table 3.1), consistent with the salinity increase.

TPM values ranged between 2.2 and 69.2 mg L^{-1} and POM ranged between 0.2 and 14.4 mg L^{-1}. In general, no seasonal trend was observed and maxima occurred in winter but also in summer. On average, the highest values were measured in the lower estuary during the flood (Table 3.1). A significant positive linear relationship ($p<0.01$) between TPM and the light extinction coefficient was found, independently of tide and location, as well as between TPM and POM. Light extinction coefficient values ranged between 0.3 and 4.1, with an average of 1.3 m^{-1}.

3.3.2 Chlorophyll *a* and photosynthetic parameters

Phytoplankton biomass, expressed in terms of chlorophyll *a* contents, showed a clear seasonal trend (Figure 3.4). Values ranged from 0.3 mg m^{-3}, during the December flood survey, to 14.9 mg m^{-3}, during the June flood survey, with higher biomass occurring generally in the upper estuary, particularly during the mid-spring early-summer phytoplankton bloom originated from the river. During this bloom period, biomass steadily decreased from the upper to the lower estuary. A second, more modest bloom was observed in most stations in late-summer early-fall, especially during the ebb. It should be noticed that maximal concentrations were observed in the upper station, during both the flood and the ebb. Variation with depth occurred only during the bloom period (June), with concentration of biomass at the surface and in August at the upper station with a reduction of biomass over depth (Figure 3.4). Phytoplankton biomass was positively correlated with temperature ($p<0.01$) and negatively correlated with river flow, phosphate and silicate ($p<0.01$). No statistical relationship was found between chlorophyll *a* and NO_3+NO_2 or ammonium.

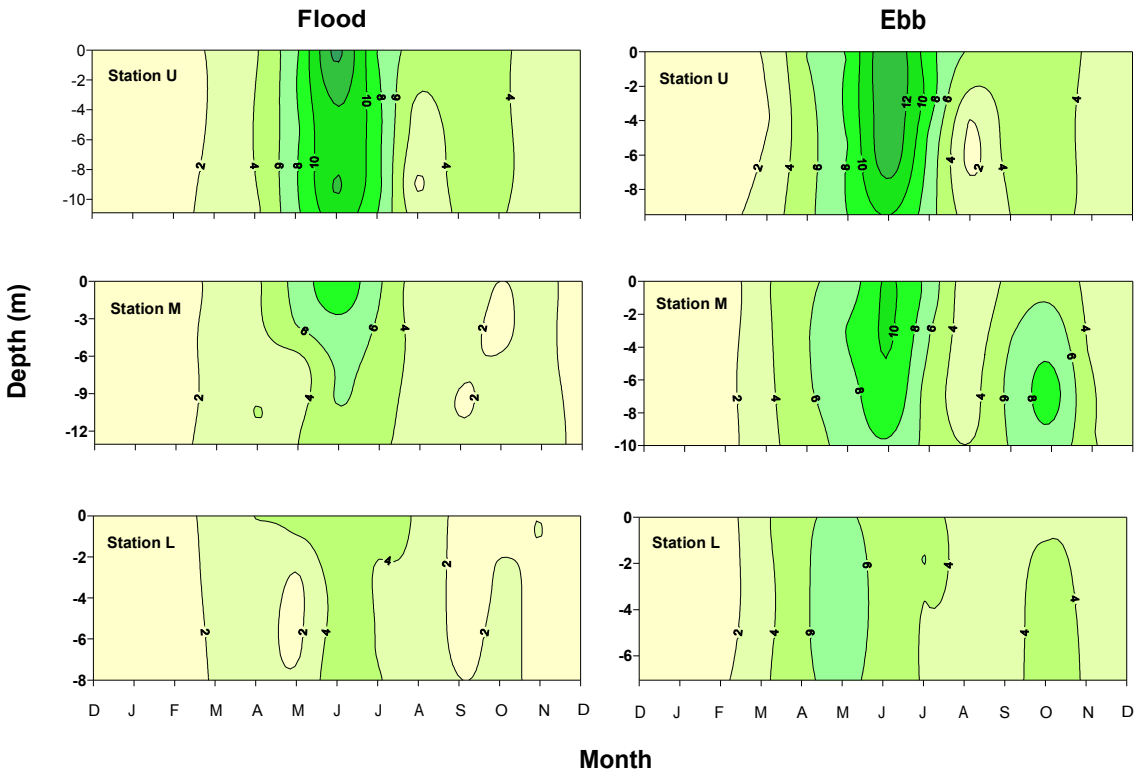

Figure 3.4. Water column chlorophyll *a* values at the lower (L), middle (M) and upper (U) estuarine stations, during the ebb and flood surveys, from December 2002 to December 2003.

Table 3.2 summarizes the results obtained by fitting Steele´s equation to P/E data (see Materials and Methods). A general good fit was obtained between model predicted values and observations as shown by the R^2 values. P_{max} values were higher in spring and summer, with the highest value during the August ebb survey at the upper station. During the ebb, higher values of P_{max} were found in June, at the lower and middle estuary, whereas during the flood, the highest values were found in July - August at the lower and middle estuary and June and August at the upper estuary. Globally, photosynthetic parameters P_{max} and E_{opt} were significantly ($p<0.01$) correlated with chlorophyll *a* and temperature (positively) and with river flow and k (negatively). The initial slope was correlated significantly and positively with temperature. The relationships between P_{max} and the initial slope versus temperature were also analysed by regression analysis. A relatively good fit was obtained with linear regression (respectively, $R^2=0.4$; ANOVA $p<0.0001$ and $R^2=0.16$; ANOVA $p<0.001$).

Table 3.2. Monthly photosynthetic parameters obtained for the PI curves for the 3 sampling stations along the year during the ebb and flood surveys. P_{max} in mg C mg $Chla^{-1}$ h^{-1}; E_{opt} in µE m^{-2} s^{-1}; Initial slope of the P/E curve in mg C mg $Chla^{-1}$ h^{-1} (µE m^{-2} s^{-1})$^{-1}$.

A) Ebb

	Station L				Station M				Station U			
Date	P_{max}	E_{opt}	R^2	**slope**	P_{max}	E_{opt}	R^2	**slope**	P_{max}	E_{opt}	R^2	**slope**
Dec-02	0.87	446.58	0.42	0.0053	1.25	508.02	0.83	0.0067	2.38	398.24	0.99	0.0162
Jan-03	1.46	450.84	0.86	0.0088	1.83	418.97	0.88	0.0119	2.91	507.30	0.94	0.0156
Feb-03	1.35	423.07	0.68	0.0086	1.66	408.89	0.72	0.0110	1.51	379.93	0.71	0.0108
Mar-03	1.76	469.45	0.83	0.0102	2.86	610.88	1.00	0.0127	2.59	535.93	0.84	0.0131
Apr-03	1.95	554.82	0.88	0.0096	2.97	540.28	0.92	0.0149	2.73	608.54	0.90	0.0122
May-03	2.29	466.31	0.88	0.0133	3.99	612.00	0.99	0.0177	3.44	631.26	0.98	0.0148
Jun-03	3.27	455.66	0.76	0.0194	5.56	1882.83	0.86	0.0080	4.09	641.63	0.96	0.0173
Jul-03	2.67	553.08	0.95	0.0131	2.57	560.27	1.00	0.0124	3.87	595.88	0.99	0.0176
Aug-03	3.21	623.17	0.84	0.0140	3.18	687.98	0.92	0.0125	9.24	626.14	0.92	0.0401
Sep-03	1.90	603.28	0.96	0.0086	2.40	684.95	0.96	0.0095	2.73	670.71	0.86	0.0110
Oct-03	2.57	522.12	0.93	0.0134	2.99	675.28	0.96	0.0120	3.79	618.67	0.95	0.0166
Nov-03	2.02	498.35	0.79	0.0110	2.32	524.11	0.80	0.0120	2.89	544.53	0.83	0.0144
Dec-03	1.00	592.37	0.98	0.0046	1.44	925.37	0.88	0.0042	1.02	440.12	0.90	0.0063

B) Flood

	Station L				Station M				Station U			
Date	P_{max}	E_{opt}	R^2	**slope**	P_{max}	E_{opt}	R^2	**slope**	P_{max}	E_{opt}	R^2	**slope**
Dec-02	2.51	374.46	0.44	0.0182	3.76	460.18	0.50	0.0222	1.18	718.43	0.84	0.0045
Jan-03	1.45	373.77	0.46	0.0105	1.42	417.60	0.90	0.0092	2.86	380.81	0.89	0.0203
Feb-03	1.74	509.36	0.91	0.0093	1.96	473.66	1.00	0.0112	1.90	505.96	0.97	0.0102
Mar-03	1.73	487.23	0.97	0.0096	2.41	427.91	0.98	0.0153	3.45	812.50	0.80	0.0115
Apr-03	2.43	508.38	0.95	0.0130	2.65	565.28	0.91	0.0127	1.93	587.68	0.93	0.0089
May-03	2.30	587.68	0.93	0.0106	4.43	516.55	0.98	0.0232	3.56	540.42	0.97	0.0179
Jun-03	2.64	582.00	0.89	0.0123	3.08	663.97	0.99	0.0126	4.66	616.00	0.96	0.0205
Jul-03	5.06	722.95	0.92	0.0190	4.52	825.55	0.96	0.0149	3.81	657.61	0.91	0.0157
Aug-03	4.40	675.82	0.94	0.0177	5.45	676.56	0.94	0.0218	4.65	606.66	0.92	0.0208
Sep-03	1.49	698.70	0.84	0.0058	3.66	657.70	0.91	0.0151	3.25	643.49	0.96	0.0137
Oct-03	1.68	489.07	0.81	0.0093	2.58	685.56	0.95	0.0102	3.84	801.13	0.99	0.0130
Nov-03	3.68	552.63	0.98	0.0181	3.38	587.42	1.00	0.0156	3.17	591.01	0.99	0.0145
Dec-03	1.44	551.88	0.90	0.0071	1.30	531.66	0.97	0.0066	1.13	539.04	0.85	0.0057

Compensation depth values are presented in Table 3.3. These values were compared with sampling stations mean depth and the depth of the halocline when present. In the majority of situations analysed, compensation depths were less than half of water column depth. During spring and summer, however, a fully euphotic water column occurred in some stations, namely at the upper station in May, during the flood, and in May through August, during the ebb; at the middle station in June, during the flood, and at the lower station in June. Only in two situations the compensation depth was higher than the halocline: at the lower station, during the July ebb survey and at the middle station, during the July flood survey, when the halocline was present at 2.8 and 4.4 m, respectively.

Table 3.3. Compensation depths calculated for the 3 sampling stations along the year during the ebb and flood surveys. Compensation depth values represented in bold type are close to or higher than water column depth.

	Ebb			Flood		
Date	Station L	Station M	Station U	Station L	Station M	Station U
Dec-02	a)	a)	a)	a)	1.1	a)
Jan-03	a)	a)	a)	a)	a)	1.2
Feb-03	a)	a)	a)	a)	a)	5.6
Mar-03	1.7	1.5	1.2	a)	0.7	1.7
Apr-03	2.8	2.7	3.1	3.2	2.2	a)
May-03	2.5	1.3	**4.6**	6.0	3.0	**6.7**
Jun-03	**7.3**	2.3	3.6	3.5	**10.3**	5.6
Jul-03	2.8	3.2	**4.8**	a)	4.4	5.3
Aug-03	a)	0.7	**6.5**	2.7	3.2	5.8
Sep-03	a)	0.5	0.4	a)	3.7	3.3
Oct-03	3.0	1.7	4.2	a)	a)	3.0
Nov-03	0.7	0.6	3.1	0.8	1.4	2.8
Dec-03	a)	a)	a)	a)	a)	a)

[a)] The solution of equation 4 resulted in an imaginary number (see Materials and Methods).

3.3.3 Estuarine metabolism

Except for the May – July period in the upper estuary, corresponding to the phytoplankton bloom, CR was always higher than photosynthetic production, *i. e.* heterotrophy was the dominant process in the estuarine water column (Figure 3.5).

A decreasing trend in integrated PP from the upper to the lower estuary was found, independently of the tide. Integrated daily values, however, were higher during the flood. Water column PP was significantly ($p<0.01$) and positively correlated with temperature and salinity but negatively correlated with river flow, k, nutrients (except ammonium), TPM and POM. No relationship was found between PP and water column CR. From the data obtained during the study period, water column PP annual averages were calculated. Values of 95, 106 and 160 g C m^{-2} y^{-1} were obtained for the lower, middle and upper estuary, respectively. It is noteworthy that these PP annual values are estimates from spring tides only, since there is no data available for neap tides, that would allow a more accurate estimate of water column annual PP.

Regarding CR, values increased steadily from the upper to the lower estuary, reaching its maximum expression during the summer months. Annual averages of 570, 478 and 199 g C m^{-2} were obtained for the lower, middle and upper estuary, respectively. Depth integrated hourly CR showed a positive significant correlation with salinity and ammonium and negative correlation with NO_3+NO_2, silicate and river flow ($p<0.01$).

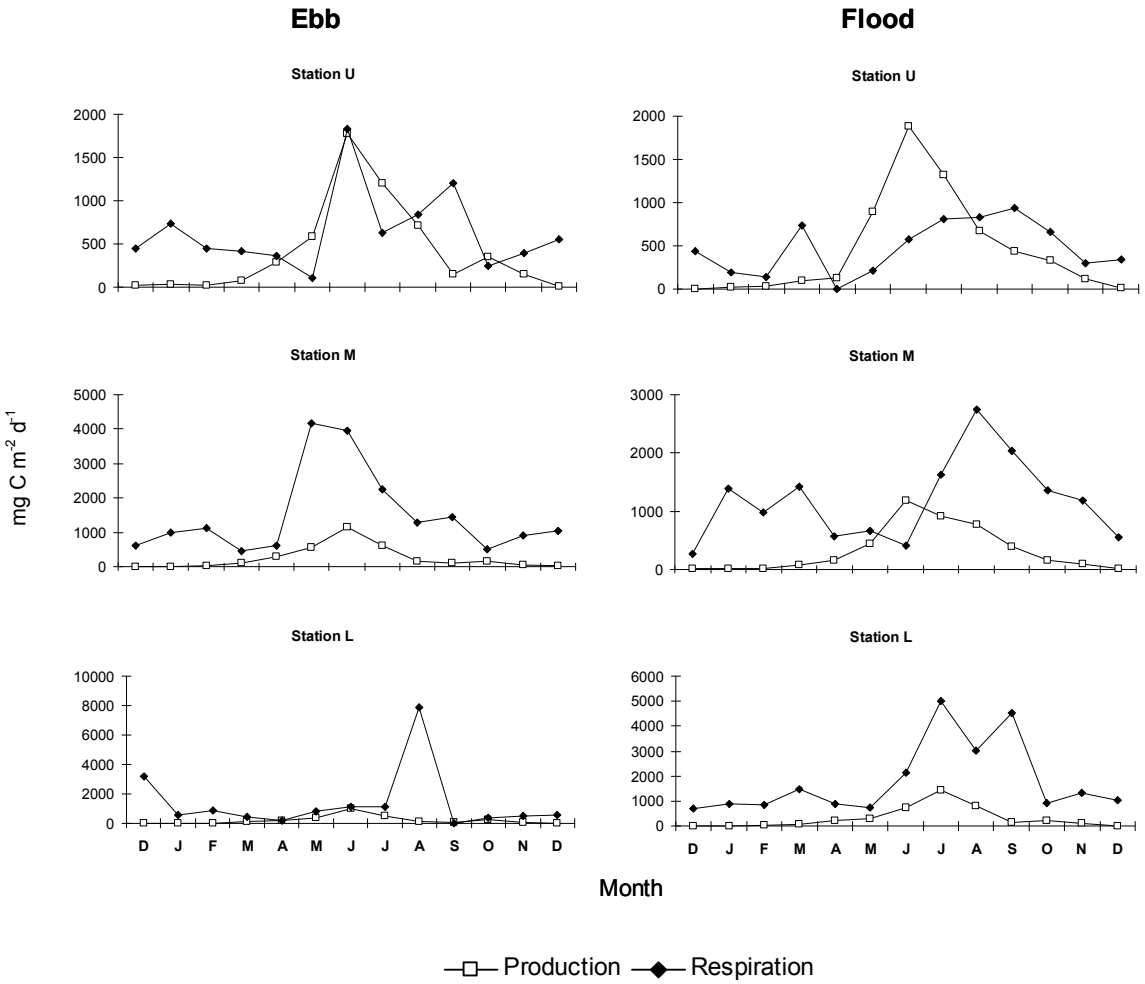

Figure 3.5. Daily integrated phytoplanktonic PP and water column CR in the lower (L), middle (M) and upper (U) estuarine stations, during the ebb and flood surveys, from December 2002 to December 2003.

3.3.4 Effect of time, tide and stations

After testing the MANOVA assumptions, it was concluded that not all variances were homogeneous, even after standardization and log transformation. The effect "time" was significant ($p<0.05$) for P_{max}, k, salinity, phosphate and ammonium. The effect "tide" was significant ($p<0.05$) for k, only.

The effect "Station" was significant for salinity, NO3+NO2, ammonium and POM. *A posteriori* comparisons with the Newman-Keuls test indicated significant differences ($p < 0.05$) between the upstream station and the other two stations. Regarding the variable

CR, there was a significant "station" effect ($p < 0.01$), unlike the variable PP. However, both results must be considered with caution, because of variance heterogeneity.

3.3.5 Patterns of similarity between samples

The eigenvalues corresponding to the 5 principal components (PCs) considered for analysis are presented in Table 3.4. These were chosen because all were greater than the unity and together explained 77.7% of the total variance contained in the original data set. The correlation coefficients between PCs and variables are presented in Table 3.5. The variables that contributed the most to PC1 were temperature and PP (positively), k and silica (negatively), suggesting a dominant influence of physical factors on primary production. PC2 was positively participated by POM, TPM, and salinity, and negatively participated by NO_3+NO_2 and the N:P ratio, mostly chemical factors. PC3 was negatively participated by N:P ratio, TPM, POM and initial slope. PC4 was highly and negatively participated by ammonium, possibly indicating an anthropogenic influence. PC5 was positively participated by chlorophyll *a* and E_{opt} and negatively by the initial slope. However these last two PCs explained only a small portion of the total variance (Table 3.4).

Table 3.4. Eigenvalues, percent variation and cumulative percent variation of the first 5 principal components.

PC	Eigenvalues	%Variation	Cum.%Variation
1	7,05	39,1	39,1
2	2,8	15,6	54,7
3	1,68	9,3	64
4	1,3	7,2	71,2
5	1,17	6,5	77,7

In Figure 3.6, a representation of the first two PCs is shown. Samples have been labelled based on season. Winter and summer samples were arranged at opposite extremes of PC1 while spring and fall were spread across the middle, showing a clear seasonal pattern. This is in agreement with the contribution of physical variables for PC1. On the other hand, Figure 3.7 represents the same projection but with the samples labelled by sampling station, highlighting spatial trends. In this case, stations are spread along the PC2 axis. The lower estuarine station samples were spread over the positive side whereas the upper station samples were located at the negative side. This agrees with the positive contribution of salinity (higher in the lower estuary) and the negative contribution of NO_3+NO_2 (higher in the upper estuary). No association between samples based on tide

was observed. Figure 3.8 shows graphically the weight of variables PP and extinction coefficient superimposed on the projection of samples, labelled by season, in the two-dimensional space defined by the first 2 principal components. The larger the circle, the greater the value of the superimposed variable. The samples with the highest values of PP are located in the positive side while the highest values of k are located on the negative side of the PC1 axis, reflecting the negative correlation found between these two variables.

Table 3.5. Eigenvectors or Coefficients in the linear combinations of variables making up PC's.

Variable	PC1	PC2	PC3	PC4	PC5
Pmax	0,282	-0,211	-0,256	0,046	-0,199
Eopt	0,217	-0,097	0,208	0,144	0,468
K	-0,3	-0,073	-0,274	-0,002	0,152
Slope	0,191	-0,168	-0,363	-0,094	-0,545
PP	0,327	-0,149	-0,125	0,193	0,093
CR	0,13	0,213	-0,013	-0,209	0,197
Chlorophyll *a*	0,241	-0,201	-0,12	0,278	0,36
Temperature	0,325	-0,049	0,038	0,206	0,05
Salinity	0,217	0,364	-0,052	-0,14	0,071
NO3+NO2	-0,238	-0,384	-0,064	-0,207	0,115
Phosphate	-0,258	-0,066	0,314	-0,108	-0,071
Silica	-0,32	-0,232	0,002	-0,036	0,004
Ammonium	0,062	0,203	-0,141	-0,595	0,332
N:P ratio	0,001	-0,365	-0,449	-0,246	0,263
Turbidity	-0,262	0,009	-0,256	0,212	0,142
TPM	-0,174	0,342	-0,385	0,27	0,056
POM	-0,125	0,411	-0,33	0,15	0,002
River Flow	-0,261	-0,06	0,058	0,371	0,126

3.4 Discussion

The Douro estuary is a highly dynamic system like most estuaries and very dependent on river flow variations which are due to seasonal changes and dominate water circulation (Vieira & Bordalo 2000). River inflow determines the extent of salt water intrusion, residence time, levels of nutrients and phytoplankton biomass. During winter, high flows often prevent coastal water from entering the estuary, even during the flood, raise nutrient levels, lower phytoplankton biomass and reduce water residence time. In this estuarine system, river flow rather than tides controls water residence time (Bordalo & Vieira 2005). The surveys were carried out during a wet year, since the average river discharge was almost twice the long term average inflow of freshwater.

Considering nutrient limitation of phytoplankton production, oceanic systems are considered to be nitrogen limited (Eppley et al. 1973) while freshwater systems are generally viewed as phosphorus limited (Schindler 1977). In estuaries, where seasonal and spatial variation of freshwater and seawater mixtures occur, this concept is not so clear (Bernhard & Peele 1997). Seasonal alternation of nitrogen and phosphorus limitation has been reported (Fisher et al. 1992, Mallin et al. 1999) as well as a spatial shift from phosphorus to nitrogen limitation in some estuaries (Yin et al. 2001). In the present study, N:P ratio was usually high and always above the Redfield ratio except for the bottom and middle depth samples collected at the lower and middle stations during the September flood tide survey. These were high salinity low nutrient samples, characteristic of seawater where nitrogen limitation is common. Hence, generally, in the Douro estuary phosphate, rather than nitrate was the potentially limiting nutrient. Nevertheless, nitrate limitation can occur in low river flow situations when scarcely diluted seawater is present within the estuary.

Table 3.6. Summary of pelagic primary production (PP) measurements (mean values or ranges) in temperate estuaries.

Site	**Pelagic PP** (mg C m^{-2} d^{-1})	Author
Bristol Channel	204	Joint (1978)
Chesapeake Bay	500 - 3500	Malone et al (1996)
Colne	24	Kocum et al (2002)
Danube	200 - 4400	Humborg (1997)
Douro	**4.7 – 1879 (mean = 320)**	**This work**
Eastern Scheldt	908	Wetsteyn & Kromkamp (1994)
Ems-Dollard	20.4	Van Es (1977)
Ems-Dollard	36	Cadée & Hegeman (1974b)
Lynher	222	Joint & Pomeroy (1981)
St. Lawrence	10 – 800	Sinclair (1978)
Swan river	2192 - 2740	Thompson (1998)
Western Scheldt	485	van Spaendonk et al (1993)
Western Scheldt	632	Kromkamp et al (1995)
Apalachicola Bay	90 - 1800	Mortavazi et al (2000)
Mississippi	50 – 1000	Thomas & Simmons (1960)

The PP obtained in the Douro estuary is within the productivity range for other temperate and subtropical estuaries (Table 3.6). The results clearly show that the Douro estuary is predominantly heterotrophic. This is an expected result, considering the shallowness (around 23%) of the euphotic layer/compensation depth compared to the depth of the estuary (Table 3.3) and it is also a normal feature in temperate tidal estuaries (Heip et al. 1995). The deficit in PP may be compensated by external sources of organic matter, such as untreated sewage discharge or treated effluent disposal by the eight WTPs (Figure 3.1). The contribution of benthic PP is limited owing to the small intertidal area of the

estuary (Magalhaes et al. 2003) and, due to land reclamation, saltmarsh areas were dramatically reduced to less than 0.1 Km^2 (Bordalo, unpublished data).

The analysis of Figures 6, 7 and the MANOVA results indicates significant ($p<0.01$) differences in CR between sampling stations and suggests different metabolic patterns over time and space in the Douro estuary. The gap between PP and CR increases towards the river mouth, with some positive values in summer in the upper and middle estuary. It is noteworthy that heterotrophy is much more evident towards the sea. The explanation for this fact lies probably in the higher TPM and POM loads at this end of the estuary, a very uncommon phenomenon that may be explained by the dam effect at the upstream end of the estuary, retaining large amounts of sediments. Also, the human-induced contamination of the lower and middle estuary (Bordalo 2003), contributed to an increased organic loading and hence of respiration, leading to the heterotrophy situation observed all year round.

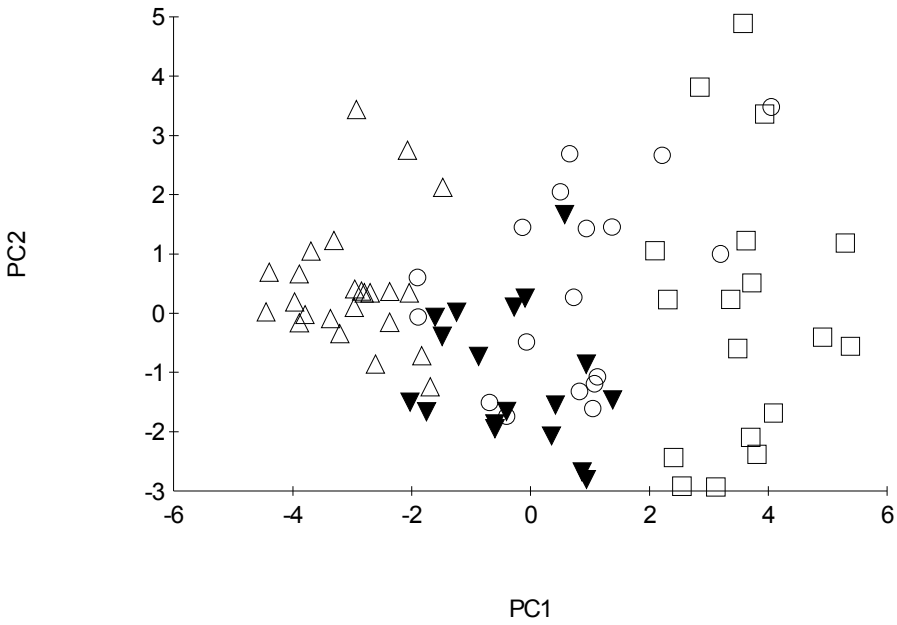

Figure 3.6. Projection of samples in two dimensions, defined by the first two principal components, labelled by season - winter (△); spring (▼); summer (□); fall (○).

The results show that different factors may control PP over space and time. From the PCA analysis, it is clear that spatial differences arose mostly along PC2, contrasting mostly larger nitrate+nitrite concentrations and N:P ratios (upper station) to higher salinities, TPM and POM concentrations (lower station). This suggests that the upper estuary is more

productive than the lower estuary as a result of higher nitrogen concentrations from riverine origin (Mallin et al. 1993, Malej et al. 1995). Also, higher chlorophyll biomass from the reservoir (Bordalo & Vieira 2005) may help to explain these trends, but to a lesser extent (Table 3.5). Regarding temporal differences, higher PP values were associated to higher temperatures, lower light extinction coefficients (k) and higher P_{max}, coinciding with the summer period. According to Heip et al. (1995), annual PP values lower than 160 g C m^{-2} y^{-1} result from light limitation in nutrient-rich or heterotrophic systems, which is the case of Douro estuary, with an annual estimate of 120 g C m^{-2} y^{-1}. This is partly confirmed from the results obtained in this work, regarding temporal variability in PP, statistically related to k values.

Probably, one of the most interesting aspects of this work is the positive correlation of chlorophyll *a* with P_{max}. In marine ecosystems, there seems to be a general decreasing trend of the P/B ratio as a function of net primary production (NPP). In one extreme there are oligotrophic ecosystems, with high P/B, low biomass and NPP, such as open ocean pelagic systems, and in another extreme there are ecosystems with low P/B, high NPP and biomass, such as algal reefs and beds (Duarte et al. 2006). These trends suggest that low biomass and NPP ecosystems are more efficient in using limiting resources. Furthermore, low biomass standing stocks may also leave more resources per unit of biomass, helping to explain higher P/B ratios. P_{max} expressed as mg C mg $Chla^{-1}$ h^{-1}, may be viewed as a potential P/B ratio. Therefore, from the results obtained, it seems that the Douro estuary has a different pattern regarding the usual relationship between P/B and biomass standing stock – higher biomass situations coincide with higher phytoplankton photosynthetic capacity. This positive feedback is reinforced by higher initial slopes (Table 3.2). The significant linear relationships between those parameters and temperature highlighted the importance of temperature in contributing to higher P_{max} and photosynthetic efficiency. Madariaga (1995) in the Urdaibai estuary (Bay of Biscay) and Van Spaendonk et al. (1993) in the Westerschelde (The Netherlands) obtained higher P_{max} values downstream than upstream, whereas the contrary was true for PP and chlorophyll concentration: exactly the opposite trends obtained in this work for P_{max} and in line with previous comments on the P/B ratios. P_{max} values reported here are well within those measured by Madariaga (1995), 2.03 and 15.21 mg C mg $Chla^{-1}$ h^{-1}, and Van Spaendonk et al. (1993), 0.08 and 16 mg C mg $Chla^{-1}$ h^{-1}.

The mentioned patterns may result from the specific characteristics of the Douro river and its estuary. The relatively low chlorophyll concentrations in the Crestuma-Lever reservoir,

within 8 – 12 mg Chl m^{-3} (Bordalo, unpublished data), discharging directly into the estuary, may explain the low phytoplankton biomass within the estuary.

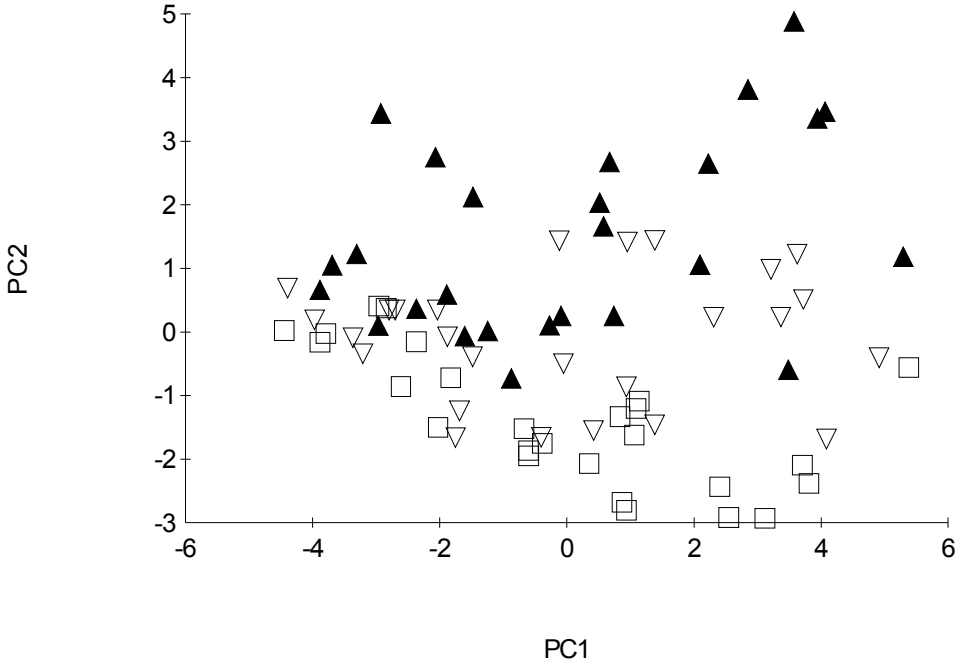

Figure 3.7. Projection of samples in two dimensions, defined by the first two principal components, labelled by station - Lower (▲); Middle (▽); Upper (□).

The river is dammed all over its course and this may justify the relatively low TPM loads to the estuary as compared to other European estuarine systems, such as the Sado estuary (Portugal), the Gironde (France) and the Scheldt (Belgium and the Netherlands). In such systems TPM concentration in the upper estuarine area were 600 mg L^{-1}, >200 mg L^{-1} and c.a. 40 mg L^{-1}, respectively (Cabecadas et al. 1999). Moreover, in the Douro estuary an increasing trend of TPM with salinity was observed (Table 3.1), whereas in the above mentioned systems an opposite trend was found. Chlorophyll concentrations were in the range of those measured in the Douro, except for the Scheldt, with maximal values above 200 mg Chl m^{-3}. For both the Sado and the Gironde, chlorophyll maxima occurred at intermediate salinities, whereas for the Scheldt, upstream maximum was reported. This was also the case of Douro, where the highest chlorophyll concentration was observed at the estuary head, indicating a riverine origin of phytoplankton.

A possible explanation for the positive correlation between photosynthetic capacity and chlorophyll concentration of the Douro phytoplankton, may be the relatively low

phytoplankton biomass, preventing intraspecific competition from lowering photosynthetic capacity, on one hand, and the physiologic characteristics of phytoplankton itself, originated from a semi-lotic (Crestuma reservoir) rather than from a true lotic ecosystem. Probably, this last hypothesis deserves further investigation, since it may clarify some impacts of river damming over estuarine metabolism in accordance to the Water Framework Directive (EC 2000).

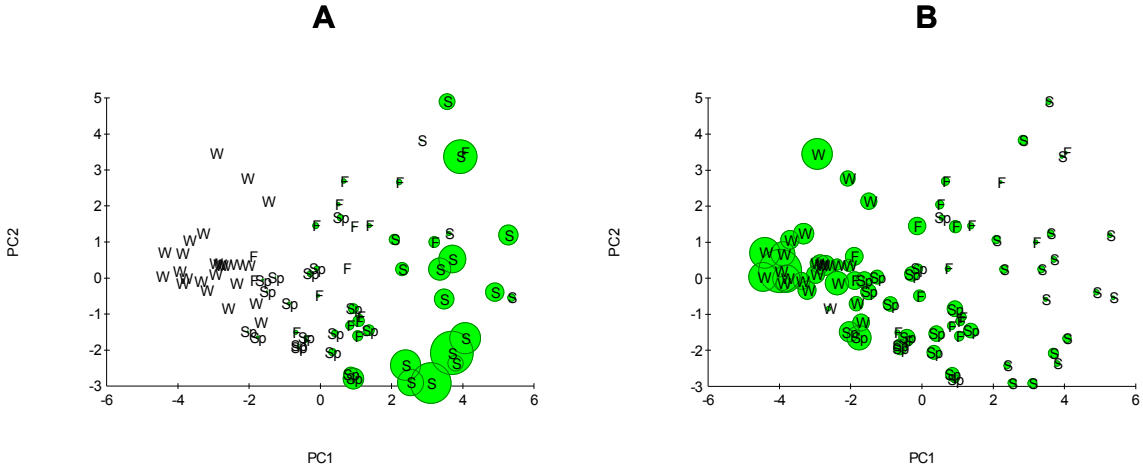

Figure 3.8. Projection of samples in two dimensions defined by the two first principal components. Bubble size is related to the magnitude of the variable represented. A – depth integrated hourly PP; B – extinction coefficient (k). Samples are labelled by season: winter (W); spring (Sp); summer (S); fall (F).

The absence of historical data to compare the obtained results with similar studies carried out before dam construction prevents any definite conclusion about the dam effect on estuarine production and metabolism. However, considering the important differences between the Douro estuary and other European estuaries, it may be acceptable that the river Douro dams lead to a reduction in TPM and chlorophyll loads into the estuary and a decrease in estuarine metabolism at its upstream end. Whilst it is generally accepted that TPM loads decrease as a result of dam retention, the same is not so clear regarding chlorophyll. However, considering that the Crestuma-Lever reservoir has an average depth above 13 m, that only about one third of the water column is euphotic and that, for most of the year, the water column is well mixed (Bordalo et al., unpublished data), it may be speculated that PP in the reservoir is not very high and therefore relatively low chlorophyll values may be expected as an input to the estuary.

Finally, significant differences between tides were not observed, as shown by MANOVA and multivariate analysis results, except for k, reflecting higher water turbidity during the

ebb. Considering spatial variability, higher turbidity in the lower estuary is rather derived from sewage discharge within that estuarine stretch or from oceanic outfalls than from sediment ressuspension, which traditionally originates the turbidity maximum. Differences between tides concerning phytoplankton biomass reported in other studies are related to a much higher difference between chlorophyll *a* coming from the river and the adjacent coastal waters (Roegner 1998); or to seasonal phytoplankton cycles (Aubry & Acri 2004).

3.5 Conclusions

The results obtained from this study suggest that:

1) The Douro estuary is predominantly heterotrophic, with some exceptions in the lower salinity upstream area in summer;
2) PP seems to be mostly controlled by temperature, being also influenced by a positive feedback from photosynthetic capacity and chlorophyll biomass;
3) No significant differences between ebb and flood were observed in what PP is concerned.
4) The reservoir located upstream may have a dominant influence on TPM concentration gradients in the estuary, which exhibit low TPM and chlorophyll *a* comparing to other systems.
5) Further studies addressing the impact of the upstream dam on the characteristics of phytoplankton arriving at the estuary, as well as its influence on estuary metabolism are needed.

CHAPTER 4

Temporal and spatial variability of phytoplankton photosynthetic characteristics in a southern European estuary (Douro, Portugal)

4.1 Introduction

The relationship between photosynthesis and light (P-E relationship) has been used for many years as a tool to estimate phytoplankton production over several temporal and spatial scales (Harding et al. 1982, Falkowski & Raven 1997). This relationship has been described by several mathematical formulations, which may be empirical, based on observations (Steele 1962, Webb et al. 1974, Jassby & Platt 1976, Platt et al. 1980), or mechanistic, based on physiological processes (Eilers & Peeters 1988). These references correspond to static formulations where P-E parameters are assumed to be constant in

---

The contents of this chapter can be found in Azevedo IC, Duarte PM, Bordalo AA. Temporal and spatial variability of phytoplankton photosynthetic characteristics in a southern European estuary (Douro, Portugal). Submitted to Marine Ecology Progress Series.

time. However, temporal variability of photosynthetic parameters is now well established, with several authors suggesting that this dynamic behaviour should be included in P-E models (Falkowski & Wirick 1981, Marra et al. 1985, Sakshaug et al. 1997, Duarte 2005).

Variability of photosynthetic parameters has been studied over different time scales and found to be related to endogenous circadian rhythms (Prezelin 1992) as well as to changes in environmental variables such as light intensity (Gallegos et al. 1983, Geider et al. 1996, Madariaga 2002), species composition (Cote & Platt 1983, Jouenne et al. 2005), water temperature (e.g. Tillmann et al. 2000) and salinity (Moisander et al. 2002).

Several of the above mentioned factors may be simultaneously implied in photosynthetic variability of natural phytoplankton assemblages, especially in systems subjected to highly variable environmental conditions, such as estuaries. MacCaull and Platt (1977) have already hypothesised that photosynthetic variability observed in the field is related to both endogenous rhythms and changing environmental factors. Actually, environmental variability can act directly at the level of physiology within phytoplankton species (Lizon et al. 1995, Duarte et al. 2006), as well as indirectly through changes on species composition, which in turn cause variations in photosynthesis-irradiance relationships (Cote & Platt 1983, Macedo et al. 2001, Jouenne et al. 2005).

Previous studies (Cote & Platt 1983, 1984) have shown that, by emphasizing the influence of environmental and biological factors on the photosynthetic parameters rather than on the instantaneous rate of photosynthesis, a better understanding of the factors controlling the activity of phytoplankton in their natural environment can be achieved. Moreover, knowledge of the relationships between environmental variables and photosynthetic response allows the development of reliable mathematical models that can be used to calculate photosynthetic rates based on light, temperature, nutrients and chlorophyll *a* concentration as input variables (Sakshaug et al. 1997).

The Douro estuary is characterised by a highly variable freshwater inflow, controlled by a network of over 50 large dams. In a previous paper (Azevedo et al. 2008), the authors presented a conceptual model of the Douro estuary, showing that the river emerges as the major source of nutrients, chlorophyll *a* and TPM (total particulate matter), although additional phosphate and TPM anthropogenic sources are present in the middle and lower, highly urbanized, estuarine streches. Water column salinity structure and freshwater residence time are dependent on river flow magnitude. Flows above 800 m^3s^{-1} prevent seawater from entering the estuary (Vieira & Bordalo 2000), whereas, for flows

below 300 m^3s^{-1}, salinity stratification occurs. During spring, when flow decreases and light availability and temperature increase, phytoplankton biomass and primary production (PP) reach their maxima within the estuary. During the summer low river flow period, when temperature and water transparency are the highest (as well as salinity), chlorophyll *a* and PP decline.

The Douro is a mostly heterotrophic estuary, with heterotrophy increasing towards the mouth, where this condition is observed all year round. Only in the upper reaches during spring, an autotrophic state was observed (Azevedo et al. 2006).

In the above mentioned study (Azevedo et al. 2006), annual primary production was estimated from P-E measurements, along the Douro estuary. Strong correlations were found between Pmax, temperature and chlorophyll *a*, suggesting that these environmental variables were responsible for most of the variability observed in that photosynthetic parameter. Those findings paved the way for the present study, whose objective is to answer the following questions:

- At which temporal scales is the variability of P-E parameters more important?
- How important is the spatial variability of the mentioned parameters, along the estuarine gradient, giving the complex mixing patterns between fresh and salt water phytoplankton?
- What are the most important environmental factors affecting variability of P-E parameters?

4.2 Material and Methods

4.2.1 Study area

The Douro estuary is a granitic drowned valley estuary, heavily modified in its last 8 Km, corresponding to the limit between upper and middle estuarine stretches. It is characterized by semidiurnal tides, with a mean tidal range of 2.8 m, and a pronounced seasonal river flow regime (0 – 13,000 m^3s^{-1}; average 505 m^3s^{-1}). During the flood and under low river discharge, the salt wedge reaches the head of the estuary (Figure 4.1),

and remains within the estuary during the next ebb. During high discharge events, the estuary is flushed completely during one tidal cycle and seawater intrusion is prevented during the flood (Vieira & Bordalo 2000).

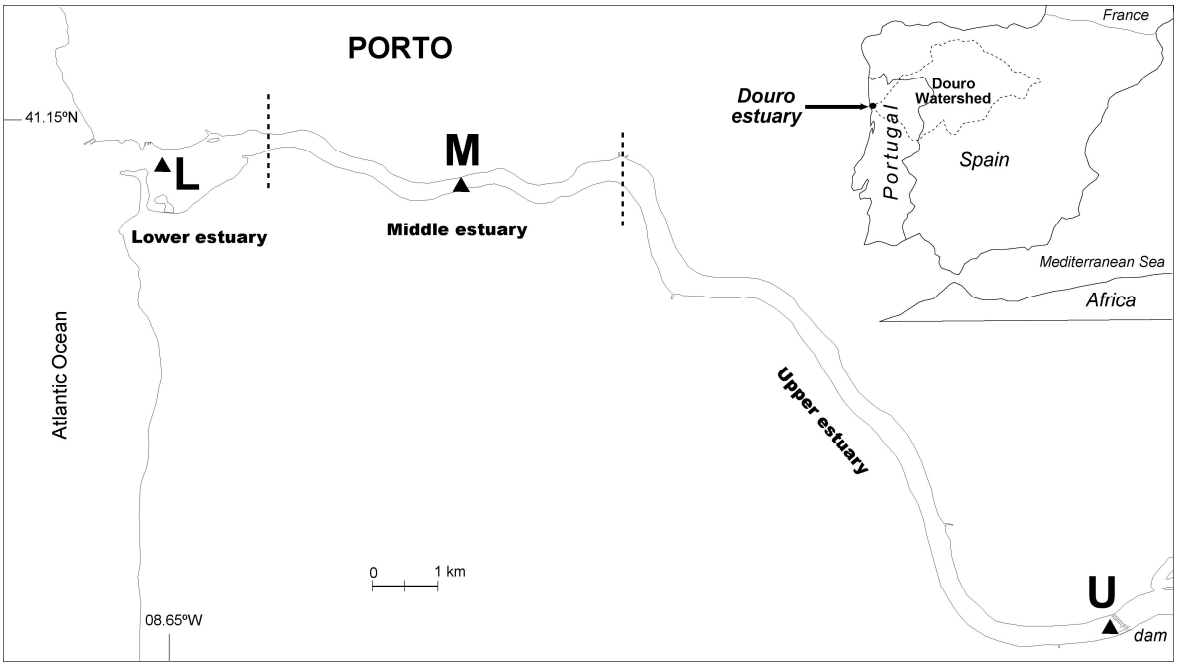

Figure 4.1. The river Douro estuary and location of sampling stations (L – lower, M – middle and U – upper estuary, WTP – Wastewater Treatment Plant).

4.2.2 Data collection

4.2.2.1 Tydal cycles

Sampling was carried out in 28 October 2003, 23 January 2004, 18 May 2004 and 29 July 2004. Quasi-continuous surface and bottom measurements (every minute) of water temperature, salinity, dissolved oxygen (DO) and pH were taken with CTD probes (YSI, 6600), whereas current velocity and direction were measured with Valeport (model 106) current meters. Incident irradiance (PAR) was measured with a spherical quantum sensor light meter (LI-COR, LI-250). Surface and bottom samples were collected every 2 hours for nutrients and chlorophyll *a* quantification. Subsurface samples for P-E incubations were collected in the morning (around 9:00 a.m.), around noon and in the afternoon (around 3:00 p.m.). Sechi disk depth was measured for water column light attenuation assessment.

4.2.2.2 Monthly surveys

From December 2002 to December 2003, monthly surveys were conducted during a 13-month cycle for primary production and pelagic metabolism assessment of the Douro estuary (Azevedo et al. 2006). Briefly, sampling design consisted in monthly visits to three stations located in the lower, middle and upper estuary, at approximately 0.7, 5.0 and 21.6 Km respectively, from river mouth (Figure 4.1). Vertical profiles of temperature, conductivity, salinity, dissolved oxygen, pH and turbidity were performed with a CTD (YSI, 6600). Photosynthetic active radiation (PAR) profiles were obtained with a spherical quantum sensor light meter, at 0.5 m depth steps (LI-COR, LI-250). Simultaneously, subsurface samples were collected for chlorophyll *a,* nutrients (nitrate, nitrite, ammonium, phosphate and silicate) and PP assessment.

4.2.3 Analytical and experimental procedures

Dissolved orthophosphate, nitrite, ammonium and silicate were analyzed following the methods described in Grasshoff et al. (1983). Nitrate was quantified by an adaptation of the spongy cadmium reduction technique (Jones 1984), subtracting nitrite from the total. Analyses were performed in triplicate. Chlorophyll *a* was assayed spectrophotometrically after extraction with 90% acetone (Parsons et al. 1984) with cell homogenization, using the SCOR-UNESCO (1966) trichromatic equation. P-E experiments were performed by the ^{14}C method (Steeman Nielsen 1952). Samples were placed in 125-ml Pyrex glass flasks and 2 µCi of aqueous solution of sodium bicarbonate was added (Carbon 14 Centralen). Incubations were conducted at 5 light levels (100%, 75%, 50%, 25%, 1%), to mimic light attenuation at different depths within the euphotic zone, for 1 – 2 hours in a water bath, at *in situ* temperature. An artificial light source providing a PAR of 920 $\mu Em^{-2}s^{-1}$ was used. A neutral screen was used to provide the different light levels. One additional dark bottle was also incubated. After incubation, samples were filtered through 0.45 µm membranes; washed, placed in 20-ml scintillation vials and 10-ml scintillation cocktail (Beckman Instagel Packard) was added. Countings, in disintegrations per minute (DPM), were performed in a Beckman LS3801 liquid scintillation analyser using internal standards for the automatic establishment of the quenching curve. Dark DPM values were subtracted from light DPM values and results were expressed in mg C m^{-3} h^{-1}. Inorganic carbon was assayed from pH and alkalinity measurements by direct titration according to Parsons et al.(1984).

4.2.4 Data analyses

4.2.4.1 P-E parameter estimation

Steele's production-light function (Eq. 1) (Steele 1962) was used to fit P-E curves to experimental data from incubation experiments, using the Gauss-Newton non-linear regression method, since photoinibition was apparent. Photosynthetic rates were normalised to chlorophyll *a*. Chlorophyll specific maximum photosynthetic rate (P_{max}) and optimal light intensity (E_{opt}), were obtained directly from the fitted P-E curves. Photosynthetic efficiency (α) was estimated as the initial slope of the P-E curves by deriving the Steele function in relation to light intensity (E) and calculating the limit of the derivative when E approaches zero.

$$P = P_{max}\left[\frac{E}{E_{opt}}\exp\left(1-\frac{E}{E_{opt}}\right)\right]^{n} \qquad \text{(Eq. 1)}$$

n = 1 (n empirical integer)

4.2.4.2 Statistical and multivariate analyses

Spearman rank correlation analysis was performed to evaluate relations between environmental and biological variables and metabolic processes.

Principal components analysis (PCA) was performed using Primer Software in order to investigate patterns of similarity between samples (Q – mode analysis) based on the contribution of environmental variables and photosynthetic parameters. The data matrix was organized with samples as rows and observations (variables) as columns. Data was log transformed to account for non-normal distribution of variables and standardized to account for the different units in which the variables were expressed.

4.2.4.3 Analysis of photosynthetic parameters variability at different timescales

In order to establish the temporal scale at which variability of photosynthetic parameters was highest, inter-seasonal (MS1) and intra-seasonal (MS2) variance were calculated, according to equations 2 and 3, respectively, using the monthly surveys dataset (cf. – 4.2.2.2).

$$MS1 = \frac{\sum_{i=1}^{n} (\bar{x}_i - \bar{x}_a)^2}{n-1} \qquad \text{(Eq. 2)}$$

$$MS2 = \frac{\sum_{i=1}^{n} \left(\sum_{j=1}^{k} (\bar{x}_{ij} - \bar{x}_i)^2 \right)}{(k-1) * n} \qquad \text{(Eq. 3)}$$

$\bar{x}_a$ - annual mean

$\bar{x}_i$ - seasonal mean

$\bar{x}_{ij}$ - monthly mean, based on results from three sampling stations X two occasions

n - number of seasons

k - number of months from each season

The tidal cycle dataset (cf. – 4.2.2.1) was used to compare seasonal and diel variability, according to the same equations, except that in this case $\bar{x}_{ij}$ is a single value corresponding to time of day and k is the number of samples taken at each day.

Each pair of variances was compared by computing their ratio and performing an F-test. Since photosynthetic parameters were not sampled randomly over time and space, this comparison between their variances at different time scales may be biased. Additionally, coefficients of variation (CV) were calculated for the same timescales.

4.2.4.4 Temperature and phosphate integration in the Steele's P-E equation

A previous study on the pelagic metabolism of the Douro estuary (Azevedo et al. 2006) showed that primary production (PP) was mostly controlled by temperature. Also, in this system, N:P ratio is generally above the Redfield ratio, suggesting an excess of nitrate availability and a potential limiting role for phosphate (Azevedo et al. 2008). Thus, in order to investigate the effect of including those factors in primary production estimation, Steele's equation was combined with an exponential limiting function for temperature and a Michaelis-Menten limiting function for phosphate. The resulting model (Eq. 4) was adjusted to data obtained from incubations performed during the monthly surveys, using the Gauss-Newton non-linear regression method.

$$P = P_{max}\left[\frac{E}{E_{opt}}\exp\left(1-\frac{E}{E_{opt}}\right)\right]^{n}\exp(k_T T)\left(\frac{Ph}{(Ph+Kp)}\right) \quad \text{(Eq. 4)}$$

k_T – temperature augmentation rate, in $(ºC)^{-1}$

T – temperature, ºC

Ph – phosphate concentration, in μM

Kp – half-saturation constant for phosphate, in μM

4.3 Results

4.3.1 Environmental variables

Results presented in the next paragraphs are based on the tidal cycle surveys (*cf.* – 4. 2.2.1), since environmental variability of monthly surveys has been presented elsewhere (Azevedo et al. 2006).

River flow into the estuary was controlled by the dam discharge activity at the head. Hourly variability was high, with abrupt changes observed during all sampling periods, according to the needs of hydroelectricity (Figure 4.2). In the autumn survey, flow rose from 800 to 1400 m^3s^{-1} and dropped back to 700 m^3s^{-1} in 3 hours. In the winter survey, a 300 m^3s^{-1} drop was observed, between 2 and 3 pm, from 900 to 600 m^3s^{-1}, whereas in the summer survey, river flow was 0 m^3s^{-1} between 8 and 11 am, rose to around 200 m^3s^{-1} until 6 pm and then dropped back to 0 m^3s^{-1} at 8 pm.

Salinity values observed during the sampling surveys were dependent on tidal conditions and river flow (Figure 4.3). At the bottom, salinity increased during the flood, except in the summer survey, when values remained high throughout the entire survey due to the absent/reduced freshwater discharge from the dam. The influence of river flow on salinity was more evident at the surface. Values decreased during the flood in all surveys, coincident with river flow increase. This was well noticed in the summer survey: surface salinity remained high throughout the period of absence of freshwater discharge, decreasing about 2.5 hours after the dam started discharging. This salinity decrease was accompanied by an increase in temperature and oxygen saturation. Moreover, salinity stratification of the water column was recurrent throughout the surveys during high tide.

Nitrate, phosphate and silicate were higher during fall, winter and spring surveys and lower during the summer, when the influence of low nutrient coastal water was more noticeable. Ammonium was higher during spring and summer surveys and lower in fall and winter. Ranges and averages obtained for each survey are presented in Table 4.1.

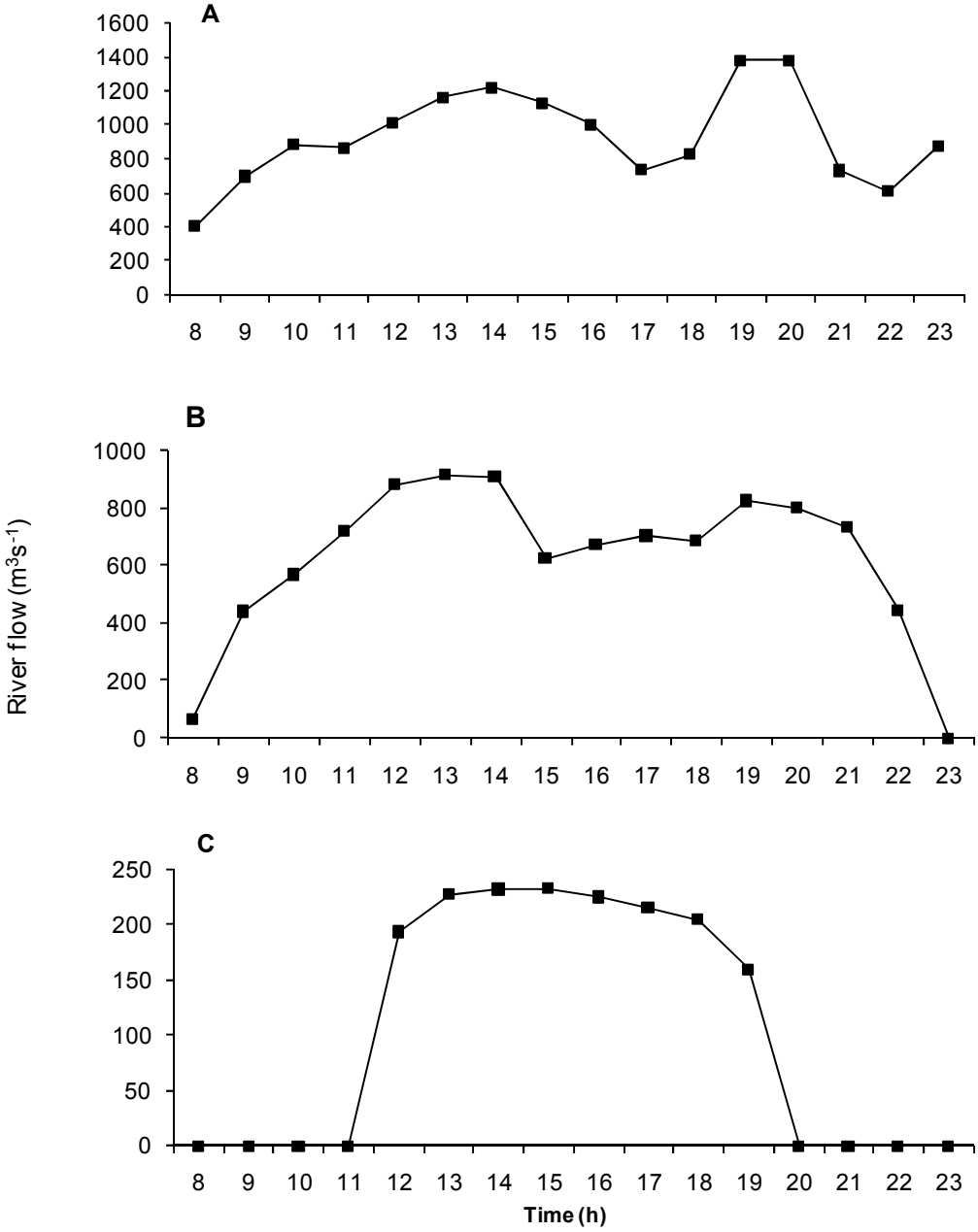

Figure 4.2. Hourly river flow (m^3 s^{-1}) during the fall, winter and summer tidal cycle surveys. Data for the spring survey were not available.

Whenever a two layer circulation was present, due to salinity stratification, nitrate and phosphate presented a vertical gradient, with higher levels at the surface, corresponding to lower salinity water (Figure 4.4). When a salinity decrease occurred at the surface, due

to river flow increase, nutrient levels increased. This was also observed at the bottom, especially during the ebb, due to water column mixing. Concerning ammonium, no clear pattern was observed, although higher values were also found at the surface.

Chlorophyll *a* concentration mean values, standard deviation, coefficient of variation (CV) and ranges obtained for each survey are given in Table 4.1. Unlike nutrients, chlorophyll *a* showed no relationship with salinity and, generally, no vertical gradient was observed for this variable during periods of water column stratification. Also, considering the different seasonal surveys, no consistent diel rhythm was observed.

4.3.2 Photosynthetic parameters

4.3.2.1 Temporal analysis

Considering the data set obtained during the seasonal tidal cycles (*cf.* – 4.2.2.2), P_{max} ranged between 0.7 and 35.2 mg C mg $Chla^{-1}$ h^{-1}; α ranged between 0.0043 and 0.1578 mg C mg $Chla^{-1}$ h^{-1} (μE $m^{-2}s^{-1})^{-1}$; E_{opt} ranged between 441.9 and 1181.0, while E_k varied between 162.6 and 434.4 μE $m^{-2}s^{-1}$. Mean values, standard deviation, coefficient of variation (CV) and ranges of photosynthetic parameters for each seasonal tidal cycle, are given in Table 4.2. Diel variability of P_{max}, α, E_{opt} and E_k was highest during the summer survey, whereas the lowest variability was observed during the spring survey for P_{max} and α, and, during winter, for E_{opt} and E_k, as shown by the CV. P_{max} and α lowest and highest values were found in winter and summer, respectively. P_{max} increased from morning to afternoon, except during the spring survey when maximum was recorded around noon, whereas α increased from morning to noon in all surveys, remaining relatively constant between noon and afternoon, except in summer when a sharp decrease was observed at this time of day. No consistent pattern was observed for E_k diel variation (Figure 4.5). P_{max} correlated positively with α, E_{opt}, E_o, E_k, temperature and salinity, and negatively with light extinction coefficient (k) and silicate ($p < 0.01$). Photosynthetic efficiency presented similar correlations with the above cited variables. No correlation with chlorophyll *a* was found for P_{max} or α, when considering the entire data set.

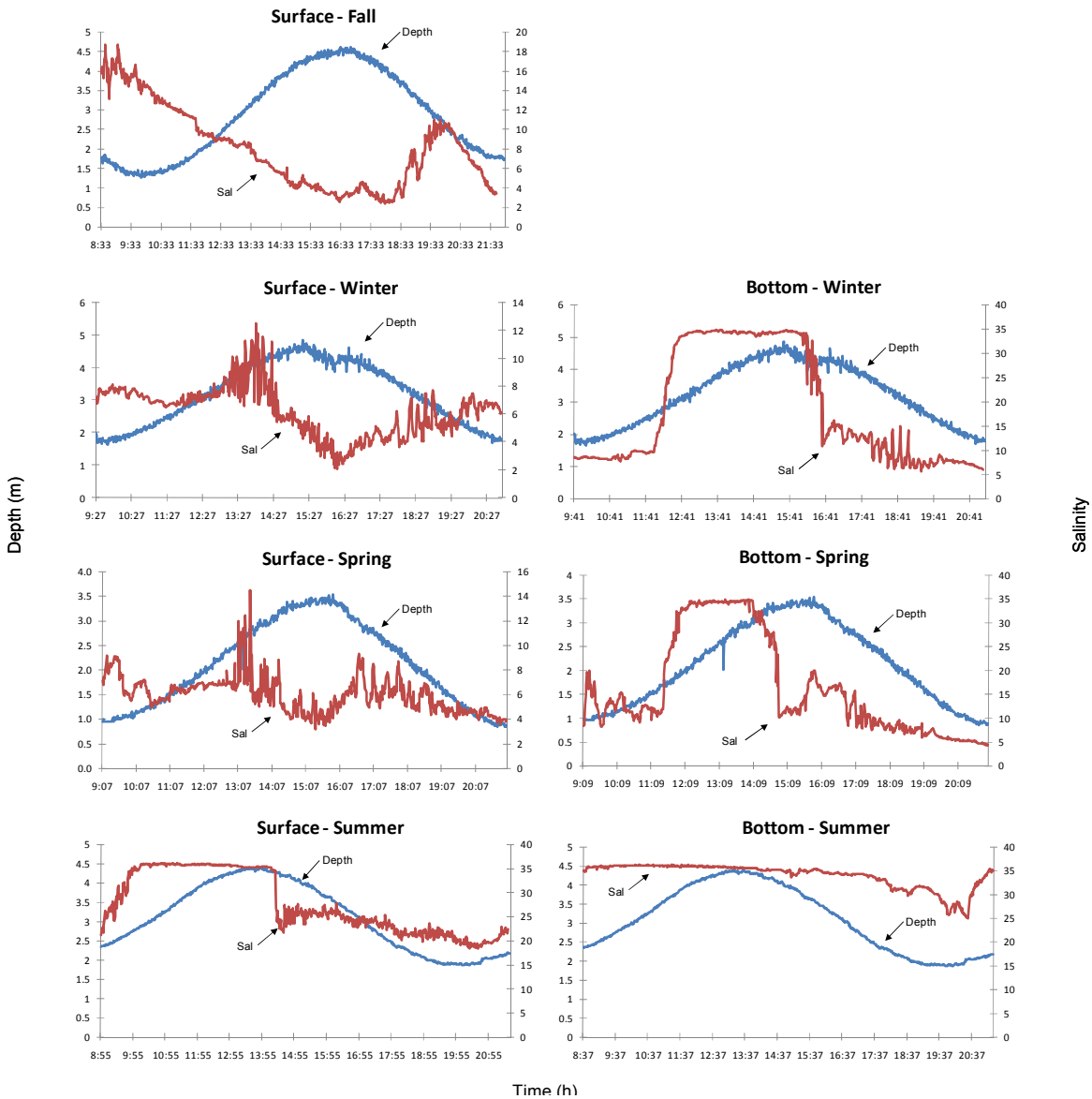

Figure 4.3. Hourly river flow (m^3 s^{-1}) during the fall, winter and summer tidal cycle surveys. Data for the spring survey were not available.

A PCA was performed in order to investigate patterns of similarities between samples based on the contribution of environmental variables and photosynthetic parameters. Projection of samples in the space limited by the first 2 PCs is presented in Figure 4.6. Samples labelled by season show winter and summer samples located at opposite extremes of PC1 (positive and negative, respectively), while fall and spring samples were located in the middle. Variables contributing the most to PC1 were PP, photosynthetic parameters P_{max} and α, E_o, temperature, salinity and ODsat (negatively) and k and nutrients (positively). Higher levels of chlorophyll *a*, E_{opt}, E_k and nutrients, variables that contributed the most to PC2, may explain the partition between spring and fall samples, in addition to the winter samples, along PC2 (Table 4.3). Samples labelled by time of day

showed a slight separation of the morning samples along PC1 in all surveys but summer. Variables contributing positively to PC1, k and nutrients, suggest that the tidal situation (low tide), and associated higher freshwater component, may have explained the observed pattern.

Table 4.1. Descriptive statistics of environmental variables measured during seasonal tidal cycles; s.d. – standard deviation; C. V. – coefficient of variation (%).

	Salinity	Temperature	Nitrate	Ammonium	Phosphate	Silicate	Osat	pH	Chla
		ºC	µM	µM	µM	µM	%		mg m^{-3}
Fall									
Mean	13.2	16.6	51.1	10.0	1.4	31.0	95.6	8.1	2.7
s.d.	9.5	0.4	21.9	4.8	0.5	9.3	5.4	0.3	0.5
Max.	31.3	17.6	86.0	16.6	2.0	46.6	104.2	8.8	3.7
Min.	3.4	16.1	11.9	1.0	0.5	13.3	83.5	7.5	1.6
CV	72.2	2.3	42.9	48.2	34.0	30.0	5.6	3.6	20.0
Winter									
Mean	12.2	10.7	69.6	11.7	1.4	48.2	92.5	9.3	1.2
s.d.	8.1	1.0	24.3	4.8	0.6	15.5	18.1	0.3	0.2
Max.	32.4	13.2	103.4	21.4	2.9	66.7	141.4	10.0	1.7
Min.	6.1	10.0	23.6	1.2	0.6	12.4	56.2	8.9	0.9
CV	66.2	9.1	35.0	41.4	38.9	32.3	19.6	3.5	17.4
Spring									
Mean	14.0	16.9	73.8	14.5	1.2	27.8	114.4	7.9	5.7
s.d.	10.1	0.9	35.6	7.5	0.5	13.2	8.8	0.2	1.2
Max.	35.3	17.9	117.9	29.3	2.0	43.5	132.3	8.2	8.2
Min.	6.5	14.8	6.2	3.1	0.4	2.8	103.9	7.3	3.7
CV	72.3	5.6	48.3	51.4	42.3	47.5	7.7	3.0	21.0
Summer									
Mean	30.2	19.2	13.4	14.2	0.9	3.7	162.7	8.5	2.8
s.d.	6.1	1.5	11.9	11.1	0.6	2.4	9.6	0.5	2.3
Max.	36.8	21.2	35.3	45.0	2.4	11.3	180.3	9.0	6.2
Min.	20.0	17.1	1.0	3.0	0.3	1.1	140.9	7.9	0.3
CV	20.2	7.9	88.5	78.0	62.4	64.6	5.9	5.4	83.6

4.3.2.2 Analysis of photosynthetic parameters variability at different timescales

Comparison of inter- and intra-seasonal variance of photosynthetic parameters (with data from the monthly surveys; *cf.* – 4.2.4.3), showed that P_{max} was significantly ($p < 0.05$) more variable between seasons than within a particular season. Inter-seasonal CVs were, as expected, higher than intra-seasonal, especially for P_{max} and E_{opt} (33 versus13% and 18 versus 7%, respectively). Using data from tidal cycles, inter-seasonal and diel variances were compared. Diel variance was higher for E_{opt} only, while the contrary was true for P_{max} and α, although no statistical significance was obtained. These observations were confirmed by the CVs calculated for the same timescales.

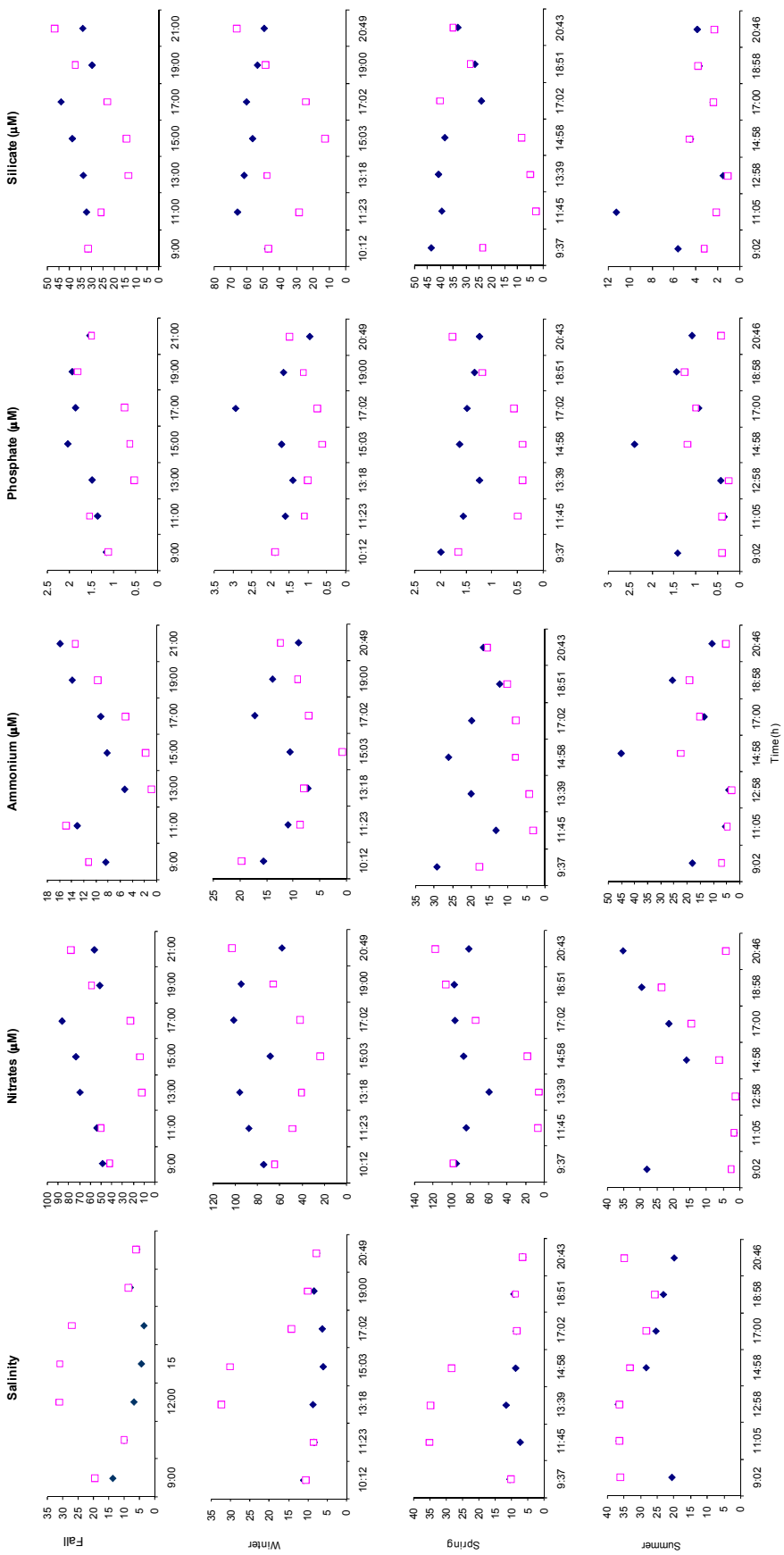

Figure 4.4. Salinity and nutrients variability along the tidal cycle surveys. Open symbols correspond to bottom samples and block symbols correspond to surface samples.

Table 4.2. Descriptive statistics of photosynthetic parameters obtained during seasonal tidal cycles. s.d. – standard deviation; C. V. – coefficient of variation (%); P_{max} in mg C mg $Chla^{-1}$ h^{-1}; α in mg C mg $Chla^{-1}$ h^{-1} (μE $m^{-2}s^{-1})^{-1}$; E_{opt}, E_o and E_k in μE $m^{-2}s^{-1}$; chlorophyll *a* in mg m^{-3}.

Fall	**P_{max}**	**α**	**E_{opt}**	**E_o**	**E_k**	**K**	**Chl *a***
Mean	2.0	0.0094	565.8	899.5	208.2	1.1	2.4
s.d.	0.8	0.0029	82.8	770.4	30.5	0.1	0.4
Max.	2.6	0.0111	644.6	1484.0	237.1	1.2	2.8
Min.	1.1	0.0061	479.4	26.5	176.4	1.1	2.2
C.V.	41.1	30.7	14.6	85.6	14.6	6.6	14.6
Winter							
Mean	1.2	0.0068	475.9	16.8	175.1	1.0	1.1
s.d.	0.4	0.0022	42.0	6.0	15.5	0.1	0.2
Max.	1.5	0.0082	522.9	23.7	192.4	1.1	1.3
Min.	0.7	0.0043	441.9	13.1	162.6	0.9	0.9
C.V.	34.7	31.9	8.8	35.6	8.8	8.5	19.6
Spring							
Mean	3.2	0.0123	704.8	1433.7	259.3	0.8	5.0
s.d.	0.6	0.0006	109.3	503.8	40.2	0.1	0.3
Max.	3.8	0.0130	800.2	1729.3	294.4	0.9	5.2
Min.	2.6	0.0119	585.5	851.9	215.4	0.7	4.7
C.V.	19.7	4.8	15.5	35.1	15.5	10.7	6.3
Summer							
Mean	24.3	0.0901	751.2	1586.8	276.3	0.6	2.4
s.d.	15.9	0.0637	372.4	262.9	137.0	0.2	3.2
Max.	35.2	0.1578	1181.0	1774.8	434.4	0.8	6.0
Min.	6.0	0.0313	525.2	1286.4	193.2	0.4	0.3
C.V.	65.5	70.8	49.6	16.6	49.6	40.6	131.0

4.3.2.3 Spatial analysis

Spatial analysis of photosynthetic parameters was performed with the monthly surveys data set (*cf.* – 4.2.2.2). P_{max} ranged between 0.9 and 9.2 mg C mg $Chla^{-1}$ h^{-1}; α between 0.0042 and 0.0401 mg C mg $Chla^{-1}$ h^{-1} (μE $m^{-2}s^{-1})^{-1}$ and E_k between 137.5 and 692.7 μE $m^{-2}s^{-1}$. Averaged P_{max} and α increased upstream (Table 4.4), as well as chlorophyll *a* concentration and temperature, variables that presented significant ($p < 0.01$) positive correlations with the above mentioned photosynthetic parameters. Positive correlations between P_{max} and chlorophyll *a* and temperature obtained for the entire annual data set were maintained when analysing each individual station.

Table 4.3. Eigenvectors or Coefficients in the linear combinations of variables making up PC's (see Figure 4.6); P_{max} in mg C mg $Chla^{-1}$ h^{-1}; α in mg C mg $Chla^{-1}$ h^{-1} (μE $m^{-2}s^{-1})^{-1}$; E_{opt} and E_o in μE $m^{-2}s^{-1}$; chlorophyll *a* in mg m^{-3}; PP in mgC mg $Chla^{-1}.h^{-1}$; nutrients in μM; temperature in ºC and ODsat in % saturation.

Variable	PC1	PC2	PC3	PC4	PC5
P_{max}	-0.306	-0.183	0.186	-0.135	0.177
E_{opt}	-0.179	0.092	0.465	-0.153	-0.43
E_o	-0.258	0.285	0.08	-0.098	-0.286
k	0.259	-0.016	0.143	-0.542	-0.092
α	-0.308	-0.188	-0.055	-0.069	0.371
PP	-0.315	-0.168	-0.036	-0.052	0.35
Chla *a*	0.024	0.529	-0.007	0.409	-0.061
Nitrate	0.293	0.072	0.13	0.215	0.316
Nitrite	0.195	0.271	-0.023	-0.566	0.302
Ammonium	-0.053	0.039	0.594	0.219	0.227
Phosphate	0.169	-0.05	0.543	0.024	0.148
Temperature	-0.256	0.349	0.093	-0.21	0.095
Silicate	0.317	-0.179	-0.002	0.086	0.086
Salinity	-0.322	-0.117	-0.114	-0.026	-0.173
ODsat	-0.339	0.005	0.066	0.112	0.138
pH	0.072	-0.532	0.164	0.026	-0.317

4.3.3 Temperature and phosphate integration in the Steele's P-E equation

The empirical model integrating light, temperature and phosphate (Eq. 4) was tested with data from incubations performed during the monthly surveys. Although 55% of variance in photosynthetic parameters was accounted for using this model, higher than the 44% of when considering only irradiation, Kp was <0, and thus without any biological meaning. Using a function combining the Steele equation and temperature only, 60% of variation was explained, with parameter estimates of 1.5 mg C mg $Chla^{-1}$ h^{-1} (μE $m^{-2}s^{-1})^{-1}$ for P_{max}, 576.6 μE $m^{-2}s^{-1}$ for E_{opt} and 0.0378 ºC^{-1} for k_T (Table 4.5). The model was also applied to data from individual seasons, in order to investigate different (seasonal) response patterns to those environmental variables. Biologically significant parameters were obtained for spring and fall, with total variance explained of 67% and 82%, respectively (Table 4. 5).

4.4 Discussion

4.4.1 Environmental variability

The high variability of environmental characteristics observed during seasonal tidal cycles was mainly due to river flow control by the dam located at the upper estuary. River flow magnitude influenced water column stratification, which was observed around high tide during all sampling periods, coincident with the increase of river flow during that tidal interval. This river flow effect was particularly noticed during the summer survey, being responsible for the sharp salinity decrease at the surface observed 2.5 hours after the dam started discharging. River flow magnitude and water column stratification also influenced nutrient temporal and vertical distribution. In most estuaries, nutrient concentration is often related to river flow magnitude (Jordan et al. 1991, Balls 1992, Snow et al. 2000, Pastuszak et al. 2003). Pereira et al (2001) reported a tide-nutrient relationship, with a nutrient decrease during the flood and high tide and an increase during the ebb. In the present study, such relationship was not found, due to water column stratification: levels at the surface remained high throughout the flood due to the presence of a lower salinity surface layer, resulting from river flow. A similar pattern would be expected for chlorophyll *a* distribution, since previous work in the Douro presented evidence that phytoplankton originates mostly from the river (Bordalo & Vieira 2005, Azevedo et al. 2008). The general absence of a vertical gradient in chlorophyll *a* concentration, during periods of water column stratification, could be explained by sinking of phytoplankton cells, due to their specific weight, generally exceeding that of the water. Sinking rates depend on morphology, motility, physiological state, density and viscosity of the medium, as well as water circulation (Pitcher et al. 1989). Sinking rates of 0.5 – 0.9 m d^{-1} for estuaries have been reported, although for oceans the range is much broader, reaching 25 m d^{-1} (Huisman & Sommeijer 2002 and references therein). Considering a sinking rate of a few meters per day, during periods of lower river flow, and higher residence times, a vertical uniform distribution of phytoplankton may be achieved. In the Douro estuary, residence time is higher than 1 day for river flows lower than 300 m^3s^{-1}, which is characteristic of spring and summer periods when phytoplankton biomass is higher.

Table 4.4. Descriptive statistics of photosynthetic parameters obtained during annual surveys at the 3 stations along the estuary. s.d. – standard deviation; C. V. – coefficient of variation (%); P_{max} in mg C mg Chla^{-1} h^{-1}; α in mg C mg Chla^{-1} h^{-1} (µE m^{-2}s^{-1})$^{-1}$; E_{opt}, E_o and E_k in µE m^{-2}s^{-1}; chlorophyll *a* in mg m^{-3}.

Station L	**P_{max}**	**α**	**E_{opt}**	**E_o**	**E_k**	**K**	**Chl *a***
Mean	2.3	0.0118	529.5	980.8	194.8	1.2	3.0
s.d.	1.0	0.0044	88.8	686.3	32.7	0.7	1.7
Max.	5.1	0.0195	722.9	2782.0	266.0	2.9	6.2
Min.	0.9	0.0046	373.8	70.0	137.5	0.3	0.7
C. V.	43.9	36.9	16.8	70.0	16.8	58.1	56.4
Station M							
Mean	2.9	0.0130	637.8	1051.3	234.6	1.5	3.7
s.d.	1.2	0.0046	278.3	722.6	102.4	0.8	2.7
Max.	5.6	0.0233	1882.8	2741.0	692.7	4.1	10.5
Min.	1.3	0.0042	408.9	70.0	150.4	0.5	0.5
C. V.	40.2	35.2	43.6	68.7	43.6	54.4	74.3
Station U							
Mean	3.1	0.0147	578.8	1051.3	212.9	1.0	4.6
s.d.	1.6	0.0066	112.0	722.6	41.2	0.0	3.8
Max.	9.2	0.0401	812.5	2741.0	298.9	1.0	14.9
Min.	1.0	0.0045	379.9	70.0	139.8	0.8	0.8
C. V.	50.4	45.0	19.3	68.7	19.3	4.1	82.3

4.4.2 Photosynthetic variability

The ranges obtained for photosynthetic parameters P_{max} and α were broader than in other systems reported in the literature (Cote & Platt 1983, Goosen et al. 1999, Basterretxea & Aristegui 2000, Tillmann et al. 2000, Macedo et al. 2001, Jouenne et al. 2005, Struski & Bacher 2006) although similar to the range reported by Boyer (1993) for the temperate Neuse river estuary (0.14 - 33.9 mg C mg chla^{-1} h^{-1} for P_{max}). The highest values were obtained during the summer tidal cycle survey, at noon / afternoon samples, when P_{max} exceeded the theoretical maximum of 25 mg C mg Chla^{-1} h^{-1}, according to Falkowski (1981). This may be explained by the low chlorophyll *a* concentration of those samples (0.40 and 0.86 mg m^{-3}, respectively), due to the influence of chlorophyll *a* poor coastal waters. This problem has also been reported by Lohrenz et al (1994) in coastal waters of the Gulf of Mexico, except that in the present study, rates of carbon fixation obtained for these samples were not low (around 10 mg C m^{-3} h^{-1}), suggesting the presence of a low biomass but highly productive phytoplankton. The presence of low biomass and high primary production was previously detected in the lower Douro estuary (Bordalo 1991). In addition, Lohrenz et al (1994) calculated the maximum theoretical limit for α of 0.11 mg C mg Chla^{-1} h^{-1} (µE m^{-2}s^{-1})$^{-1}$. Values above these limits were obtained only for one of the samples mentioned above, the noon summer survey sample.

Table 4.5. Parameters obtained by integration of temperature and phosphate limiting functions with Steele equation; T – temperature (ºC); Ph – phosphate (µM); Kp – phosphate half-saturation constant (µM); k_T – temperature augmentation rate (ºC)$^{-1}$

	P/E with T				P/E with T and Ph				
Dataset	P_{max}	E_{opt}	k_T	Variance explained	P_{max}	E_{opt}	k_T	Kp	Variance explained
All data	1.47	576.7	0.0378	0.60	1.41	578.1	0.0334	a)	0.56
Winter	1.25	454.4	0.0292	0.37	1.27	452.3	0.0182	a)	0.38
Spring	1.24	566.0	0.0546	0.73	1.48	564.4	0.0601	0.3443	0.69
Summer	2.04	643.4	0.0325	0.76	1.29	643.3	0.0502	a)	0.77
Fall	3.56	606.8	a)	0.74	3.77	608.9	0.0150	1.1373	0.82

a) value <0, thus without biological meaning.

E_k has been frequently used to describe the physiological adjustments of algal populations to changing environmental conditions (Cote & Platt 1983, Macedo et al. 2001), expressing phytoplankton photoacclimational state (Sakshaug et al. 1997, Behrenfeld et al. 2004). In the present study, E_k levels were within the range reported for other coastal systems (Lohrenz et al. 1994, Tillmann et al. 2000, Macedo et al. 2001, Struski & Bacher 2006).

4.4.2.1 Temporal variability

Positive correlation of P_{max} with temperature is a common feature to most studies (Cote & Platt 1983, Lohrenz et al. 1994, MacIntyre & Cullen 1996, Tillmann et al. 2000), and is consistent with P_{max} being a function of the enzymatic reactions carried out in photosynthesis (Cote & Platt 1983). P_{max} also presented a positive correlation with salinity and incident light but negative with k and silicate, reflecting the seasonal variability observed for this parameter. From PCA analysis it is clear that seasonal variability is higher than diel variability, since samples from the same seasonal tidal cycles were grouped together, with the exception of summer samples, which were spread along PC2, reflecting changes in light and chlorophyll *a* concentration during that survey. Summer and winter surveys were projected at opposite extremes relative to PC1, contrasting higher P-E values, irradiance, temperature and salinity (summer) to higher k and nutrient levels (winter).

Variability in P-E parameters has been divided by Behrenfeld et al (2004) in E_k-dependent variability, associated with independent changes in P_{max} and α that alter E_k; and E_k-independent variability, associated with parallel changes in P_{max} and α , with little influence on E_k. The former results predominantly from physiological adjustments to changing light conditions (photoacclimation), whereas for the latter no clear physiological explanation has been found. The positive correlation between P_{max} and α observed in the present study was also reported by other authors (Cote & Platt 1983, Lohrenz et al. 1994,

Jouenne et al. 2005, Struski & Bacher 2006), suggesting a predominance of E_k-independent variability. This phenomenon could be due to the high environmental variability observed throughout the surveys. The high physicochemical and biological variability that characterises estuarine systems, may complicate short term photoacclimation (Jouenne et al. 2005).

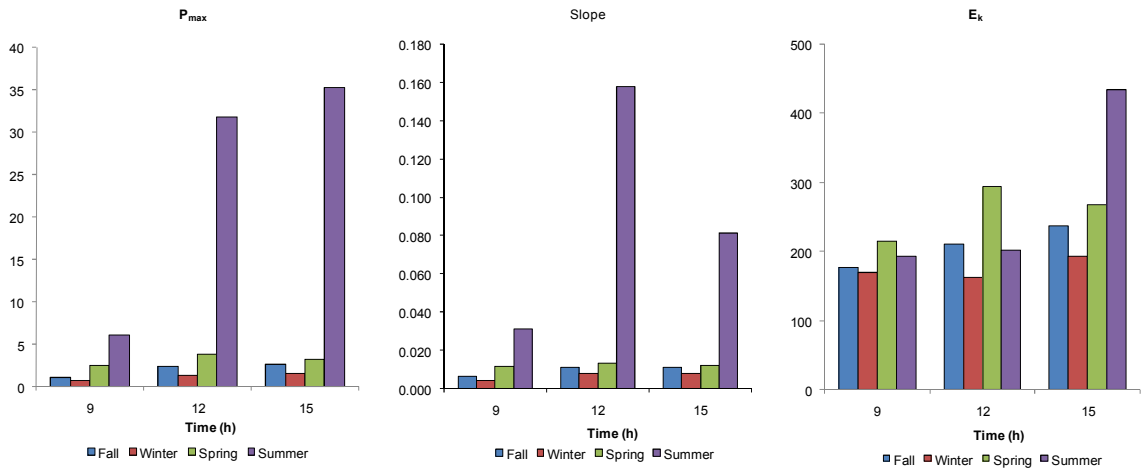

Figure 4.5. Diel variation of photosynthetic parameters P_{max} (in mg C mg $Chla^{-1}$ h^{-1}), α (in mg C mg $Chla^{-1}$ h^{-1} (µE $m^{-2}s^{-1})^{-1}$) and E_k (in µE $m^{-2}s^{-1}$).

Diel variability has been attributed to a combination of endogenous physiological oscillations as well as responses to environmental factors (Prezelin 1992, Binder & DuRand 2002). In highly variable systems, such as estuaries, in which photic and mixing conditions may vary in an hourly basis, consistent patterns of diel variability of photosynthetic parameters are more difficult to observe. The subtle separation of morning samples in PCA reflected adaptation to lower light levels and higher riverine influence on the estuary, since the variables contributing the most (positively) to PC1 were nutrients and k, as well as the tidal situation during that period (ebb). This doesn't imply low diel variability, however, as shown by the CV calculated for each tidal survey (Table 4.2). Maximal P_{max} values observed around noon or in the afternoon in the Douro estuary, were consistent with previously reported observations in other coastal systems (Lohrenz et al. 1994, Basterretxea & Aristegui 2000, Jouenne et al. 2005). Previous studies in other temperate estuaries observed a tidal signal in P_{max} variability: lower P_{max} at low tide and higher at high tide (Goosen et al. 1999, Jouenne et al. 2005). In the present study, tidal cycles were always initiated in the morning during low tide, which means that high tide coincided with noon. This allowed the reduction of variability due to different tidal situations but, on the other hand, prevented the analysis of tidal influence on P-E parameters

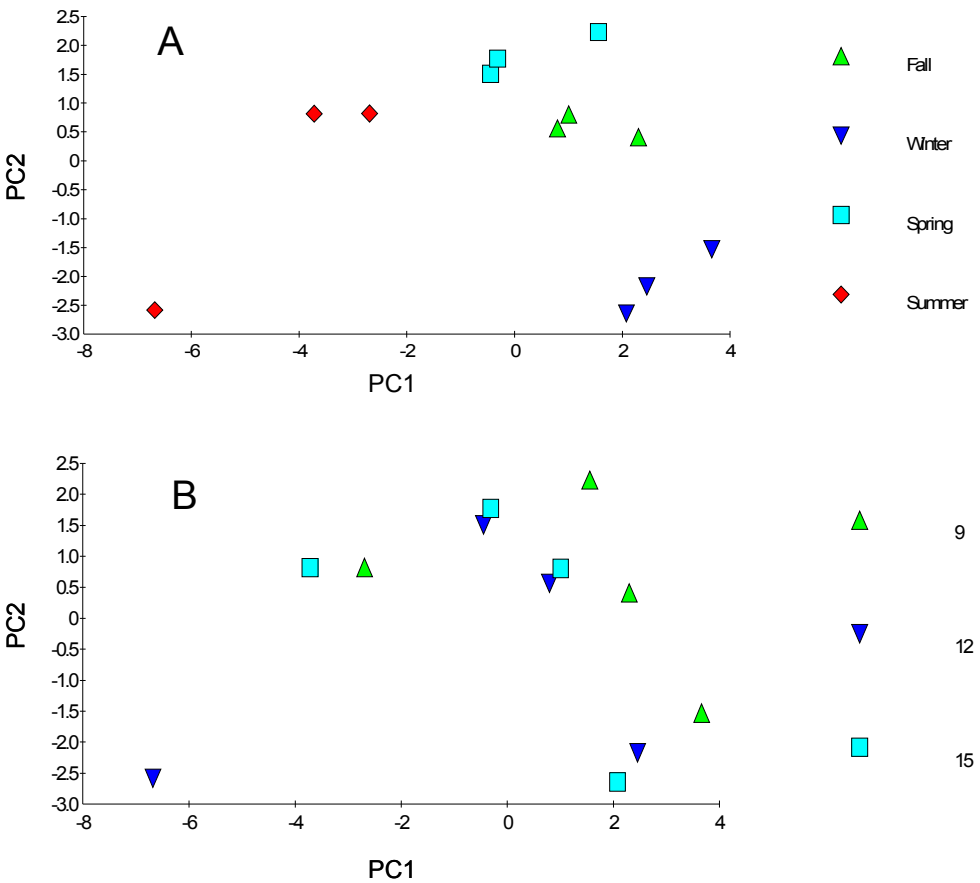

Figure 4.6. Projection of samples in the space defined by the first two principal components. A – samples labelled by season; B – samples labelled by time of day.

Analysis of inter-seasonal, intra-seasonal and diel timescales of variability in photosynthetic parameters, suggests that in the Douro, photosynthetic parameters P_{max} and α are most variable at a seasonal timescale, while for E_{opt}, diel variability was highest, as expected. Thus, predictive models of primary productivity should take into account this seasonal variability, when used to estimate primary production over larger timescales.

4.4.2.2 Spatial variability

In the Douro estuary, P_{max} highest values were found at the upstream station, although the spatial pattern of variability was not the same in all surveyed periods. This trend is opposite to observations in other systems. In the Neuse River estuary, Boyer (1993) found an inverse spatial pattern, a declining P_{max} with distance from the estuary mouth, attributed to acclimation to lower light levels of the riverine phytoplankton communities. In the maximum turbidity zone of the Westerschelde, Goosen (1999) observed a lower specific rate of photosynthesis in the more upstream stations, attributed to riverine

phytoplankton meeting saline conditions. The pattern observed in the Douro may be explained by higher temperatures in the upstream station, which is confirmed by a positive correlation between those two variables. A positive correlation was also obtained with chlorophyll *a*, unusual in coastal ecosystems, attributed to the relatively low phytoplankton biomass, preventing intraspecific competition from lowering photosynthetic capacity, on one hand, and the physiology of phytoplankton related to their origin in a semi-lotic (reservoir) ecosystem (Azevedo et al. 2006).

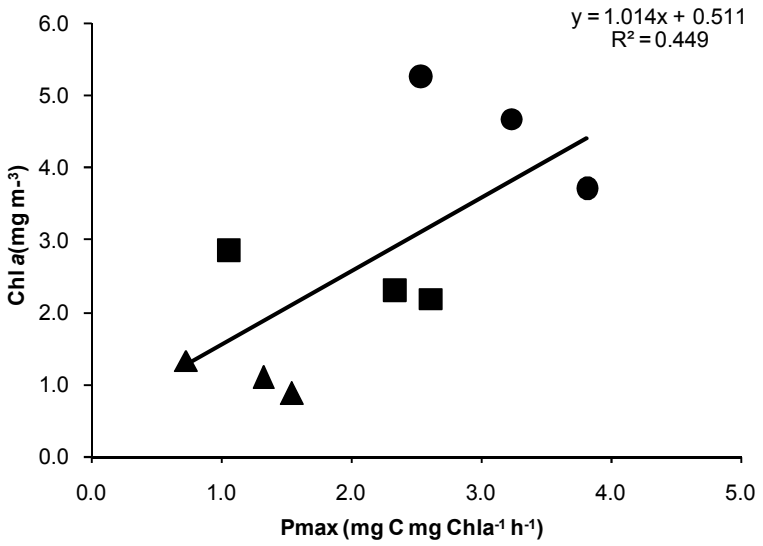

Figure 4.7. Relationship between P_{max} and Chl *a* obtained during spring, fall and winter tidal surveys. ● - Spring; ■ - Fall and ▲ - Winter.

The positive correlation between P_{max} and chlorophyll *a* obtained during annual surveys was not observed during seasonal tidal cycles, when considering the entire data set. However, if the summer survey is not considered, a significant positive relationship between those variables emerges, although analysis of this relationship for data collected during individual surveys shows this correlation to be somewhat misleading. For each individual survey, an inverse relationship between those variables seems to exist (Figure 4.7), suggesting that other factors, such as temperature, should also influence P_{max} variability over a seasonal time scale. These observations enhance the multivariate facet of photosynthetic response control of natural phytoplankton assemblages within highly dynamic systems. Changes in environmental conditions may influence phytoplankton photosynthesis directly (temperature, light, nutrients) through physiological adaptations or indirectly, through changes in species composition, induced by hydrodynamic alterations.

This will depend on the physiologic adaptation time of phytoplankton and whether it is higher or shorter than the hydrodynamic changes of the system.

The attempt to integrate temperature and phosphate limiting functions in PP estimation showed that the inclusion of temperature improves model performance, while including the phosphate potential limiting effect, only works for spring and fall. In fact, modelling of phytoplankton nutrient limitation is not straightforward, since it depends not only on the water N:P ratio, but also on factors such as nutrient regeneration and intracellular concentration.

4.5 Conclusions

The results obtained from this study suggest that:

- The most important timescale of P_{max} and α variability was seasonal, although diel variability in summer was also considerable.
- Diel analysis showed that P_{max} highest values were found around noon or in the afternoon, while α maxima were observed around noon.
- P_{max} was generally higher upstream, decreasing towards the estuary mouth.
- Light, temperature and salinity were the most influential factors on P-E parameters variability. Additionally, PP prediction accuracy was increased by combining light and temperature limiting functions.
- The relationship observed between salinity and P-E parameters may indicate that variability in these parameters could also be caused by species composition shifts, changing photosynthetic response of the phytoplankton assemblage. Since species composition was not in the framework of this study, it deserves further research.

CHAPTER 5

Influence of river discharge patterns on the hydrodynamics and contaminant dispersion in the Douro estuary (Portugal)

5.1 Introduction

The issue of freshwater inflows to estuaries and the consequences of changes brought about by human activities in the magnitude and timing of these inflows has been thoroughly debated (e.g. Hopkinson & Vallino 1995, Alber 2002). Changes in freshwater inflow cause alterations in water circulation, stratification and residence time, as well as in dissolved and particulate materials delivered to estuaries by river runoff, such as nutrients and sediments. Moreover, changes in estuarine hydrodynamics will affect dispersion of contaminants and other substances originated from runoff and wastewater discharges, which is particularly critical in urban estuaries. The ability to predict water quality in estuaries as a function of river discharge is fundamental to the management of these water bodies, as required by the European Water Framework Directive.

Hydrodynamic models have been used to predict water circulation and salinity distribution patterns in estuaries and coastal systems in response to controlling factors. The influence of those forcing factors, which are mainly freshwater inflow, tidal action and weather

events, depend on system characteristics (Dyer 1997). Several three-dimensional (3D) hydrodynamic models have been recently developed, validated and applied in studies concerned with the understanding of how the systems respond to those forcing factors (e.g. Ulses et al. 2005, Ji et al. 2007, Levasseur et al. 2007, Liu et al. 2007). For example, river discharge was found to be a dominant factor influencing salt intrusion in the Danshuei River estuary (Liu et al. 2007) and freshwater inflow influence on estuarine stratification and flushing was analysed for St. Lucie estuary (Ji et al. 2007).

Frequently, hydrodynamic modelling is also performed as a basis for water quality studies or for coupling with biogeochemical models (Larson et al. 2005, Ulses et al. 2005, Levasseur et al. 2007). Water quality modelling has been used to predict contaminant transport, distribution and fate in estuaries and coastal zones (e.g. Falconer & Lin 1997, Thouvenin et al. 1997, Passone et al. 2003). In fact, the use of mathematical models to address environmental and ecological problems is increasing, evidencing their role as scientific tools, to increase understanding of ecosystems properties, as well as management tools, to predict the results of human action affecting the environment (Jørgensen & Bendoricchio 2001).

The Douro estuary is limited upstream by a dam, built in 1985, at 21.6 Km from the mouth, for electric power production. Therefore, freshwater inflow to the estuary is strongly dependent on electric power demand, especially during the summer low river flow period. As a consequence, river inflow to the estuary is characterised by high short-term variability, between zero flow and > 1,000 m^3s^{-1}, in a matter of hours (Bordalo, unpublished data). The estuary was defined as a salt wedge under low river flow by Vieira & Bordalo (2000). This feature was attributed by those authors to its tidal behaviour, close to a standing wave, produced by the reflection of the tidal wave on the dam wall. These authors implemented a salt budget box model and estimated residence time between 8 hours and 16 days, depending on river flow. Urbanization levels of the banks are high, especially in the middle and lower estuary, responsible for increased levels of bacterial and ammonium contamination (Azevedo et al. 2008).

In a previous work, a two-dimensional hydrodynamic model was implemented for the lower estuarine stretch as a decision support tool within the scope of a project regarding hard stabilization of the Douro estuary mouth (Silva 1996). Some of the constraints enhanced by the author, in implementing the model, concerned the presence of water column saline stratification even under low river flow, as well as a highly variable flow pattern. Temporal and spatial variability of these characteristics were previously

addressed and included in a conceptual model of the river flow influence on the Douro estuary biogeochemistry (Azevedo et al. 2008). In the present work, a three-dimensional (3-D) hydrodynamic model was implemented, in order to improve understanding of hydrodynamic characteristics of the estuary and the effects of river flow management on estuarine water circulation and quality. The questions to be answered are the following:

- What is the impact of river flow magnitude and discharge patterns on estuarine hydrodynamic behaviour?
- What is the influence of those variables on salinity distribution and contaminant dispersion along the estuary?

Answering these questions may help understanding the effects of changes induced in the estuary by river flow regulation at the dam, as a function of electric power production.

5.2 Methodology

5.2.1 Study site

The Douro estuary is part of the largest watershed in the Iberian Peninsula (98,000 km^2). More than 50 large dams have been built in the watershed for irrigation and electric power generation. The construction of the most downstream dam, at 21.6 Km from the mouth, in 1985, reduced estuarine length by 60% (Bordalo, unpublished data). The Douro drains into the Atlantic Ocean, at the west coast of Portugal, near the city of Porto (41.14ºN and 8.66ºW; Figure 5.1). It is a drowned valley estuary, narrow in the middle and upper reaches, widening towards the mouth, reaching an average width of 645 m in the lower stretch. The mouth is partially obstructed by a concrete stabilized sand bar, with ongoing hard work alterations for navigation accessibility improvement. Bathymetry is characterized by a regularly dredged 6-m deep navigation channel and a V-shaped cross-section, with asymmetric slopes. Daily freshwater discharge by the Douro River ranges from 0 to more than 13,000 m^3s^{-1}, with an average of 505 m^3s^{-1}. Other sources of freshwater are present along the estuary, originated from 13 small rivers, with average flows in the range 0.1-5 m^3s^{-1} (Figure 5.1).

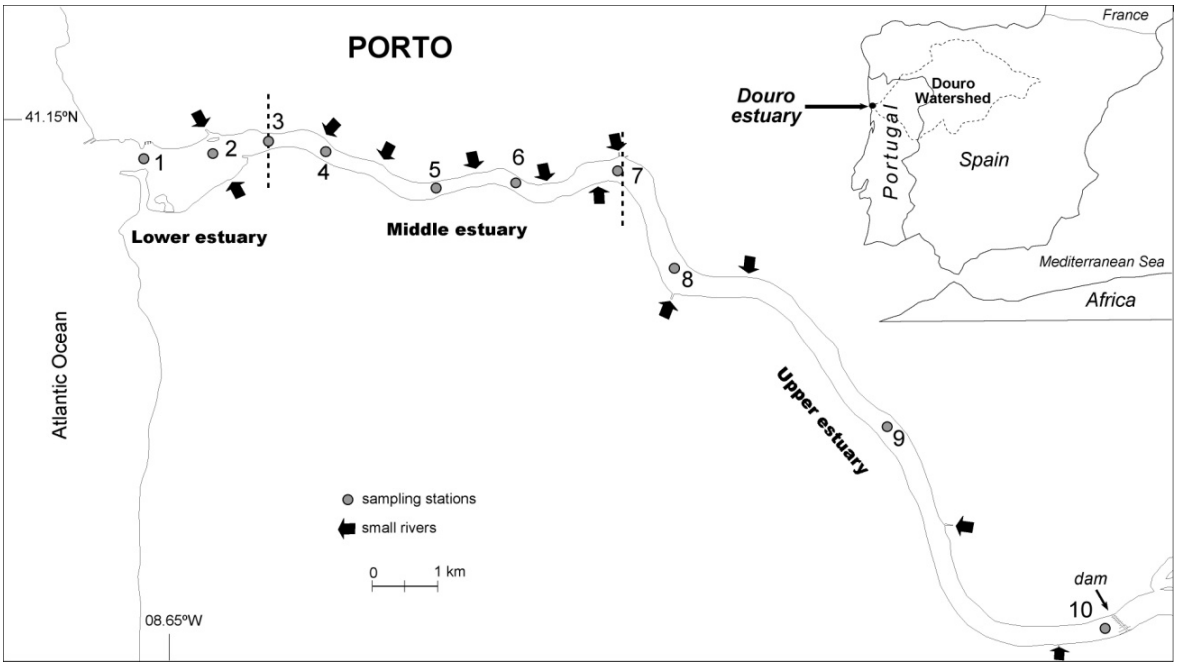

Figure 5.1. Study site, showing the 3 estuarine stretches and the upstream limit. Arrows represent location of main small rivers discharging into the estuary.

5.2.2 Model description

The model used in this work is a 3-D hydrodynamic model, based on a finite difference staggered grid (Vreugdenhil 1989) with a spatial resolution of 75 m. Model implementation was carried out using EcoDynamo - an object oriented modelling software (Pereira & Duarte 2005). EcoDynamo is based on a shell, providing the user interface and allowing the interaction between different objects. These objects simulate several hydrodynamic, thermodynamic, and biogeochemical processes and variables. EcoDynamo allows the use of different models and model setup definitions, such as simulation time, time-step, object activation, output formats and selection of simulated variables for output. In the present study, 5 objects simulating forcing conditions and 2 objects simulating state variables were used (Table 5.1).

Wind object reads wind speed and direction time series and returns corresponding values to the water temperature and the hydrodynamic objects. Air temperature object reads air temperature values, which are also returned to the water temperature object. Light object returns light intensity values at sea level and at any depth. Water column light intensity is computed from the Lambert–Beer law, using the water light extinction coefficient computed by a suspended matter object. Water temperature object uses outputs from the previous objects to calculate water temperature from heat losses through evaporation,

sensible heat and radiative exchanges between the water and the atmosphere. Light intensity and water temperature objects use standard formulations described in Brock (Brock 1981) and Portela and Neves (Portela & Neves 1994). Tide object uses the equations and harmonic components described in SHOM (SHOM 1984, 1992) to calculate water level at the sea boundary. Boundary water levels are returned to the hydrodynamic object, where they are used to calculate the propagation of the tidal wave into the estuary.

Table 5.1. EcoDynamo objects implemented for the Douro estuary.

Object type	Object name	Object outputs
Forcing conditions	Wind	Wind speed
	Air temperature	Air temperature
	Water temperature	Water temperature
	Light	Water column total and photosynthetically active radiation (PAR)
	Tide	Tidal height
State variables	3D-Hydrodynamic	Sea level, current velocity and direction, salinity, water density
	Suspended matter	Total particulate matter (TPM), particulate organic matter (POM) and water column light extinction coefficient

The hydrodynamic object implements a three dimensional baroclinic solution of the equations of motion and continuity (Eq. 1 – 4) (Knauss 1997), to calculate the velocity field and water level, under the Boussinesq and Hydrostatic assumptions. Horizontal and vertical diffusions are treated as a Fick law. Horizontal diffusivity is used as a calibration parameter, while vertical diffusivity is computed with a mixing length model following Nihoul (1982) and Santos (1995).

$$\frac{d_{u_x}}{dt} + \frac{\partial(uu)}{\partial x} + \frac{\partial(uv)}{\partial y} + \frac{\partial(uw)}{\partial z} - v_x \frac{\partial^2 u}{\partial x^2} - v_y \frac{\partial^2 u}{\partial y^2} - v_z \frac{\partial^2 u}{\partial z^2} = -\frac{\partial P}{\rho \partial x} - \frac{Cf|u|u}{H} + \frac{\partial \tau x}{\rho \partial z} + f v_y \quad \textbf{(1)}$$

$$\frac{d_{v_y}}{dt} + \frac{\partial(vv)}{\partial y} + \frac{\partial(vu)}{\partial x} + \frac{\partial(vw)}{\partial z} - v_x \frac{\partial^2 v}{\partial x^2} - v_y \frac{\partial^2 v}{\partial y^2} - v_z \frac{\partial^2 v}{\partial z^2} = -\frac{\partial P}{\rho \partial y} - \frac{Cf|v|v}{H} + \frac{\partial \tau y}{\rho \partial z} + f u_x \quad \textbf{(2)}$$

$$\frac{d\xi}{dt} = \frac{\partial_{u_x}}{\partial x} + \frac{\partial_{v_y}}{\partial y} + \frac{\partial_{w_z}}{\partial z} \quad \textbf{(3)}$$

$$\frac{\partial_{u_x}}{\partial x} + \frac{\partial_{v_y}}{\partial y} + \frac{\partial_{w_z}}{\partial z} = 0 \quad \textbf{(4)}$$

Where:

u, *v* and *w* - velocity components along the east – west (*x*), north-south (*y*) and vertical (*z*) directions, respectively (ms^{-1});

ξ - water elevation (m);

v_x, v_y, and v_z - diffusivities along the three dimensions ($m^2 s^{-1}$);

P – pressure ($N m^{-2}$);

Cf - rugosity coefficient calculated from a turbulent kinetic energy closure scheme following Santos (1995) and Dyke (2001);

ρ - water density ($kg m^{-3}$);

H - water depth (m);

Tx and *Ty* - wind stress coefficients along the two horizontal dimensions and

f - Coriolis parameter.

Equations (1) and (2) represent the horizontal momentum equations; (3) and (4) represent the equation of continuity for the surface and remaining layers, respectively. Vertical velocities are calculated by continuity using (4). In the model, equation 3 is integrated vertically. Therefore, vertical velocities cancel, with elevations resulting from the horizontal balance of momentum. The model uses an Alternate Direction Implicit Scheme (ADI) for numerical stability.

The general model algorithm is:

$$v_{ijk}^{t+1} \rightarrow \xi_{ij}^{t+1/2} \rightarrow u_{ijk}^{t+1} \rightarrow w_{ijk}^{t+1} \rightarrow V_{ijk}^{t+1} \; and \; \xi_{ij}^{t+1} \rightarrow S_{ij}^{t+1}$$

Where,

i, *j* and k - lines, column*s* and layers of model domain;

V_{ijk},- cell volume and

S_{ijk} - concentration of any property at a particular cell.

One of the horizontal equations of motion (e.g. v_{ijk}) is solved implicitly (*t+1*) and used in the equation of continuity, integrated vertically. At this point, only past estimates of velocities and elevations are known. However, the mentioned vertical integration eliminates vertical diffusivities, allowing an implicit solution of water elevations, used as a surrogate for barotropic pressure, to be obtained. Thereafter, these water elevations are used in the horizontal equations of motion to solve for the corresponding velocity

components. Afterwards, the updated horizontal velocity components are used to estimate vertical velocities by continuity and the volume of each surface cell. Finally, the velocity field and diffusion are used in the transport equation for dissolved and suspended properties. For all technical details on the numerical solution of equations (1 – 4) see Duarte (2008). The model is forced by tidal height at the sea boundary, river discharges, wind drag forces and density gradients.

5.2.3 Model calibration and validation

Data used for model calibration and validation were retrieved from a dataset compiled from monthly sampling surveys conducted in 2003, along the entire estuary, during flood and ebb, as well as from 13-hour tidal cycles, conducted at an anchor station (station 1, Figure 5.1) near the mouth, in October 2003 and January and July 2004. Analysis of those data was presented in previous works (Azevedo et al. 2006, Azevedo et al. 2008). The model was calibrated for horizontal diffusion and maximum vertical diffusivity, using September surveys data. The procedure used for calibration and afterwards for model validation was as follows: model initialization was performed with data from flood surveys and obtained results were compared to data (salinity and water temperature) measured in ebb surveys of the same month. The parameter values that produced the best fit with observations were used for subsequent simulations.

Model validation was carried out with data from May, June, July, August, October, November and December 2003, as well as the tidal cycle data mentioned above. These periods were chosen as representative of the river flow range observed in the Douro. Simulated periods varied between 44 hours (September) and 167 hours (June). Model results were also compared to Admiralty Tables data for tidal height, as well as tidal lag and amplification of the tidal range between estuary mouth and head.

Model performance was assessed by comparing observations and predictions using “goodness of fit” and absolute error measures. For an overview of advantages and limitations of several of these measures, see Legates and McCabe (1999). In the present work, the Modified Index of Agreement, d1 (Willmott et al. 1985) and the Modified Coefficient of Efficiency, E1 (Nash & Sutcliffe 1970, Legates & McCabe 1999) were used as “goodness of fit” evaluation measures:

$$d_1 = 1 - \frac{\sum_{i=1}^{n}|Oi-Pi|}{\sum_{i=1}^{n}(|Pi-\bar{O}|+|Oi-\bar{O}|)} \quad \textbf{(5)}$$

$$E_1 = 1 - \frac{\sum_{i=1}^{n}|Oi-Pi|}{\sum_{i=1}^{n}|Oi-\bar{O}|} \quad \textbf{(6)}$$

Where,

Oi - observed values at each time i

Pi - predicted values at each time i

$\bar{O}$ - mean of observations

n - number of observations.

Additionally, absolute error was estimated using the Root Mean Square Error (RMSE) and the Mean Absolute Error (MAE):

$$RMSE = \sqrt{\frac{1}{n}\sum_{i=1}^{n}(Oi - Pi)^2} \quad \textbf{(7)}$$

$$MAE = \frac{1}{n}\sum_{i=1}^{n}|Oi - Pi| \quad \textbf{(8)}$$

5.2.4 Simulation Scenarios

In order to evaluate the effects of river flow magnitude and variability on the hydrodynamic behaviour and contaminant dispersion in the Douro estuary, three discharge regimes were combined with three flow magnitudes in a total of nine scenarios (Table 5.2).

Table 5.2. Scenarios representing different river flow variability and magnitude (see text).

	Flow variability		
Flow magnitude	Hourly	Daily	Constant
Standard	S1	S2	S3
Half	H1	H2	H3
Double	D1	D2	D3

Each regime differed in the way flow was distributed over time. The “hourly” regime was similar to the real one observed in June 2003 – with a large hourly variability. The second

regime was obtained by calculating daily mean flows, therefore reducing flow variability – "daily" regime. Finally, the third regime was obtained by averaging flow over the simulation period and was therefore constant – "constant" regime (Figure 5.2). The idea of simulating scenarios of different flow variability was based on the assumption that, in summer, under low freshwater input, low variability regimes are representative of conditions in the estuary before the dam was built. Therefore, comparing high with low flow variability scenarios was used as a proxy for comparing estuarine behaviour before and after the dam was built. For each regime, the measured ("standard") flow was halved and doubled to investigate the effects of its magnitude on estuarine hydrodynamics.

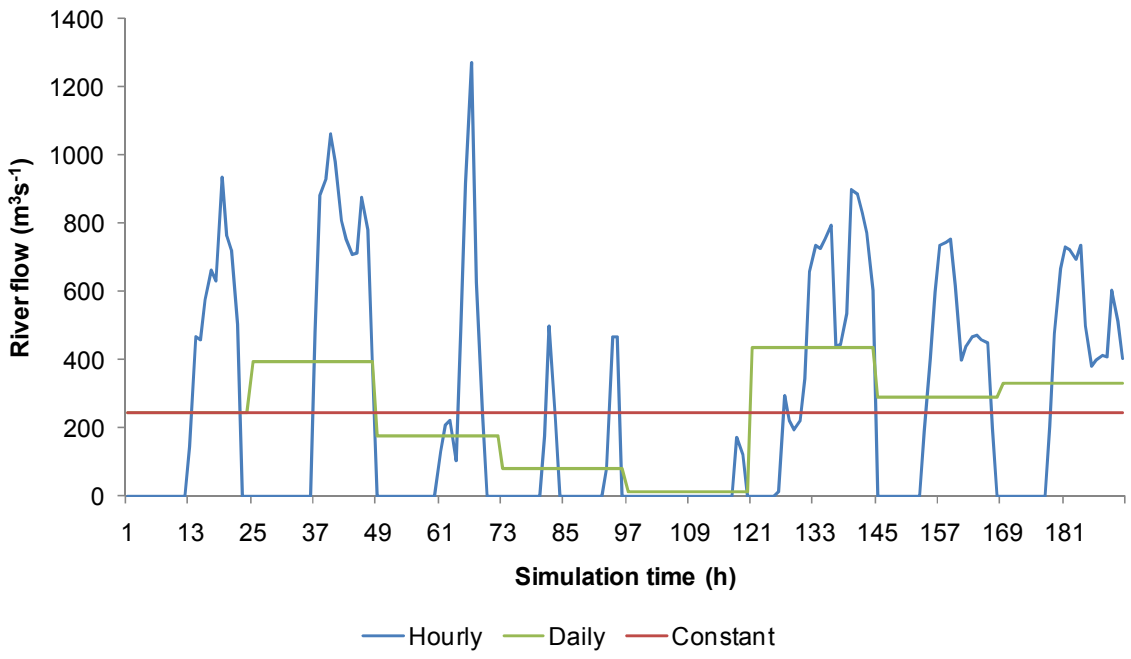

Figure 5.2. River flow regimes tested: 1) the observed, highly variable flow; 2) daily averaged flow, and 3) constant flow throughout the simulation period, corresponding to the averaged value of the flow measured for the entire simulation period (*cf.* – Methodology – simulation scenarios).

For these model runs, salinity and temperature conditions from June 2003 were used to initialise the model, corresponding to the river flow values used in scenario S1 ("hourly standard" flow).

For evaluation of the hydrodynamic response, results from the different scenarios were compared in terms of averaged salinity, residual flow, stratification, seawater intrusion and freshwater residence time. Stratification was assessed by calculating the stratification index Estuary Number, Ne (Dyer 1997):

$$Ne = \frac{P(Fm)^2}{TR} \quad \textbf{(9)}$$

$$Fm = \frac{uf}{\sqrt{gh(\Delta\rho/\rho)}} \quad \textbf{(10)}$$

$$uf = \frac{R}{AT} \quad \textbf{(11)}$$

Where,

P - tidal prism volume (m^3)

Fm - densimetric Froude number

T - tidal period (s^{-1})

R - river discharge (m^3 s^{-1})

uf - crosssectional average of the vertically averaged mean velocity (ms^{-1})

g - acceleration due to gravity (ms^{-2})

h - estuary depth (m)

Δρ-density difference between surface and bottom (kg m^{-3})

ρ- vertically averaged mean density (kg m^{-3})

Freshwater residence time (Tr) was calculated as:

$$Tr = \frac{Vf}{Q} \quad \textbf{(12)}$$

$$Vf = fV \quad \textbf{(13)}$$

$$f = \frac{S_0 - S}{S_0} \quad \textbf{(14)}$$

Where,

Tr - residence time (d)

Vf - freshwater volume (m^3)

Q - inflow (m^3s^{-1})

f - freshwater fraction

S_0 - ocean salinity

S - salinity at any part of the estuary

For contaminant dispersion analysis, a conservative tracer was used. Tracer river loads of 100 μM were introduced, for tributaries located in the estuary (Figure 5.1), simulating contaminant discharges from these sources. Contaminant dispersion effects were analysed by comparing average tracer levels concentration and dispersion over the estuary.

5.3 Results

5.3.1 Model calibration and validation

Model calibration was performed by using September data, a low river flow period when water column stratification reached half the estuarine length. The criteria for parameter selection were mainly salinity stratification and seawater intrusion, features whose simulation is not straightforward in the Douro, as acknowledged by previous works (Silva 1996). A horizontal diffusion coefficient of 5 m^2s^{-1} and a maximum vertical diffusivity of 0.005 m^2s^{-1} were selected.

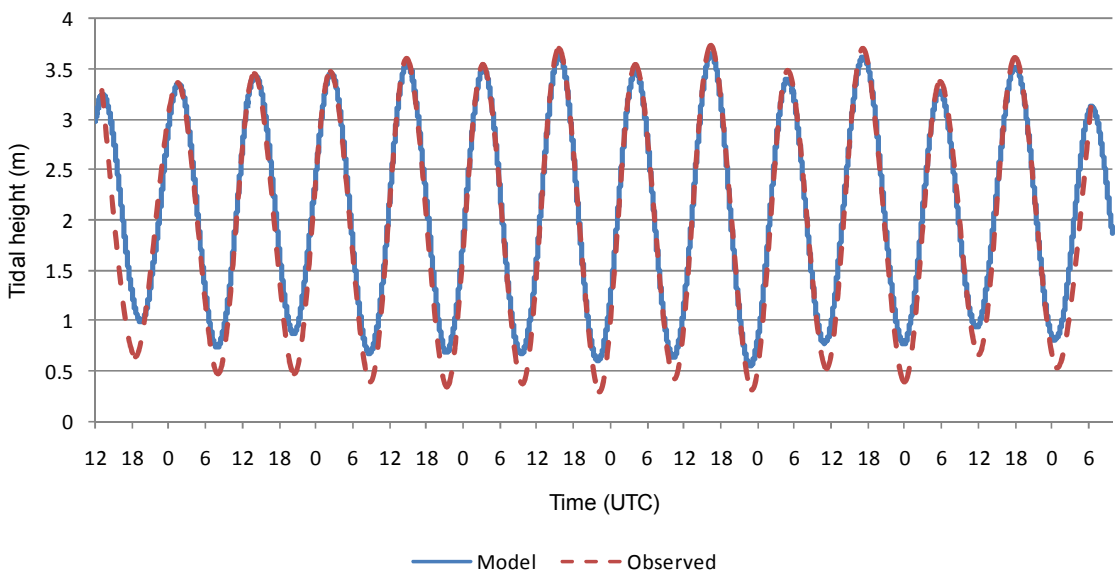

Figure 5.3. Tidal heights predicted by the model versus observed values (obtained from Admiralty Tables) at the estuary mouth.

Analysis of calibration results showed that the model presented good predictions of salinity and water temperature distributions at the surface and middle depth whereas, at

the bottom layer, saline intrusion was underestimated. Thus, in order to improve model performance, an increase in vertical resolution from 3 to 10 layers was tested for June, August and September. However, the small improvement in model predictions did not compensate for the larger computation overhead. Therefore, subsequent simulations were performed with a 3 layered morphology.

A good agreement was achieved between model predictions and tidal height and phase data from Admiralty Tables (Figure 5.3). Small discrepancies observed in tidal height may be explained by the fact that the model was forced by harmonics for the closest commercial port (Leixões, at 4 km to the North), whereas observations correspond to Admiralty Table values corrected for the Douro mouth. Cross-correlation analysis of simulated tidal height at the estuarine mouth and head resulted in a tidal lag estimate of one hour, similar to values from Admiralty Tables (1h 02min at high water and 1h 49min at low water, for spring tides). Analysis of tidal height time series predicted by the model, suggests upstream tidal amplification (Figure 5.4) in direct relation with river flow. In the absence of flow, an amplification of approximately 20 cm was predicted at high water, similar to Admiralty Tables data (23 cm), whereas at low water, no amplification was apparent in model results, although expected from Admiralty Tables (41 cm). Probably, this discrepancy may be explained by average river flow conditions over the period used to produce the mentioned tables.

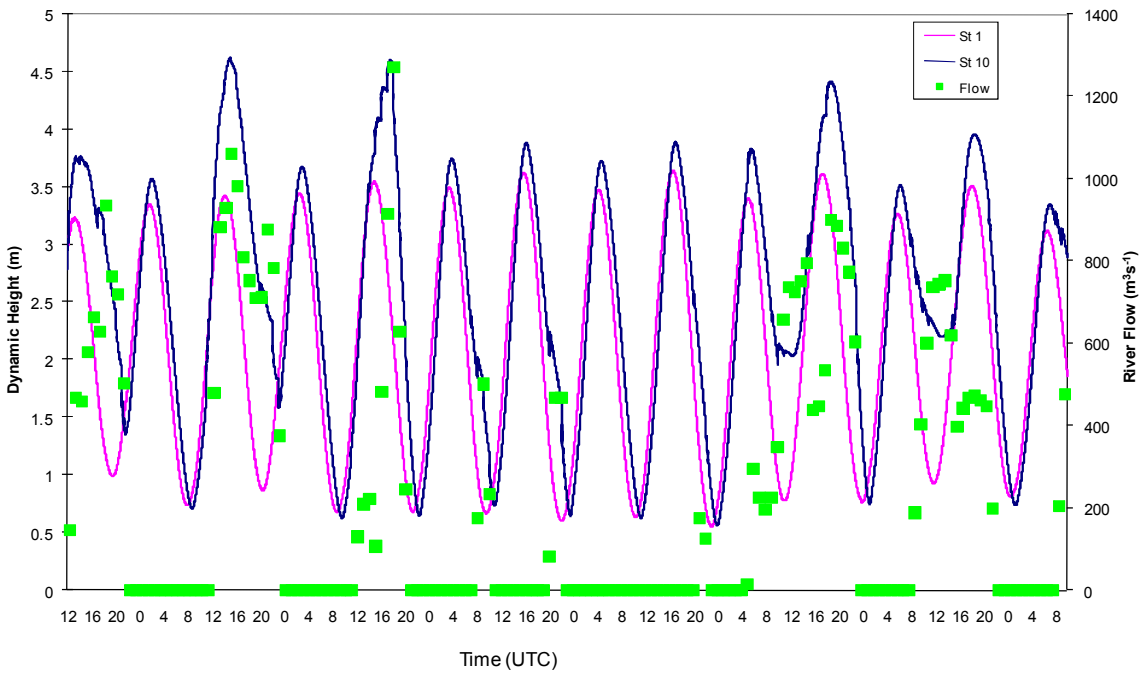

Figure 5.4. Tidal height predicted by the model at 2 extreme locations: station 1, near the mouth and station 10 near the dam, the estuary upstream limit (*cf.* – Figure 5.1). Squares correspond to river flow hourly values.

Observed data from the tidal cycles at station 1 are shown in Figure 5.5. Surface and bottom data were available for comparison.

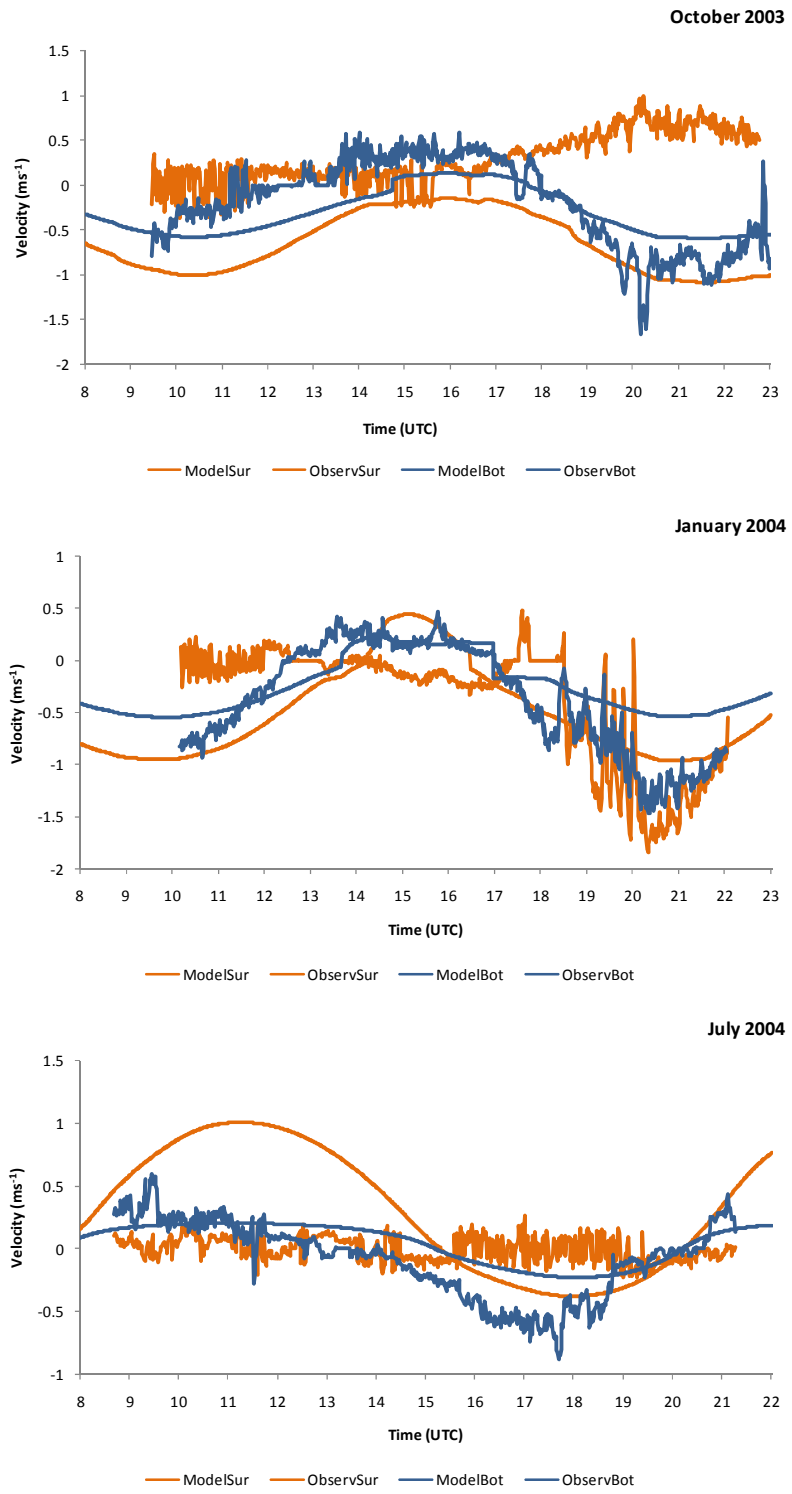

Figure 5.5. Current velocities predicted by the model and observed values, from seasonal tidal cycles conducted at the estuary mouth.

Measurements at the surface presented a somewhat random pattern, indicative of turbulence, whereas at the bottom, a similar pattern was observed for all surveys: higher velocities during the ebb with values exceeding 1.5 ms^{-1}. A good agreement was found between model and observations at the bottom, but not at the surface (Figure 5.5).

Comparisons between observed and predicted values of salinity and temperature for June (Figure 5.6), August (Figure 5.7) and October (Figure 5.8), confirm that these variables were reasonably predicted by the model for the upper and middle layers. Differences between observed and predicted values were higher at the bottom layer, especially in periods of low river flow, reflecting model underestimation of seawater intrusion, a fact already observed in the calibration experiments.

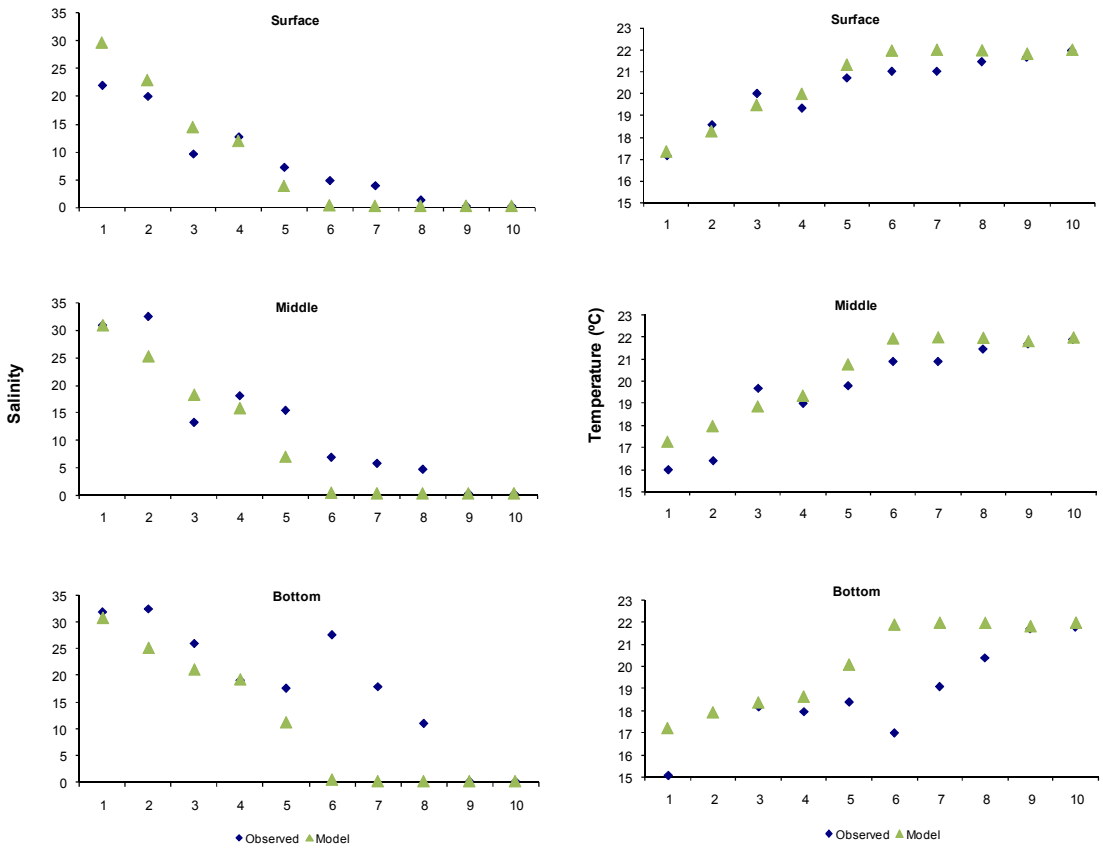

Figure 5.6. Observed versus predicted values for salinity and temperature at 10 stations along the estuary (*cf.* – Figure 5.1) and at 3 depths for June simulation.

Model performance evaluation by the Modified Index of Agreement (d1) and the Modified Coefficient of Efficiency (E1), resulted in values of 0.8 and 0.6, respectively, for salinity and 0.9 and 0.8, respectively, for temperature. Those results are indicative of a good model performance, considering that d1 varies between 0 (poor model) and 1 (perfect

model), and E1 >0 means that model predictions are better than the observed mean (Legates & McCabe 1999). Absolute error measures, RMSE and MAE, yielded values of 7.0 and 3.9 for salinity and 1.5 and 0.9 (ºC) for water temperature, respectively.

5.3.2 Scenario analysis

As expected, average salinity increased with decreasing river flow. The "hourly" flow regime (scenarios S1, H1 and D1) yielded the highest values whereas the "constant" flow regime (scenarios S3, H3 and D3) yielded the lowest. Ne values were always higher than 0.1, indicating that the estuary as a whole was not classified as stratified. Since this is an estuarine wide index, some stratification may be present in some parts of the estuary, namely in the most downstream sector. The lowest Ne (0.39) was obtained for scenario H2 ("daily" regime, half river flow), and values increased with river flow magnitude for all regimes (Table 5.3).

Table 5.3. Average salinity, Ne, freshwater residence time and tracer concentration for the different river flow magnitudes and regimes tested. Ne < 0.1 indicative of stratified conditions; Rt – freshwater residence time (days); Tracer in µM.

	Hourly				Daily				Constant			
Flow	Salinity	Ne	Rt	Tracer	Salinity	Ne	Rt	Tracer	Salinity	Ne	Rt	Tracer
Half	10.29	0.41	3.95	4.54	10.27	0.39	3.95	4.64	10.06	0.42	3.98	4.16
Standard	**8.93**	**0.63**	**2.08**	**3.19**	**8.67**	**0.57**	**2.10**	**3.26**	**8.28**	**0.55**	**2.13**	**2.86**
Double	7.77	1.05	1.09	2.33	6.98	1.18	1.12	2.35	6.31	1.22	1.15	1.97

Residual velocity increased with river flow, as expected. Higher velocities were obtained for the "hourly" river flow regime. Maximal residual velocities of 1.08, 0.80 and 0.78 ms^{-1} were obtained for simulations S1, S2 and S3, respectively. Halving the river flow resulted in decreased residual velocities of 0.89, 0.78 and 0.75 ms^{-1}, for simulations H1, H2 and H3, respectively, whereas doubling the river flow resulted in increased velocities: 1.61, 1.02 and 0.86 ms^{-1}, for simulations D1, D2 and D3, respectively. Freshwater residence time (Tr) was calculated for each river flow regime and magnitude. As expected, residence time increased with decreasing flow magnitude whereas, concerning the different flow regimes, similar results were obtained, with slightly increasing values from the "hourly" to "constant" regimes (Table 5.3).

The influence of river flow variability and magnitude on the conservative tracer behaviour was analyzed by comparing its mean concentration values for each scenario, as well as its highest levels and spatial distribution for different tidal conditions: high versus low tide

and spring versus neap tide. Considering river flow magnitude, tracer mean and highest levels always increased with decreasing flow (Table 5.3 and Figure 5.9), whereas regarding river discharge regimes, mean tracer concentration was highest for the "daily" regime and lowest for the "constant" regime. Tidal dynamics influenced tracer levels and dispersion (Figure 5.9). Tracer dispersion over the estuary was always higher at low tide as well as, generally, its concentration. For S3 and D3 scenarios, an increasing gradient towards the mouth was observed, at low tide, probably due to flushing, in agreement with the lower average tracer levels obtained for these simulations.

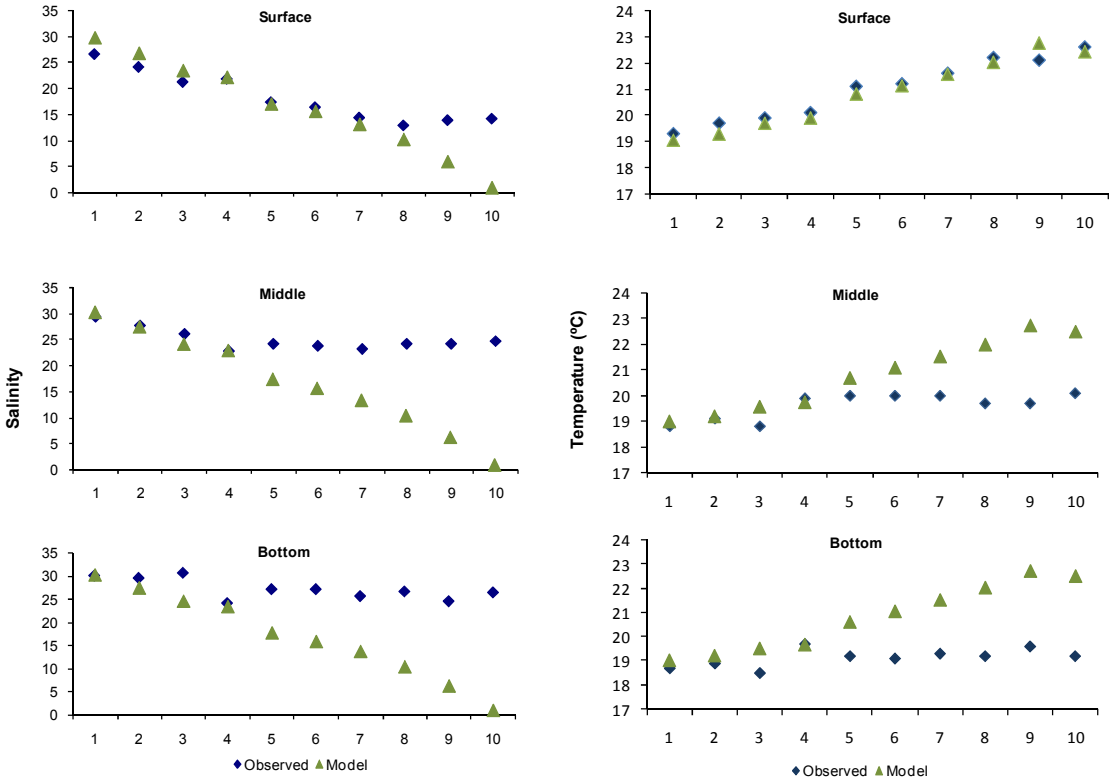

Figure 5.7. Observed versus predicted values for salinity and temperature at 10 stations along the estuary (*cf.* – Figure 5.1) and at 3 depths for August simulation.

Comparison of spring versus neap tide was performed using constant flow conditions, to avoid flow variation effects. No obvious differences arose, except for a higher tracer dilution downstream at spring tide, caused by a higher seawater intrusion. Thus, the best situation, concerning estuary contamination, was obtained for D3 scenario, corresponding to "constant" double flow, whereas the worst situation was obtained for H2 scenario, corresponding to "daily" half flow.

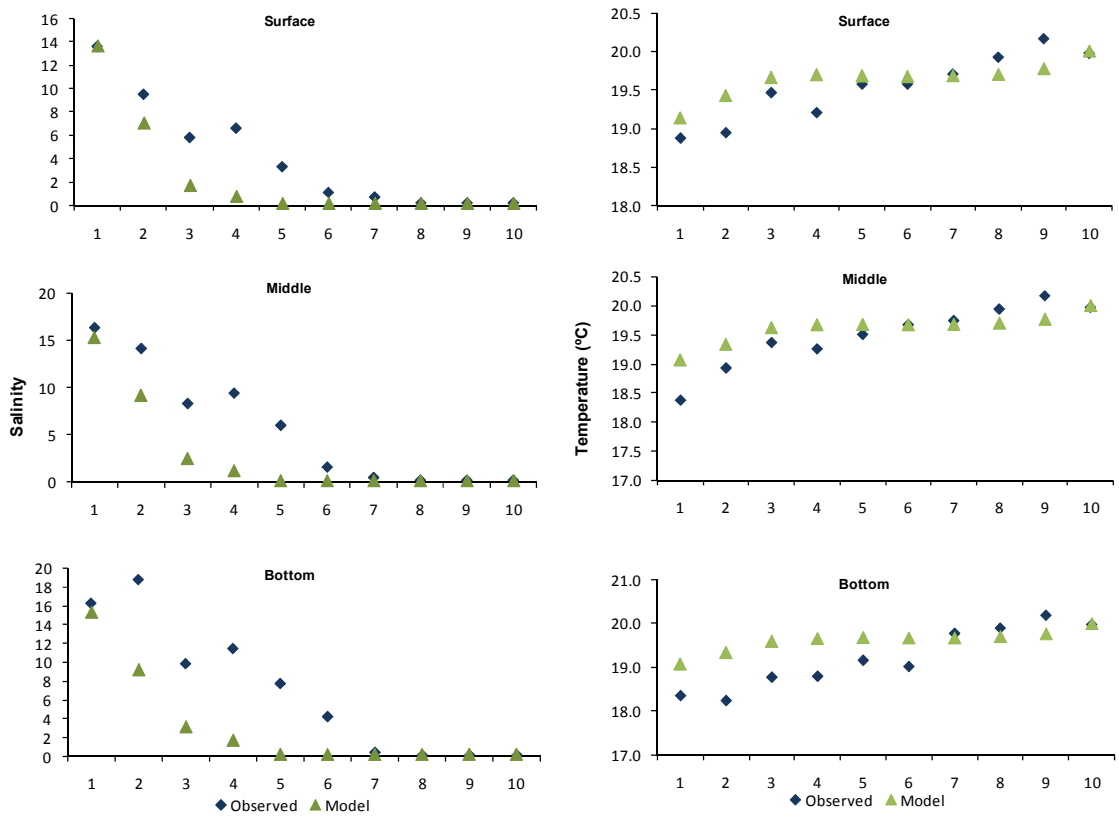

Figure 5.8. Observed versus predicted values for salinity and temperature at 10 stations along the estuary (*cf.* – Figure 5.1) and at 3 depths for October simulation.

5.4 Discussion

5.4.1 Model calibration and validation

For model calibration and validation, time series observations were used for tidal dynamics whereas for salinity and temperature, longitudinal data for individual sampling surveys were used.

Results obtained from applying goodness of fit (d1 and E1) and error measures (RMSE and MAE) to model predictions of salinity and temperature are indicative of good model performance. A detailed analysis of those data (Figures 5.6 – 5.8), considering temporal and spatial variability confirms that, generally, good predictions of salinity and temperature were obtained. The only exceptions were the extremely low river flow periods, as in

August, when high salinity levels were found at the bottom layer near the dam, during the ebb. In this situation, model predictions tended to underestimate salt water intrusion. One possible explanation for this underestimation may be the location of the sea boundary. Tidal height variability at this boundary is one of the major forcing functions. Moreover, since the boundary is located at the estuary mouth, the water within model domain picks up momentum, during the flood, only from this point upstream, whereas in reality, advection from distances further away from the estuary mouth may be an important energy input to estuarine circulation. One way to overcome this problem would be to relocate model boundary further away from estuarine mouth. However, this was not done due to the lack of detailed bathymetric data outside the river mouth. Current velocity prediction could also beneficiate from this improvement, since modelled values were lower than observations, at the bottom layer. General agreeing trends were nevertheless found between predictions and observations.

Tidal lag, or the delay between the tidal phase at the mouth and at the head of the estuary, was well predicted by the model. Tidal amplification was also well predicted by the model, although for high tide situation only. In the Douro, tidal amplification is caused by resonance effects due, on one hand, to the frequency of the ocean tide being close to the frequency of free oscillation of the main estuary channel (dictated by its length and depth) and, on other hand, to the narrowing of the channel cross-section in the upstream direction (Vieira & Bordalo 2000). Discrepancies with observed values found for low tide may be explained by river flow values during the period when Admiralty Table results were obtained. Another explanation may lay in an insufficient resolution of model morphology. Bearing in mind the weaknesses stressed above, quantitative and qualitative evaluation of model performance allowed a reasonable validation of the model and its use for scenario testing.

5.4.1 Scenario analysis

The influence of river flow regime on the estuary hydrodynamics was translated in higher mean salinity for the “hourly” regime, decreasing for “daily” and “constant” regimes, suggesting that, as freshwater inflow becomes more regular, salinity levels decrease. Increased salinity obtained for the more variable flow regime appears to result from salt water intrusion during periods of low river flow and incomplete flushing of this sea water during periods of higher flow. Results suggest that as flow variability increases, under

periods of low average flow (summer), the estuary tends to become saltier than under a stable discharge.

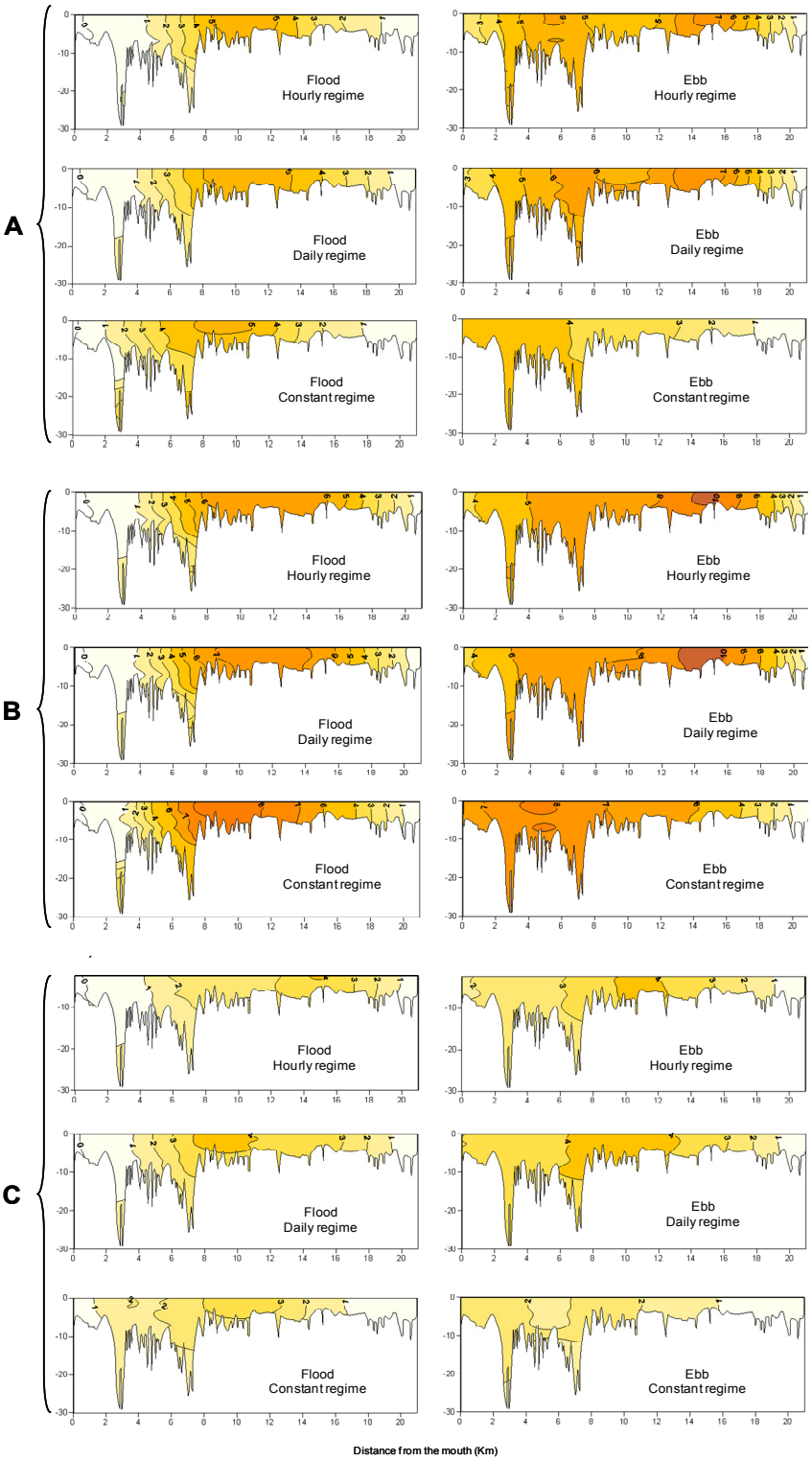

Figure 5.9. Spatial distribution of tracer concentration during flood and ebb periods, for the, 9 scenarios of flow variability and magnitude: A) standard flow magnitude; B) halved river flow; C) doubled river flow.

Ne results for the different flow scenarios did not follow the same pattern for all flow magnitudes tested. Ne increased with river flow magnitude, which means that departure from stratified conditions occurred for higher river inflows. This is in agreement with previous work in the Douro, when an inverse relationship between river flow magnitude and Ne was found (Azevedo et al. 2008). It was suggested that overall stratification of the Douro estuary is expectable for river flows lower than 300 m^3s^{-1}. The relationship between density stratification and river flow is dependent on systems characteristics; in estuaries where freshwater inflow is generally low, this relationship is positive and stratification is enhanced by flow increases (Snow et al. 2000, Uncles & Lewis 2001). On the other hand, in systems characterised by high freshwater inflows, or river dominated systems, this relationship is negative and stratification develops when river discharges are reduced (Kurup et al. 1998, Liu et al. 2007). Schroeder et al (1990), in Mobile Bay, reported that low river flow lead to weak stratification, which increased with increasing flow, collapsing under high discharges, due to flushing rather than mixing.

Concerning conservative tracer dispersion, two main factors controlled its behaviour - tidal action and Douro river discharge. Since neither was a source to the estuary, their action resulted in tracer dilution. For this reason, it appears straightforward the increase in tracer levels obtained with decreased flow (reduced dilution by river flow), and higher levels and dispersion for low tide situation (decreased dilution by sea water). Lower mean tracer levels obtained for the “constant” flow regime for all flow magnitudes tested, together with the lower salinity obtained for the same scenarios suggest that dilution by river flow was the factor responsible for the encountered pattern. Higher freshwater residence time obtained for these conditions, which results in a lower flushing time, was related to the lower salinity levels obtained, since residence time is defined as the time to replace the freshwater volume present in the estuary. Thus, dilution by freshwater, was the process responsible for the lower tracer levels obtained for this discharge regime (constant river flow).

Differences in contaminant behaviour between spring and neap tide are likely to be limited to the lower estuarine reaches, near the mouth, since they result from a higher dilution by increased sea water intrusion during spring tides. Passone et al (2003), in a study about effluent discharge policies found that the spring tide with high freshwater inflow was the best situation concerning pollutant distribution in the Upper Milford Haven estuary. In the present study, under the conditions tested, the worst situation in the case of contaminant release from tributaries would be under low river flow periods and during the ebb, with a daily constant flow regime. Since this was the scenario that resulted in the lowest Ne, it

may be suggested that water column stratification may enhance contamination hazards, additionally to decreased river inflow.

The consequences of contaminant discharges from freshwater sources along estuaries are known to be dependent on river flow magnitude as well as tidal conditions. Results presented here suggest that, apart from average magnitude, river flow variability may also play a role in dispersing contaminants. Stable flows seem to be the most effective in dispersing contaminants in the Douro. The fact that contaminant dispersion does not depend only on average river flow, points out to the existence of non-linear interactions between flow magnitude and variability.

5.5 Conclusions

A three-dimensional hydrodynamic model was implemented for the Douro estuary and used to analyse several scenarios in terms of river flow magnitude and variability. Results obtained lead to the following conclusions: (i) Apart from river flow magnitude, its variability also plays an important role in estuarine hydrodynamics; (ii) Stable flows seem to reduce average salinity and to be more effective in dispersing contaminants than highly variable flows of the same average magnitude.

From these conclusions, it seems reasonable to infer that flow management may have important effects on estuarine hydrodynamics through interactions between flow magnitude and variability. Furthermore, considering that stable summer freshwater inputs are a proxy for estuarine behaviour before the dam was built (cf. – Methodology – Simulation scenarios), when those inputs depended mostly on Douro base flow, it may be speculated that flow regulation through the dam may be responsible for increasing estuarine salinity during the summer months and reducing its dilution potential for contaminant dispersion.

CHAPTER 6

Influence of freshwater inflow variability on the Douro estuary biogeochemistry: a modelling study

6.1 Introduction

The dynamic nature of estuaries at different time scales, from annual to seasonal, is related to several factors, being freshwater inflow variability one of the most important. Alterations to natural river flow variability have been increasingly affecting these ecosystems worldwide, due to climate change or direct human intervention. One of the most drastic interventions is dam construction, which may introduce important alterations in the amount, timing and quality of freshwater delivered to estuaries (Hopkinson & Vallino 1995, Alber 2002). When damming has consumptive purposes, freshwater input is likely to decrease; whereas if its purpose is flood regulation, discharge pulses are attenuated or eliminated. In all cases, water quality changes caused by impoundment will occur, namely in suspended and dissolved materials. The response of biological communities to these alterations may include changes in species composition, diversity, abundance and distribution, with repercussions on estuarine productivity (Cloern et al. 1983, Sklar & Browder 1998, Snow et al. 2000, Alber 2002, Kimmerer 2002a, Yamamoto & Hatta 2004, Chicharo et al. 2006a).

Phytoplankton is affected by changes in freshwater inflow by several mechanisms, mainly associated with physical-chemical processes, such as density driven estuarine circulation (Cloern et al. 1983), advection from the euphotic zone (Zakardjian et al. 2000), nutrient input (Malone et al. 1988, Mallin et al. 1993, Testa & Kemp 2008), increased suspended solids (which reduces light availability) and residence time (e.g. Sin et al. 1999). More than one of these processes may be involved in phytoplankton control within a given system, at different times. For example, during winter, phytoplankton production may be limited by light, whereas during the growing season, nutrient limitation may occur (Pennock & Sharp 1994, Thompson 1998).

Coupled hydrodynamic-biogeochemical models have been used to increase understanding of the relationship between physical-chemical processes and phytoplankton dynamics. For example, Robson & Hamilton (2004) found that the inclusion of three-dimensional (3D) processes in a phytoplankton growth model improved the reproduction of a *Microcystis* bloom formation and collapse in the Swan River Estuary. Huret et al (2005) implemented a coupled 3D physical-biogeochemical model in the Rio de la Plata estuary and plume and were able to simulate the spatial dynamics of primary production corresponding to the different physical-chemical conditions in each estuarine region. Xu and Hood (2006) applied a coupled physical-biological model to Chesapeake Bay for simulation of biogeochemical dynamics under dry and wet conditions. Trancoso et al (2005) applied a 3D hydrodynamic-ecological model to Ria de Aveiro (Portugal) to simulate dynamics and productivity of phytoplankton and macroalgae, finding that hydrodynamic conditions may be important for the competition between those two primary producers. Saraiva et al (2007) used a coupled hydrodynamic-biogeochemical model for eutrophication risk assessment in several Portuguese estuaries with different characteristics. Coupled hydrodynamic-biogeochemical models have also been used to predict phytoplankton responses to changes in freshwater inflow due to increased nutrient loads (Chan et al. 2002) or to reduction in vertical mixing (Byun et al. 2005).

In biogeochemical models, primary production is often modelled based on photosynthesis-irradiance (P-E) equations. There are several formulations available in the literature, which may be empirical or mechanistic, according to whether they are based on observations or on physiological processes. P-E equations may also be static or dynamic, according to whether the photosynthetic parameters are considered constant or variable in time. When a time-dependent behaviour of the P-E relationships is observed, dynamic formulations should be used in ecosystem models (Duarte 2005).

In the Douro estuary, freshwater inflow is controlled by a dam located 21.6 Km from the mouth, whose operation is based on commercial strategies rather than on environmental issues. As a result, the discharge regime is highly variable, especially during low flow periods.

In a previous work (Chapter 5), a 3-dimensional hydrodynamic model was implemented for the Douro estuary, and used to evaluate the influence of different freshwater discharge regimes in estuarine water circulation, salinity and contaminant dispersion. Results indicated that stable flows seemed to reduce average salinity and to be more effective in dispersing contaminants when compared to the present, highly variable flows of the same average magnitude. In the present study, biogeochemical processes were coupled to the above mentioned hydrodynamic model in order to address the influence of freshwater flow variability and magnitude in the estuarine phytoplankton, nutrient and suspended matter dynamics. Thus, the objectives of this work are to:

- Calibrate and validate a biogeochemical model coupled to a previously implemented hydrodynamic model for the Douro estuary.
- Use the model to understand how phytoplankton biomass and production, nutrient and suspended matter temporal and spatial dynamics are influenced by freshwater flow variability and magnitude.
- Analyse the benefits of including P-E parameters variability in primary production modelling of the Douro estuary.

6.2 Methodology

6.2.1 Study site

The Douro estuary is a drowned valley, narrow estuary, located at the end of the largest watershed of the Iberian Peninsula, draining into the Atlantic Ocean, at 41.14°N and 8.66°W, near the city of Porto, Portugal (Figure 6.1). The main freshwater source to the estuary is the Douro River. Freshwater inflow to the estuary is controlled by a dam built at

21.6 Km from the mouth, representing its upstream limit. The estuary is subjected to a highly variable discharge regime, ranging from 0 to 13,000 m^3s^{-1}, with a present average of 505 m^3s^{-1}. Tidal regime is mesotidal and semi-diurnal, being characterized by a standing wave behaviour which promotes stratification of the water column for flows lower than 800 m^3s^{-1} (Vieira & Bordalo 2000). These authors reported a residence time ranging from 8 hours to more than two weeks, depending on river flow. The middle and lower estuarine reaches are highly urbanized, presenting high bacterial levels originated from untreated wastewater discharges (Bordalo & Vieira 2005, Azevedo et al. 2008).

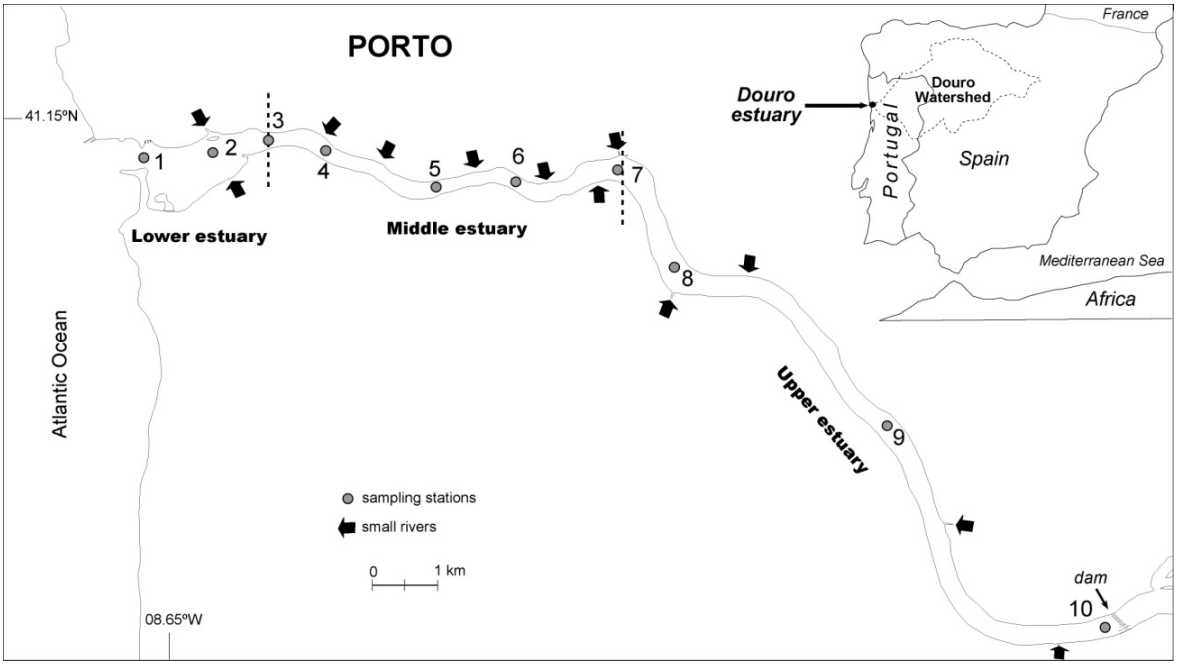

Figure 6.1. Study site, showing the 3 estuarine stretches and the upstream limit. Arrows represent location of main small rivers discharging into the estuary.

6.2.2 Model description

The model used in the present work is a 3-D model based on a finite difference staggered grid (Vreugdenhil 1989) with a spatial resolution of 75m. It was implemented with EcoDynamo - an object oriented modelling software (Pereira & Duarte 2005), which provides a user interface allowing the interaction between different objects. These objects simulate hydrodynamic, thermodynamic and biogeochemical processes and variables. EcoDynamo also allows the use of different models and model setup through selection of simulation time, timestep, objects, output formats and variables. For the present work, 4 objects simulating state variables and 5 objects simulating forcing functions were used (Table 6.1).

Table 6.1. EcoDynamo objects implemented for the Douro estuary.

Object type	Object name	Object outputs
State variables	3D-Hydrodynamic	Sea level, current speed and direction, salinity, water density
	Nutrients	Dissolved inorganic nitrate, nitrite, ammonium and phosphate
	Suspended matter	Total particulate matter (TPM), particulate organic matter (POM) and water column light extinction coefficient
	Phytoplankton	Phytoplankton biomass, productivity and cell nutrient quotas
Forcing conditions	Wind	Wind speed
	Air temperature	Air temperature
	Water temperature	water temperature
	Light	Water column total and photosynthetically active radiation (PAR)
	Tide	Tidal height

The description of the hydrodynamic object, as well as its calibration and validation for the Douro estuary, were presented in a previous chapter (Chapter 5). This object is forced by tidal height at the sea boundary, river discharges, wind drag forces and density gradients. The velocity field is calculated with the equations of motion and the equation of continuity (Knauss 1997), solving the transport equation for all pelagic variables.

Wind object reads wind speed and direction time series, returning the corresponding values to the water temperature and hydrodynamic objects. Air temperature object reads air temperature values, returning them to the water temperature object. Light object returns light intensity values at sea level and computes water column light intensity from the Lambert–Beer law, using the water light extinction coefficient delivered by a suspended matter object. Water temperature object uses outputs from the previous objects to calculate water temperature from heat losses through evaporation, sensible heat and radiative exchanges between the water and the atmosphere. Light intensity and water temperature objects use standard formulations described in Brock (1981) and Portela and Neves (1994). Tide object uses the equations and harmonic components described in SHOM (1984) to calculate water level at the sea boundary. Boundary water levels are returned to the hydrodynamic object, where they are used to calculate the propagation of the tidal wave into the estuary.

Dissolved substances object computes the concentrations of dissolved inorganic nutrients - ammonium, nitrite, nitrate and phosphorus - and oxygen in each of the model grid cells as a function of biogeochemical and transport processes, including exchanges with the sea, loads from rivers and waste water treatment plants (WTPs) and, in the case of

oxygen, exchanges with the atmosphere. Both the nitrogen and phosphorus cycles are simulated using equations and parameters described in Chapelle (1995), except for the raeration coefficient, calculated as a function of wind speed following Burns (2000). Phytoplankton removes nutrients from flowing water.

Suspended matter object computes total particulate matter (TPM in mg L^{-1}) and particulate organic matter (POM in mg L^{-1}) from deposition and resuspension rates, exchanges with the sea and net contribution of phytoplankton biomass. POM mineralization is calculated as in Chapelle (1995), returning inorganic nitrogen and phosphorus to the dissolved substances object. Deposition of TPM in each grid cell is based on sinking velocity and cell depth (returned by the hydrodynamic object). A constant value for sinking velocity is considered, with different values for inorganic and organic matter. Resuspension of TPM in each grid cell is calculated as a function of current velocity and bottom drag, returned by the hydrodynamic object. Below a critical velocity value, resuspension does not occur. Above a certain threshold for the product of bottom drag and current velocity (velocity shear), resuspension is assumed constant, in order to avoid unrealistically high resuspension rates. This object is partly based on a model developed by Grant and Bacher (unpublished). The light extinction coefficient (m^{-1}) is calculated from an empirical relationship with TPM (Azevedo et al. 2006).

Phytoplankton object computes phytoplankton productivity as a function of light intensity (depth integrated Steele's equation) (Steele 1962), temperature and a limiting nutrient – nitrogen or phosphorus. In this model, phytoplankton is represented through chlorophyll, carbon, and nitrogen pools, allowing the necessary accounting calculations on cell quotas. Nutrient limitation is simulated as a two-stage process: nutrient absorption by phytoplankton cells and limitation using the Liebig's law of minimum on the basis of internal nutrient quotas. A nutrient limiting factor in the range 0 – 1 is calculated both for internal nitrogen and phosphorus and the lowest value obtained is then multiplied by light and temperature limited photosynthesis (Jørgensen & Bendoricchio 2001). For a complete list of model equations and parameters see Duarte et al. (2007).

6.2.3 Model setup

The model is forced by tidal height at the sea boundary, river discharges, wind drag forces and density gradients. Douro river flow values were obtained from the Portuguese Water

Institute (INAG). Small rivers discharging into the estuary were treated as point source loads, whose flows were estimated from Reis (2002).

Data used for model setup, calibration and validation were retrieved from a dataset compiled from sampling surveys conducted in 2003, at 10 stations covering the entire estuary, twice a month, during flood and ebb. Analysis of those data was presented in previous works (Azevedo et al. 2006, Azevedo et al. 2008).

Due to the lack of specific data, nutrients, suspended matter and phytoplankton biomass loads from small tributaries were considered equal to values from the river Douro. These were obtained by interpolating data collected near the dam at the surface (from the above mentioned data set). Consequently, anthropogenic loads to the lower and middle estuary were not considered in the present study, with consequent underestimation of those loads. For the sea boundary forcing, in terms of dissolved substances, suspended matter and phytoplankton biomass, daily values were used, obtained by interpolating observed values at the most downstream sampling station, according to the simulated period.

6.2.4 Model calibration and validation

Calibration and validation followed a similar procedure: the model was initialized with data from flood surveys and results were compared with data collected during ebb surveys of the same month. For calibration, September data were used, whereas validation was performed using June, August and October data. Therefore, in this work, model performance was analysed for timescales in the order of one week. The model was first calibrated for the parameters erosion rate and sinking velocity of the suspended matter object, since preliminary tests indicated that TPM and POM presented large discrepancies when model results were compared to observed data. Calibration continued with parameters maximum production rate (P_{max}) and optimal light intensity (E_{opt}) of the phytoplankton object. P_{max} and E_{opt} values used in the calibration procedure were based in previous studies concerned with photosynthetic parameters variability in the Douro estuary (Chapters 3 and 4). Values yielding the best fit between model results and observations were chosen for subsequent simulations.

For model performance evaluation, 2 measures of “goodness-of-fit” and 2 measures of absolute error were used: d1, Modified Index of Agreement (Willmott et al. 1985); E1, Modified Coefficient of Efficiency (Nash & Sutcliffe 1970, Legates & McCabe 1999); Root

Mean Square Error (RMSE) and the Mean Absolute Error (MAE), whose equations are presented below.

$$d_1 = 1 - \frac{\sum_{i=1}^{n}|Oi-Pi|}{\sum_{i=1}^{n}(|Pi-\bar{O}|+|Oi-\bar{O}|)} \quad (1)$$

$$E_1 = 1 - \frac{\sum_{i=1}^{n}|Oi-Pi|}{\sum_{i=1}^{n}|Oi-\bar{O}|} \quad (2)$$

Where,

Oi - observed values at each time i

Pi - predicted values at each time i

$\bar{O}$ - mean of observations

n - number of observations.

$$RMSE = \sqrt{\frac{1}{n}\sum_{i=1}^{n}(Oi - Pi)^2} \quad (3)$$

$$MAE = \frac{1}{n}\sum_{i=1}^{n}|Oi - Pi| \quad (4)$$

6.2.5 Sensitivity analysis

A previous work concerned with variability of photosynthetic parameters on the Douro estuary (Chapter 4), revealed that P_{max} presented the highest variability on a seasonal timescale while E_{opt} was most variable at a diel timescale. Since one of the main concerns of the present work was the study of primary production variability, a sensitivity analysis was performed, in order to test model sensitivity to changes in these parameters. Each parameter was increased and decreased by 10 % and model results were compared with a standard simulation, performed with P_{max} and E_{opt} obtained from model calibration. Model sensitivity was assessed by comparing predictions of mean chlorophyll *a*, nitrate, phosphate, net primary production per unit mass (NPP) and gross primary production per unit mass (GPP) for the different simulations with results from the standard simulation.

6.2.6 Simulation Scenarios

In order to evaluate the effects of river flow variability and magnitude on phytoplankton biomass and production, nutrients and suspended matter concentrations, three flow regimes and three flow magnitudes were combined, resulting in nine different scenarios. These scenarios were already used in the previous chapter, concerned with estuarine hydrodynamic response to changes in flow variability and magnitude (see Table 5.2 and Figure 5.2). The first regime "hourly" corresponded to the observed flow, characterised by a high hourly variability; the second regime - "daily" - was obtained by calculating daily mean flows for each day; and the third was obtained by calculating the mean flow for the entire simulation period, and was therefore constant – "constant" regime. Additionally, for each regime, the measured - "standard" – flow was halved and doubled for the studying the effects of river flow magnitude on estuarine biogeochemistry. Comparison between variable and constant flows, under low river flow periods, may be used as a proxy for comparison of the situation in the estuary before and after the dam was built.

The model was run from 11 to 18 June 2003, dates corresponding to flood and ebb sampling surveys, respectively. This period was characterised by high chlorophyll *a* levels (average of 9.8 mg m^{-3}) and medium river flow (average 244 m^3s^{-1}). The different simulations were compared in terms of average levels of chlorophyll *a*, NPP and GPP, nutrients and suspended matter, its temporal evolution and spatial distribution.

6.3 Results

6.3.1 Model calibration and validation

Calibration simulations, using September data, were evaluated by applying goodness of fit and error measures (*c.f.* Methods – Model calibration and validation) to predicted and observed values of TPM, POM, and chlorophyll *a*. The parameters that yielded the best fit between observations and predictions were chosen for subsequent simulations (Table 6.2).

Table 6.2. Calibrated parameters and respective values.

Object	Parameter (units)	Value
Suspended matter	Erosion Rate (m^{-2} day^{-1})	0.0005
	Sinking velocity (m day^{-1})	25
Phytoplankton	Pmax (h^{-1})	0.05
	Eopt (µE m^{-2} s^{-1})	850

P_{max} was very similar to the average obtained in that period from P-E experiments (0.051 mg C (mg C)$^{-1}$ h^{-1}), whereas E_{opt}, was higher than measurements. In the latter case, average E_{opt} from P-E experiments was 660 µE$m^{-2}s^{-1}$. Results obtained are overall indicative of good model performance, although high error estimates were obtained for some variables, namely TPM, POM and ammonium (Table 6.3).

Table 6.3. Model performance after calibration, in simulated key variables, using September data.

Measure	TPM	POM	Chlorophyll *a*	Nitrate	Phosphate	Ammonium
	mg L^{-1}	mg L^{-1}	mg m^{-3}	µM	µM	µM
d1	0.7	0.8	0.9	0.9	0.9	0.8
E1	0.5	0.7	0.7	0.7	0.7	0.5
RMSE	16.7	2.1	2.2	15.2	0.4	2.5
MAE	10.8	1.3	1.5	11.5	0.3	2.2

Afterwards, validation was carried out for June, August and October, using the calibrated parameters. Chlorophyll *a* predictions were reasonably good, according to the goodness of fit and error measures obtained (Table 6.4). In June, predicted vales of chlorophyll *a* were higher than observations (Figure 6.2). Model results suggested an increase in chlorophyll *a* in the middle estuary which was only verified in observations at the bottom layer. In August, there was a good agreement between predicted and observed values, except in the upper estuary, at the middle and bottom layers, where predictions were considerably higher than observations, due to a sharp decrease in observed chlorophyll *a*. In October, although predictions were in the range of observations, an increase in observed chlorophyll *a* in the middle estuary was not predicted by the model (Figure 6.2).

Model performance evaluation results for nitrate predictions were good for June and October but not for August, when a negative value was found for E1, which means that the observed mean is a better predictor than the model (Legates & McCabe 1999) (Table 6.4). From the analysis of Figure 6.3, it is apparent that this result is a consequence of the

poor prediction of nitrate values in the upper estuary, at the surface, and in the middle and upper estuary, at the middle and bottom layers, during the August simulation.

Table 6.4. Goodness of fit and error measures obtained for model performance, in key variables simulation.

June

Measure	Chlorophyll *a* mg m^{-3}	Nitrate µM	Phosphate µM	Ammonium µM	TPM mg L^{-1}	POM mg L^{-1}
d1	0.8	0.9	0.8	0.9	0.7	0.7
E1	0.5	0.8	0.7	0.8	0.3	0.3
RMSE	6.4	18.7	0.2	2.9	7.0	1.0
MAE	5.5	13.6	0.2	2.2	6.0	0.8

August

Measure	Chlorophyll *a* mg m^{-3}	Nitrate µM	Phosphate µM	Ammonium µM	TPM mg L^{-1}	POM mg L^{-1}
d1	0.9	0.6	0.8	0.6	0.6	0.7
E1	0.7	-0.2	0.6	0.2	0.3	0.5
RMSE	1.7	44.2	1.0	28.8	18.1	3.9
MAE	1.0	33.9	0.5	16.2	13.4	2.7

October

Measure	Chlorophyll *a* mg m^{-3}	Nitrate µM	Phosphate µM	Ammonium µM	TPM mg L^{-1}	POM mg L^{-1}
d1	0.9	0.9	0.9	0.8	0.7	0.7
E1	0.8	0.7	0.8	0.7	0.6	0.6
RMSE	1.5	22.2	0.5	2.7	20.2	3.4
MAE	1.0	16.2	0.4	2.2	12.7	2.4

Model results for phosphate in June suggest a non conservative behaviour of this variable, which may be related to the increase in chlorophyll *a* verified for the same period. Observed values, however, did not present a clear trend, although higher values were registered for the lower estuary. For the August and October simulations, predictions were well in the range of observations, with observed values presenting a large variability (Figure 6.4).

Considering ammonium, model results reproduced the observed increasing trend downstream, as well as observed ammonium levels, for June and October simulations. Again, August was the period when predictions were less satisfactory (Figure 6.5), due to an overestimation of ammonium levels at the middle and bottom layers, in the middle and upper estuarine stretches and the extremely high values observed at the surface layer at stations 1 and 7. These observations were probably caused by loads to the estuary, unaccounted for in model set up. These loads were most likely originated from wastewater treatment plants, in the vicinity of the above mentioned stations.

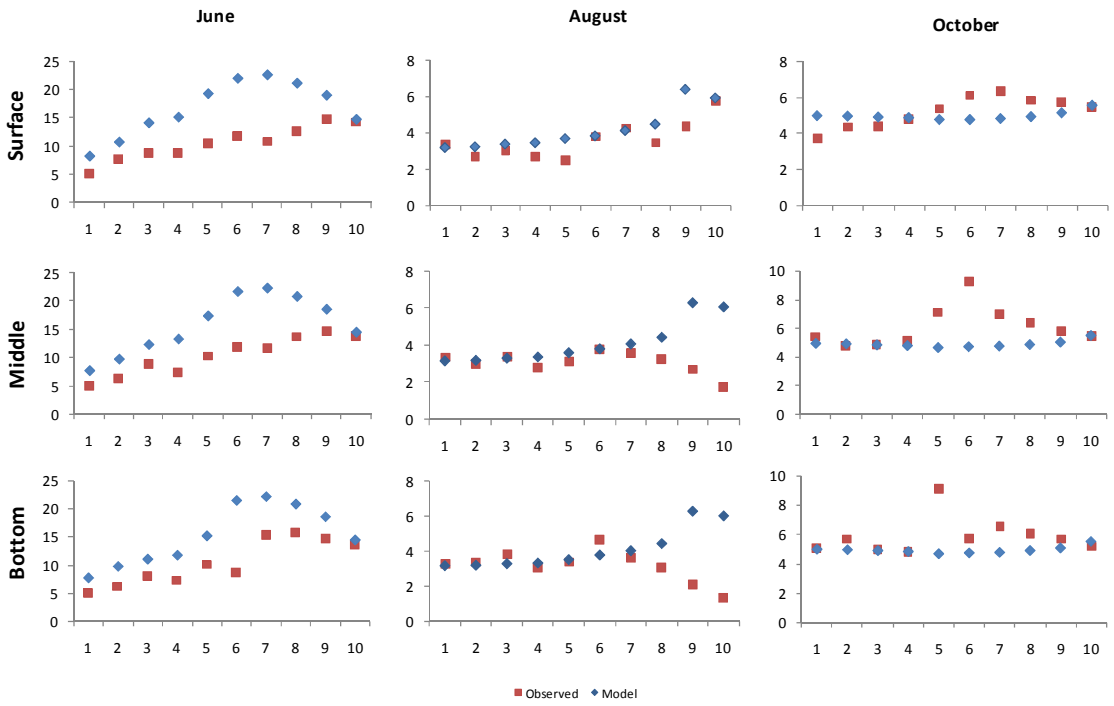

Figure 6.2. Observed and predicted chlorophyll *a* values for the June, August and October periods, in mg m^{-3}**.**

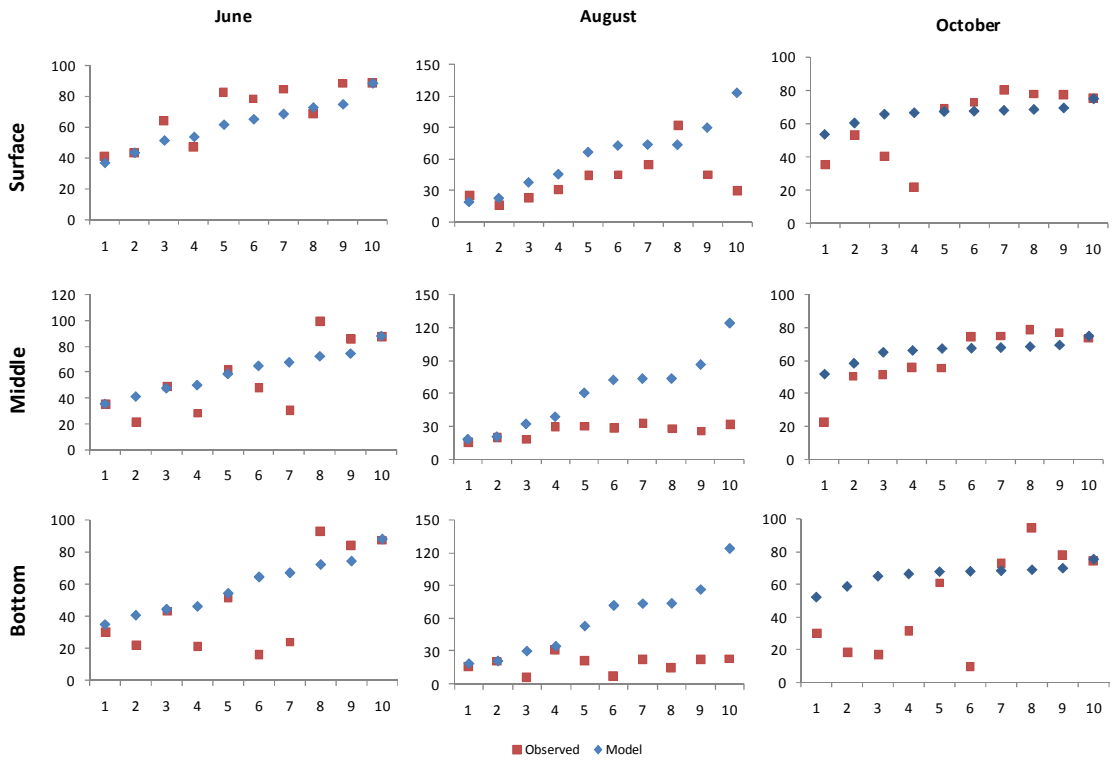

Figure 6.3. Observed and predicted nitrate values for the June, August and October periods, in µM.

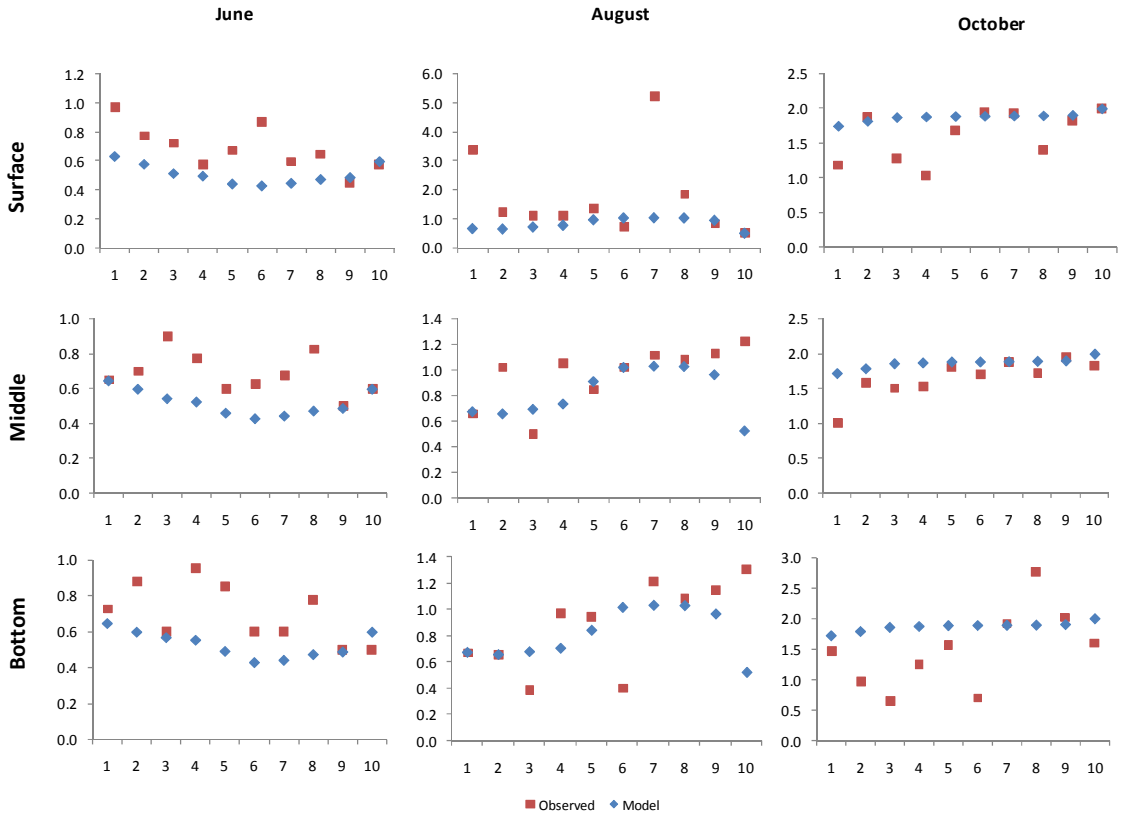

Figure 6.4. Observed and predicted phosphate values for the June, August and October periods, in µM.

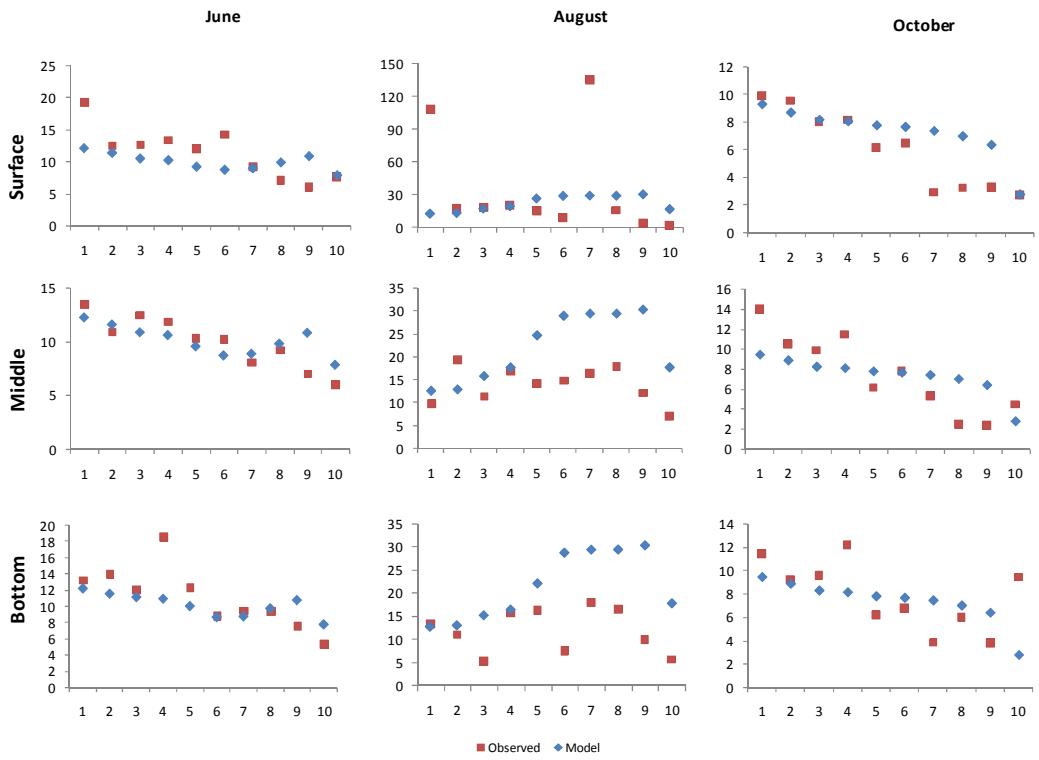

Figure 6.5. Observed and predicted ammonium values for the June, August and October periods, in µM.

TPM model results for June showed an increase in the middle estuary, similar to chlorophyll *a* predictions for that period, not found in observed values. In the August simulation, levels increased from the upper to the middle estuary, in agreement with observations, but the model was unable to predict the high values observed in the lower estuary, again probably due to unaccounted external loads to the estuary. In October, predictions followed the observed increasing trend towards the mouth (Figure 6.6).

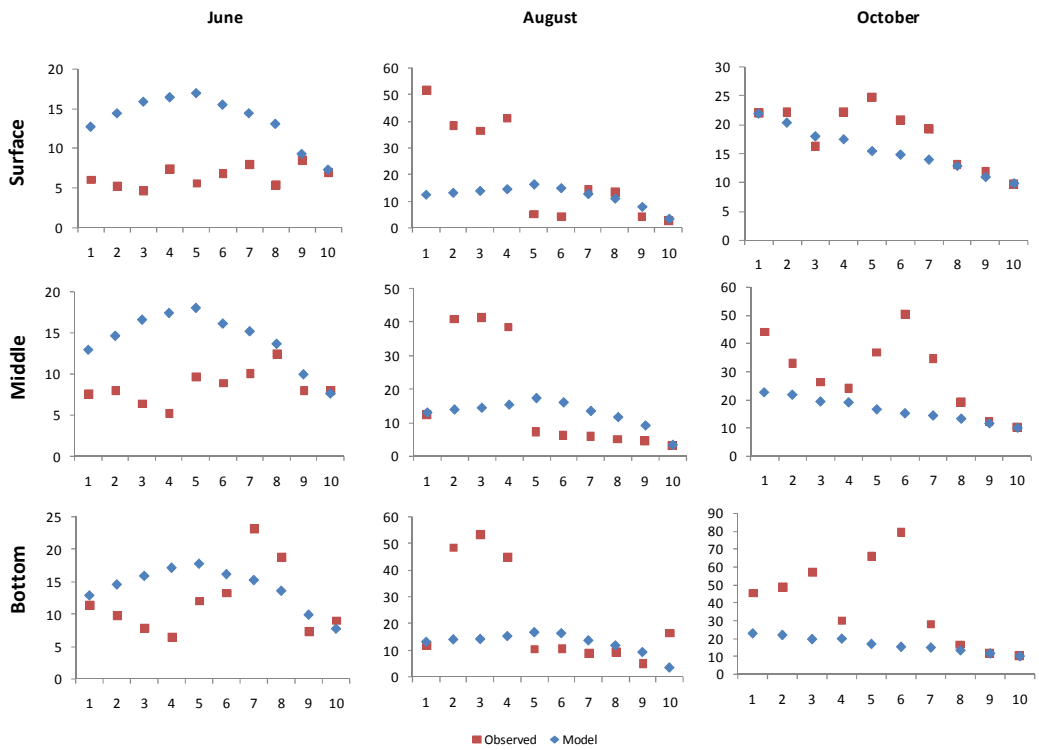

Figure 6.6. Observed and predicted TPM values for the June, August and October periods, in mg L^{-1}.

POM predictions were higher than observations at the surface and middle layers and within observed range at the bottom, for June. For August, predictions agreed well with observations in the middle and upper estuary, but the model was unable to predict the high values observed for this variable in the lower estuary, similarly to TPM results. For October, predictions were somewhat lower than observations, but increased in the lower estuary, in agreement with the observed trend (Figure 6.7).

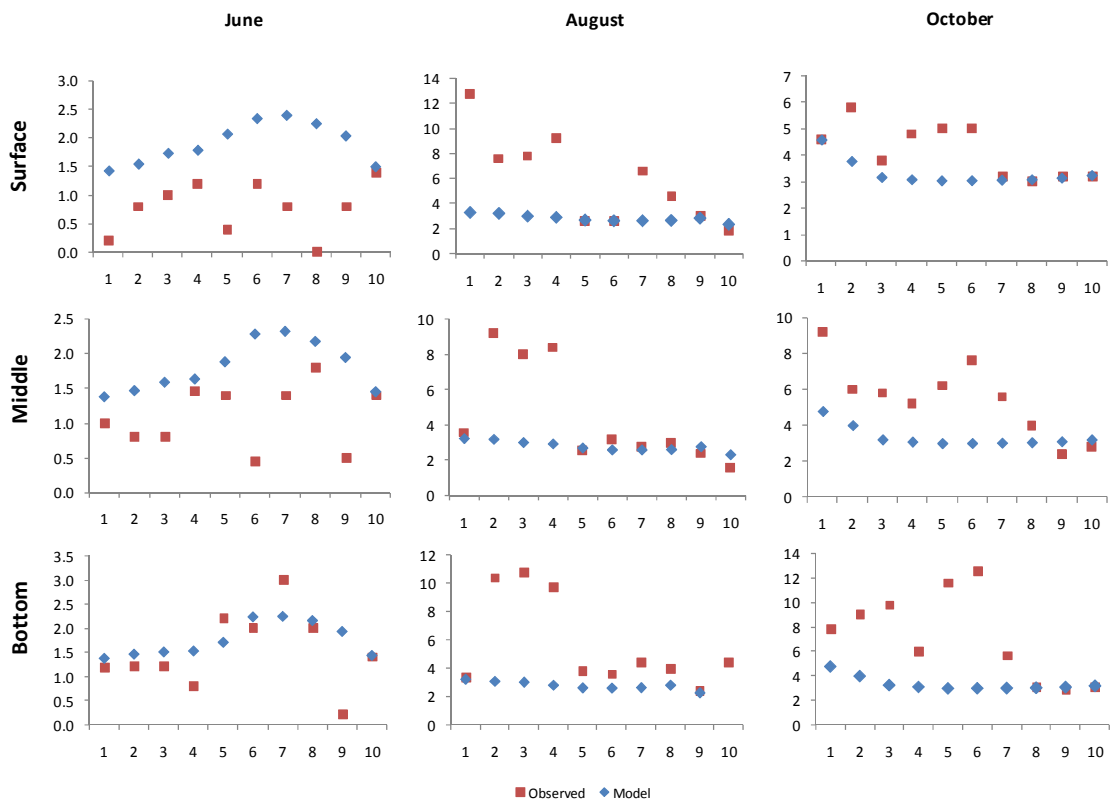

Figure 6.7. Observed and predicted POM values for the June, August and October periods, in mg L^{-1}.

Model performance in estimating phytoplankton production was assessed by comparing mean NPP and GPP per unit mass predictions for June, August, September and October, for sampling stations 1, 5 and 10, corresponding to the lower, middle and upper estuary, respectively, with measurements from P-E experiments, using the ^{14}C method. These correspond to mean hourly values integrated over one day. Model results for GPP were closer to measurements than NPP (Table 6.5), which is expectable if we consider that ^{14}C short-term incubations reflect gross PP (see discussion). Considering this assumption, model results did not present high divergences from measurements; model predictions were slightly lower than observations for June, August and October and higher for September. Temporal patterns obtained with the model were also similar to observations, except for September and October, when predicted GPP was higher for September, whereas measurements yielded higher values for October.

Table 6.5. Measured primary production and model results for net (NPP) and gross primary production (GPP) in mg C (mg C)$^{-1}$ h^{-1}, obtained in June, August September and October.

Month	^{14}C PP	Model NPP	Model GPP
June	0.025 ± 0.004	0.012	0.021
August	0.034 ± 0.008	0.010	0.025
September	0.014 ± 0.005	0.006	0.019
October	0.015 ± 0.003	0.003	0.012

6.3.2 Sensitivity analysis

Nitrate and phosphate variability in response to changes in Pmax and Eopt was very low, between -0.008% and 0.009%, for nitrate and between -0.5% and 0.5%, for phosphate, thus those nutrients were weakly affected by changes in these photosynthetic parameters (Table 6.6). As expected, mean chlorophyll *a*, GPP and NPP increased and decreased for increased and decreased P_{max}, respectively. Increasing and decreasing E_{opt} led to decreased and increased values of those variables. Results are indicative that model is more sensitive to P_{max} than to E_{opt}. However, comparing chlorophyll *a* and GPP percent variability to the error associated with observations compared to its mean (8.9 and 28%, respectively), model sensitivity to changes in those photosynthetic parameters may be considered low (Table 6.6).

Table 6.6. Sensitivity analysis results for parameters P_{max} and E_{opt}.

		Chlorophyll *a* (mg m^{-3})		Nitrate (µM)		Phosphate (µM)		GPP (mg C (mg C)$^{-1}$ h^{-1})	
		- 10 %	+ 10 %	- 10 %	+ 10 %	- 10 %	+ 10 %	- 10 %	+ 10 %
Pmax	Result	4.4	4.6	38.22	38.23	1.2	1.2	0.021	0.0253
	% variation	-2.4%	2.5%	-0.008%	0.009%	-0.50%	0.52%	-9%	10%
Eopt	Result	4.6	4.5	38.23	38.22	1.24	1.24	0.0244	0.022
	% variation	1.4%	-1.2%	0.004%	-0.004%	0.29%	-0.26%	6%	-5%

6.3.3 Scenario analysis

Analysis of averaged values obtained for each scenario showed that nitrate and ammonium levels increased with river flow, whereas phosphate presented similar values for all river flow magnitudes (Table 6.7). No clear influence of river flow magnitude was found on TPM and POM mean values. Chlorophyll *a* mean levels were highest for the standard flow magnitude. Both increasing and decreasing river flow seemed to result in

decreased phytoplankton biomass, whereas mean NPP and GPP increased with river flow magnitude.

Table 6.7. Scenario analysis - Averages obtained for key variables, in each simulation performed. Phytoplankton biomass is in mg m^{-3}, nutrients in µM, TPM and POM in mg L^{-1} and NPP and GPP in mg C (mg C)$^{-1}$ h^{-1}.

Scenarios	Phytoplankton_biomass Chl *a* (mg m^{-3})	Nitrate µM	Ammonia µM	Phosphate µM	TPM mg L^{-1}	POM mg L^{-1}	NPP h^{-1}	GPP h^{-1}
S1	15.1	46.0	10.8	0.36	17.8	3.1	0.0080	0.018
S2	15.8	47.0	10.6	0.36	17.1	3.1	0.0077	0.0182
S3	16.5	48.4	10.6	0.37	16.9	3.1	0.0084	0.0198
H1	14.0	41.4	10.7	0.36	17.4	3.0	0.0050	0.014
H2	14.7	41.7	10.5	0.37	16.8	3.0	0.0051	0.0144
H3	15.7	42.8	10.5	0.38	16.9	3.1	0.0058	0.0156
D1	14.9	49.8	11.5	0.36	17.3	3.0	0.0109	0.0213
D2	15.8	52.1	11.3	0.37	17.4	2.9	0.0101	0.0211
D3	15.6	54.2	11.8	0.37	17.1	2.8	0.0118	0.0234

Considering the different discharge regimes, higher mean nitrate levels were obtained for the “constant” regime. Higher chlorophyll *a* was also obtained for the “constant” flow scenarios S3 and H3. For the increased flow D3 scenario, chlorophyll *a* mean values were similar to D2 scenario. NPP and GPP were also highest for the “constant” flow regime. For the remaining variables, no obvious differences were found between different scenarios.

Tidal dynamics influenced the temporal pattern of nitrate and chlorophyll *a*, at the lower and middle estuary (Figures 6.8A and 6.8B), with levels rising during the ebb and lowering during the flood. Temporal variability of nitrate and chlorophyll *a* concentrations at the upper estuary for the different regimes (Figure 6.8C) showed the influence of flow variability, especially on chlorophyll *a* dynamics. For the S1 and S2 regimes, chlorophyll *a* peaks corresponded to low flow periods, whereas the “constant” S3 regime yielded nearly constant chlorophyll *a* levels. Considering flow variability, although higher chlorophyll *a* and nitrate peaks were registered for the “hourly” more variable flow, it appears that flow stabilisation may have a positive effect in nitrate and chlorophyll *a*, leading to increased levels in the estuary.

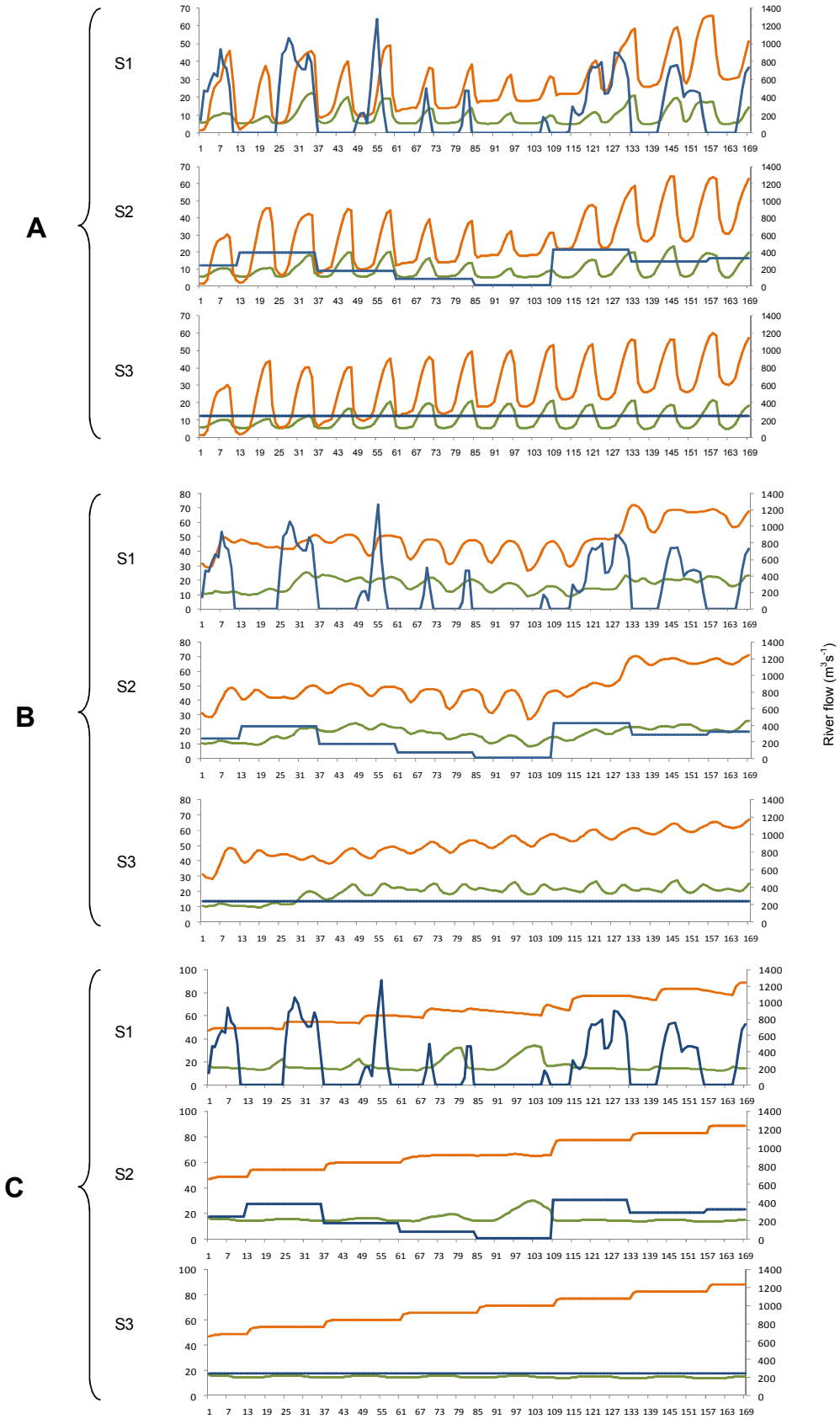

Figure 6.8. Time series of surface nitrate (in µM) and phytoplankton biomass (chlorophyll *a*, in mg m^{-3}) predictions for June at different locations: A – near the mouth; B – at the middle estuary (5.3 km from the mouth) and C – near the dam. S1, S2 and S3 correspond to the different river flow regimes. River flow is in m^3s^{-1}.

A spatial analysis of chlorophyll *a* distribution predicted by the model at flood and ebb suggested that the main origin of phytoplankton biomass was the river, since a close (inverse) relationship with salinity was evident (Figure 6.9). High salinity levels during the flood at the mouth corresponded to low chlorophyll concentration, which increased towards the head as salinity levels decreased. Nevertheless, some chlorophyll *a* accumulation was predicted at the middle and lower estuary, during the ebb for all scenarios, and during the flood, for the S2 and S3 scenarios. Comparing the different regimes, whereas chlorophyll *a* build up extended more downstream in the "constant" regime, leading to a higher mean chlorophyll *a* (Table 6.7), the highest peaks were obtained for the "hourly" and "daily" regimes.

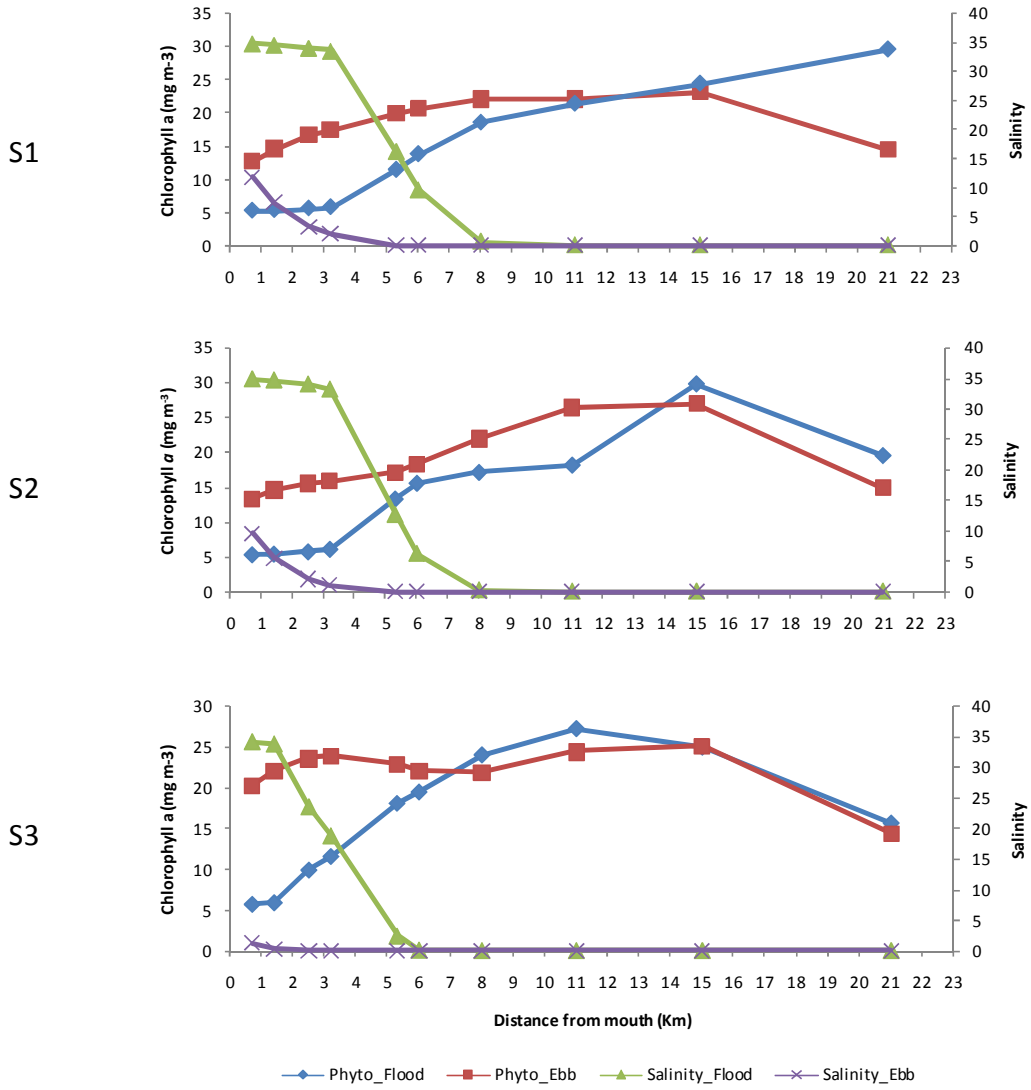

Figure 6.9. Chlorophyll *a* and salinity, predicted in simulations S1, S2 and S3 (*c.f.* Table 5.2) along the estuary, during the ebb and the flood

6.4 Discussion

6.4.1 Model calibration and validation

Overall model performance after calibration was reasonably good, considering the results of goodness of fit and error measures. These measures indicate that model performance was good for June and October period, whereas in August some variables were less well predicted by the model, namely nitrate, ammonium and TPM, as discussed below.

Model predictions for chlorophyll *a*, in June, suggested a build up of phytoplankton biomass in the middle estuary. Positive mean net primary production (NPP) predicted for this period, indicates that this accretion was due to phytoplankton growth in the estuary. Although in the period used for comparison, chlorophyll *a* build up was only observed at the bottom layer, it is not an unusual event its increase across the water column. In fact, chlorophyll *a* accretion in the middle estuary during the ebb has been observed in previous works in the Douro (Bordalo & Vieira 2005). In October, although some biomass build up was observed, chlorophyll *a* model predictions presented a decreasing trend downstream. In August, predicted and observed values were very similar, except for the upper estuary, where, at the middle and bottom layers, predictions were higher than observations and similar to surface values. The observed vertical gradient in chlorophyll *a* resulted from strong stratified conditions in the estuary in this period, with surface freshwater presenting higher chlorophyll *a* concentrations than the bottom, brackish water. Since during low flow periods, salinity stratification is underestimated by the model, a mixed water column was predicted, with vertically homogeneous chlorophyll *a*.

Underestimation of salinity stratification may also be the reason for the poor model performance obtained for nitrate prediction in August. The discrepancy between predictions and observations, especially at the middle and bottom layers may be explained by the lower salinity intrusion predicted by the model, preventing the reproduction of the vertical gradient observed for nitrate, during low river flow conditions. For the remaining simulation periods, June and October, model predictions were characterized by a decreasing trend towards the mouth, similar to the observed overall trend, suggesting a quasi-conservative behaviour for nitrate along the estuary.

Model performance results concerning phosphate levels predictions were good, with predicted values well in the range of observations. The apparent sink for phosphate

predicted for June, related to a chlorophyll *a* accumulation during that period in the middle estuary may suggest a limiting role for phosphate. In fact, observed N:P ratios indicate that phosphate is the most likely potential limiting nutrient in the Douro estuary (Azevedo et al. 2008). On the other hand, the high variability in observations may be indicative of external sources along the estuary.

Ammonium levels predicted by the model were very similar to observations in June and October, reproducing the observed increasing trend towards the mouth, whereas in August, model performance was worse, probably due to the already mentioned model stratification underestimation at the middle and lower layers, on one hand, and some high observed values, probably caused by loads to the estuary.

TPM and, especially, POM predictions in June seemed to follow the predicted chlorophyll *a* pattern, presenting higher values than observations, at the surface and middle layers, and indicating a close relationship between those variables. In August and October, discrepancies between predictions and observations were related to the high values observed at the middle and lower estuary, possibly caused by external loads, not accounted for in the model.

Phytoplankton production is simulated by the model as net and gross production per unit mass. Model results of GPP approach measurements made using ^{14}C incubation method. Although there has been a debate on what this method really measures (Mingelbier et al. 1994, and references here in), the traditional view has been that short term incubations reflect GPP, whereas 24 h long incubations reflect NPP (Li & Harrison 1982), and this interpretations has been used in more recent studies (Harding et al. 2002). Thus, considering that measurements are primarily of GPP, model predictions for phytoplankton production are in the range of observations.

Therefore, according to the discussion above, improvements in salinity stratification modelling are needed as well as a better quantification of the anthropogenic loading to the lower and middle estuary, before the model is considered fully validated. Nevertheless, considering phytoplankton biomass spatial and temporal trends, the model is able to capture estuarine behaviour. The highest chlorophyll *a* was obtained for the spring period, followed by a decline in summer, which is in accordance with the conceptual model presented previously for the estuary (Azevedo et al. 2008). Spatially, although the river acts as the main source for phytoplankton biomass, some accretion is predicted within the estuary, in accordance with observations.

6.4.2 Sensitivity analysis

A previous work in the Douro estuary (Chapter 4) revealed that P_{max} and E_{opt} presented the highest variability on seasonal and diel timescales, respectively. Those findings raised the question of the benefits of considering a dynamic modelling of primary production in the Douro estuary. Analysis of model sensitivity to P_{max} and E_{opt} was thus performed, testing the effect of increasing and decreasing the values of those photosynthetic parameters on chlorophyll *a*, nitrate, phosphate, NPP and GPP. Chlorophyll *a*, NPP and GPP were more affected by changes in P_{max} and E_{opt} than nitrate and phosphate. Nevertheless, globally, sensitivity analysis suggests that the model sensitivity to changes in those parameters is low, which indicates that the adopted parameterization of primary production is adequate.

6.4.3 Scenario analysis

River flow magnitude effects were observed mainly in nitrate, ammonium, chlorophyll *a* and NPP levels. Nitrate mean concentration increased with flow, reflecting its river origin, in agreement with the seasonal pattern observed in the Douro. Ammonium also increased with flow, although differences between flow regimes were smaller in this case. Nevertheless, the river was not a source to the estuary, according to observed data, since higher ammonium levels were consistently found at the middle and lower estuary (Azevedo et al. 2008).

Chlorophyll *a* concentration response to flow was characterised by decreased biomass mean values both for river flow increase and decrease. This parabolic relationship with flow may be related to phytoplankton growth controlling factors. In fact, in a previous study, an inverse relationship was found between river flow and chlorophyll *a* in the estuary (Azevedo et al. 2008), reflecting lower residence time and light availability. The same study also found that for August, when the flow was drastically reduced, chlorophyll *a* levels also decreased, possibly due to lower input from the river of phytoplankton biomass and nutrients. These results indicate that the model was able to reproduce the observed temporal patterns of phytoplankton biomass response to flow, in agreement with the conceptual model previously presented.

These patterns were also observed in other systems. For example, Cloern et al (1983) found that a diatom bloom occurs in the northern San Francisco Bay when river discharge falls within 100 – 350 m^3s^{-1}, whereas in other systems, phytoplankton biomass increases with river flow, due to nutrient input (Malone et al. 1988, Mallin et al. 1993, Ramus et al.

2003). Thus, the pattern obtained from these scenarios is likely to be explained by decreased nutrient and biomass input for lower flow magnitude and decreased residence time for higher flow magnitude. On the other hand, modelled PP increased with flow magnitude. This trend is opposite to the inverse relationship observed between river flow and primary production in a previous study (Azevedo et al. 2008). Nevertheless, this inverse relationship was obtained using data from one year, reflecting seasonal variability in light and temperature. Thus, since similar temperature and light conditions were used for all scenarios (differences in TPM were small, Table 6.7), other factors may be influencing NPP as a function of river flow. One may be decreased salinity, which may favour freshwater phytoplankton production.

Considering the different river discharge regimes, decreased salinity may also explain why a constant regime yielded higher PP, as well as higher nitrate and chlorophyll *a* mean levels than the more variable one. In fact, in the previous chapter, analysis of the hydrodynamic response to flow variability resulted in lower salinity for the more stable regime. Lower salinity implies more river water and, therefore, higher chlorophyll and nitrate levels, leading to higher PP.

A temporal analysis of the behaviour of chlorophyll *a* and nitrate, for the three scenarios, showed that they were greatly influenced by tidal dynamics, at the lower and middle estuary (although a slight oscillation was also visible at the upper estuary), with higher values during the ebb and lower during the flood, which corroborates their river origin. Although higher peaks were found in the variable flow regime for both variables, stable conditions resulted in higher mean levels, due to the above discussed hydrodynamic response to flow variability.

6.5 Conclusions

A 3D coupled hydrodynamic-biogeochemical model was implemented for the Douro estuary to analyse the influence of different scenarios of river flow variability and magnitude on phytoplankton biomass and production, nutrients and suspended matter dynamics.

A parabolic relationship between phytoplankton biomass and flow magnitude was found, with biomass decreasing for both increased and decreased river flow. A pattern probably related to lower residence time and lower nutrient and biomass input, for increased and decreased flow, respectively, since nitrate and primary production per unit mass increased with flow magnitude. Flow variability influence was translated in a higher mean phytoplankton biomass and production for stable flows, compared to the more variable flows, presently dominating in the Douro.

Therefore, flow management is likely to affect estuarine phytoplankton production. Moreover, the currently implemented freshwater discharge regime by the dam, with high hourly variability has probably decreased spring and summer blooms, in the estuary, due to increased salinity levels in the estuary, comparing to pre-dam conditions.

Although the model was able to reproduce most of the estuarine biogeochemical temporal and spatial dynamics, some issues arose that need further work before full validation can be achieved. One of them is underestimation of density stratification, which prevents a better prediction of estuarine properties spatial distribution and another is improvement of anthropogenic loads setup, namely ammonium and suspended matter, in the middle and lower estuary.

CHAPTER 7

General conclusions and future directions

Freshwater inflow to estuaries has been a matter of concern for the last decades, as human need for water and energy increases. The effects of river damming and consequent changes in the amount and timing of freshwater delivered to estuaries are now well acknowledged. Changes in water circulation and quality affecting estuarine communities and production are dependent on the ecosystems characteristics, thus management of estuaries should rely on the understanding of its functioning and the ability to predict its response to changes in controlling factors.

In the Douro, freshwater inflow to the estuary is managed based on electric power demand only, forsaking other environmental concerns. The highly variable regime imposed by the dam operation is likely to have consequences on estuarine hydrodynamic behaviour, water quality and primary production.

This thesis began with the spatial and temporal characterization of key environmental variables, and the study of relationships between them, resulting in the design of a conceptual model of the Douro estuary biogeochemistry (Chapter 2). The river emerges as the major source of nutrients, chlorophyll *a* and TPM for the estuary, although additional anthropogenic sources are noticeable at the middle and lower estuary. Phytoplankton biomass and primary production reaches their maxima during spring, when flow decreases and light availability and temperature increase. In summer, when river flow is the lowest, and temperature and water transparency are the highest, (as well as salinity), chlorophyll *a* and PP decline. This decline may be partly explained by the lower

phytoplankton input and the inability of freshwater phytoplankton to thrive in high salinity water that dominates the estuary during this period. This analysis also highlighted that water quality in the Douro estuary is strongly affected by increasing nitrate inputs from the river, as well as by high ammonium and bacterial levels caused by discharge of untreated wastewater within the lower and middle estuarine stretches. Although eutrophication risk is not reflected in severe phytoplankton biomass build up, it was suggested that monitoring of benthic algae dynamics should be performed additionally to phytoplankton biomass in order to understand the occurrence of large macroalgae blooms at the lower estuary. Semi-quantitative relationships of nitrate, suspended matter and primary production with river flow were derived for assisting in the implementation of an ecological model for the Douro estuary.

Alteration of the regime of freshwater discharge by river damming is expected to affect estuarine metabolism, due to changes in inorganic and organic matter loads to the estuary. Pelagic metabolism of the Douro estuary was studied, as well as factors controlling primary production (Chapter 3). The estuary was found to be predominantly heterotrophic, except for the upper reaches in summer, with heterotrophy increasing in the lower estuary, mostly related to increases in community respiration, derived from allochthonic organic matter inputs from untreated wastewater discharge. Primary production was mostly controlled by temperature with positive feedbacks from maximum production rate (P_{max}) and phytoplankton biomass. The dam appeared to have a dominant effect on suspended matter gradients in the estuary, since an increasing trend towards the mouth was observed for TPM. Moreover, TPM and chlorophyll *a* levels were low comparing to other estuarine ecosystems, which was suggested to be due to water impoundment by the dam.

The strong positive correlations obtained between P_{max}, temperature and chlorophyll *a* in the Douro suggested that these variables were responsible for most of the variability observed in that photosynthetic parameter. Thus, a further investigation on the variability of photosynthetic parameters, its controlling factors and the relative importance of temporal and spatial scales of variability was conducted (Chapter 4). It was found that the most important timescale of variability for P_{max} and photosynthetic efficiency (α) was seasonal, although diel variability in summer was also considerable, and that the highest P_{max} values were obtained around noon or in early afternoon. Light, temperature and salinity were the most influential factors on photosynthesis-irradiance (P-E) parameters variability. Additionally, PP prediction accuracy was increased by combining light and temperature limiting functions.

These findings about spatial and temporal trends, as well as relationships between the different variables that drive estuarine dynamics, were used for the adaptation, calibration and validation of a 3D coupled hydrodynamic-biogeochemical model for the Douro estuary. The model was then used to approach the problem under study: assessment of the impact of the dam and its highly variable discharge regime on estuarine water quality and primary production.

In a first step, the hydrodynamic model was implemented, calibrated, validated and used for analysing the influence of river flow magnitude and variability on estuarine water circulation (Chapter 5). Several scenarios combining different river flow magnitudes and discharge regimes were evaluated. The results of flow magnitude influence are straightforward, with reduced flows leading to higher salinity levels and stratification. On the other hand, it was found that flow variability also played an important role; stable flows seemed to reduce average salinity and to be more effective in dispersing contaminants than highly variable flows of the same average magnitude. From these conclusions, it seems reasonable to infer that flow management may have important effects on estuarine hydrodynamics through interactions between flow magnitude and variability. Furthermore, considering that stable summer freshwater inputs may be used as a proxy for the estuarine behaviour before the dam was built, when those inputs depended mostly on Douro base flow, it may be suggested that flow regulation through the dam may be responsible for increasing estuarine salinity during summer months and reducing its dilution potential for contaminant dispersion.

In a second step, coupling of the hydrodynamic and biogeochemical models was performed, followed by calibration and validation of the latter (Chapter 6). Again, the same scenarios of river flow magnitude and variability were applied, in order to study the influence of river flow magnitude and variability on estuarine water quality and primary production. Model predictions suggest a direct relationship between flow magnitude and nutrient concentration, whereas a parabolic relationship between phytoplankton biomass and flow magnitude was found, with biomass decreasing for both increases and decreases in river flow. This pattern is probably related to lower residence time and lower nutrient and biomass input, for increased and decreased flow, respectively, since nitrate and primary production per unit mass increased with flow magnitude.

Considering the different discharge regimes, stable flows yielded higher mean phytoplankton biomass and production than the more variable flows, suggesting that the

currently implemented freshwater discharge regime by the dam activity, with high hourly variability, has probably decreased spring and summer blooms, in the estuary, with overall decrease in primary production.

The model implemented in the present work was able to reproduce most of the estuarine biogeochemical temporal and spatial dynamics. Nevertheless, some problems were detected, which imply that further improvements are needed.

Future directions

The present study contributed to improve the understanding of the Douro estuary ecosystem functions through results from field and modelling work. From the results obtained, some questions arose that deserve further investigation:

- What are the temporal and spatial characteristics of the estuarine phytoplankton community structure?
- What is the influence of river damming on the physiologic conditions of the phytoplankton arriving at the estuary from the river?
- How do phytoplankton organisms, originated from the dam reservoir, respond to the estuarine gradients in salinity, temperature and light conditions, as they are advected along the estuary?

Additionally, the fine-tuning of the 3D hydrodynamic-biogeochemical model is needed, considering the discrepancies found during the modelling work. The main problems encountered in the model were related to the underestimation of salinity intrusion and stratification, observed in the estuary during periods of moderate to low flow, and the insufficient knowledge abut the loads from the small tributaries. In order to deal with these problems, some improvements should be included in the model:

- A better definition of the sea boundary, further away from the mouth, for which additional bathymetric data should be collected;
- Improved estimates of the loads from small tributaries, through the use of hydrologic models, based on catchment area, land use and precipitation;
- A better characterization of wastewater treatment plants effluent loads.

The model implemented in this thesis, with the improvements mentioned above, constitutes a useful predictive tool of the influence of stressors or mitigation measures applied to the estuary, which may be a major benefit for a future management plan, in the vein of the Water Framework Directive.

References

Anon (1958) The Venice System for the Classification of Marine Waters According to Salinity. Limnology and Oceanography 3:346-347

Alber M. (2002) A conceptual model of estuarine freshwater inflow management. Estuaries 25:1246-1261

Alpine A. E., Cloern J. E. (1992) Trophic Interactions and Direct Physical Effects Control Phytoplankton Biomass and Production in an Estuary. Limnology and Oceanography 37:946-955

APHA, WWA, WEF (1992) Standard Methods for the examination of Water and Wastewater, American Public Health Association, Washington, DC

Aubry F., Acri F. (2004) Phytoplankton seasonality and exchange at the inlets of the Lagoon of Venice (July 2001-June 2002). Journal of Marine Systems 51:65-76

Azevedo I., Duarte P., Bordalo A. (2006) Pelagic metabolism of the Douro estuary (Portugal) - Factors controlling primary production. Estuarine Coastal and Shelf Science 69:133-146

Azevedo I., Duarte P., Bordalo A. (2008) Understanding spatial and temporal dynamics of key environmental characteristics in a mesotidal Atlantic estuary (Douro, NW Portugal). Estuarine, Coastal and Shelf Science 76:620-633

Balls P. W. (1992) Nutrient Behavior in 2 Contrasting Scottish Estuaries, the Forth and Tay. Oceanologica Acta 15:261-277

Basterretxea G., Aristegui J. (2000) Mesoscale variability in phytoplankton biomass distribution and photosynthetic parameters in the Canary-NW African coastal transition zone. Marine Ecology Progress Series 197:27-40

Behrenfeld M. J., Prasil O., Babin M., Bruyant F. (2004) In search of a physiological basis for covariations in light-limited and light-saturated photosynthesis. Journal of Phycology 40:4-25

Bernhard A., Peele E. (1997) Nitrogen limitation of phytoplankton in a shallow embayment in northern Puget Sound. Estuaries 20:759-769

Binder B. J., DuRand M. D. (2002) Diel cycles in surface waters of the equatorial Pacific. Deep-Sea Research Part II -Topical Studies in Oceanography 49:2601-2617

Bordalo A. (1991) Ecologia do Estuário do rio Douro: abordagem da evolução espaço-temporal e inter-relações na componente planctónica do compartimento microbiológico. PhD dissertation, Universidade do Porto

Bordalo A. (1993) Effects of Salinity on Bacterioplankton - Field and Microcosm Experiments. Journal of Applied Bacteriology 75:393-398

Bordalo A. (2003) Microbiological water quality in urban coastal beaches: the influence of water dynamics and optimization of the sampling strategy. Water Research 37:3233-3241

Bordalo A., Vieira M. (2005) Spatial variability of phytoplankton, bacteria and viruses in the mesotidal salt wedge Douro Estuary (Portugal). Estuarine, Coastal and Shelf Science 63:143-154

Boyer J. N., Christian R. R., Stanley D. W. (1993) Patterns of Phytoplankton Primary Productivity in the Neuse River Estuary, North-Carolina, USA. Marine Ecology Progress Series 97:287-297

Brock T. (1981) Calculating solar radiation for ecological studies. Ecological Modelling 14:1-19

Burns L. (2000) Exposure analysis modelling system (EXAMS): User manual and system documentation. US Environmental Protection Agency

Byun D. S., Wang X. H., Hart D. E., Cho Y. K. (2005) Modeling the effect of freshwater inflows on the development of spring blooms in an estuarine embayment. Estuarine Coastal and Shelf Science 65:351-360

Cabecadas G., Nogueira M., Brogueira M. J. (1999) Nutrient dynamics and productivity in three European estuaries. Marine Pollution Bulletin 38:1092-1096

Cadee G. C., Hegeman J. (1974b) Primary production of the benthic microflora living on tidal flats in the Dutch Wadden Sea. Netherlands Journal of Sea Research 8:260-291

Calbet A., Landry M. (2004) Phytoplankton growth, microzooplankton grazing, and carbon cycling in marine systems. Limnology and Oceanography 49:51-57

Carpenter J. (1965) The accuracy of the Winkler method for dissolved oxygen Limnology and Oceanography 10:135-140

Catalano M. J., Allen M. S., Murie D. J. (2006) Effects of variable flows on water chemistry gradients and fish communities at the Hillsborough River, Florida. North American Journal of Fisheries Management 26:108-118

Cermeno P., Maranon E., Pérez V., Serret P., Fernández E., Castro C. (2006) Phytoplankton size structure and primary production in a highly dynamic coastal ecosystem (Ría de Vigo, NW-Spain): Seasonal and short-time scale variability. Estuarine, Coastal and Shelf Science 67:251-266

Chan T. U., Hamilton D. P., Robson B. J., Hodges B. R., Dallimore C. (2002) Impacts of hydrological changes on phytoplankton succession in the Swan River, Western Australia. Estuaries 25:1406-1415

Chapelle A. (1995) A Preliminary Model of Nutrient Cycling in Sediments of a Mediterranean Lagoon. Ecological Modelling 80:131-147

Chicharo L., Chicharo M. A., Ben-Hamadou R. (2006a) Use of a hydrotechnical infrastructure (Alqueva Dam) to regulate planktonic assemblages in the Guadiana estuary: Basis for sustainable water and ecosystem services management. Estuarine Coastal and Shelf Science 70:3-18

Chicharo M., Chicharo L., Morais P. (2006b) Inter-annual differences of ichthyofauna structure of the Guadiana estuary and adjacent coastal area (SE Portugal/SW Spain): Before and after Alqueva dam construction. Estuarine Coastal and Shelf Science 70:39-51

Cloern J. (1991) Tidal Stirring and Phytoplankton Bloom Dynamics in an Estuary. Journal of Marine Research 49:203-221

Cloern J., Alpine A., Cole B., Wong R., Arthur J., Ball M. (1983) River Discharge Controls Phytoplankton Dynamics in the Northern San-Francisco Bay Estuary. Estuarine Coastal and Shelf Science 16:415-429

Cloern J. E., Cole B. E., Wong R. L. J., Alpine A. E. (1985) Temporal Dynamics of Estuarine Phytoplankton - a Case-Study of San-Francisco Bay. Hydrobiologia 129:153-176

Cloern J. E., Nichols F. H. (1985) Temporal Dynamics of an Estuary - San-Francisco Bay - Preface. Hydrobiologia 129:153-176

Cole B. E., Cloern J. E. (1987) An Empirical-Model for Estimating Phytoplankton Productivity in Estuaries. Marine Ecology-Progress Series 36:299-305

Costanza R., dArge R., deGroot R., Farber S., Grasso M., Hannon B., Limburg K., Naeem S., ONeill R. V., Paruelo J., Raskin R. G., Sutton P., vandenBelt M. (1997) The value of the world's ecosystem services and natural capital. Nature 387:253-260

Cote B., Platt T. (1983) Day-to-Day Variations in the Spring-Summer Photosynthetic Parameters of Coastal Marine-Phytoplankton. Limnology and Oceanography 28:320-344

Cote B., Platt T. (1984) Utility of the Light-Saturation Curve as an Operational Model for Quantifying the Effects of Environmental-Conditions on Phytoplankton Photosynthesis. Marine Ecology Progress Series 18:57-66

delGiorgio P., Cole J., Cimbleris A. (1997) Respiration rates in bacteria exceed phytoplankton production in unproductive aquatic systems. Nature 385:148-151

Duarte P. (2008) Implementação de um modelo hidrodinâmico tridimensional com o EcoDynamo. Relatório Técnico. Universidade Fernando Pessoa

Duarte P. (2005) Photosynthesis-Irradiance Relationships in Marine Microalgae. In: Rao DVS (ed) Algal Cultures Analogues of Blooms and Applications, Vol 2. Science Publishers Enfield (NH), Plymouth,UK, p 639-670

Duarte P., Azevedo B., Ribeiro C., Pereira A., Falcão M., Serpa D., Bandeira R., Reia J. (2007) Management oriented mathematical modelling of Ria Formosa (South Portugal). Transitional Waters Monographs 1:13-51

Duarte P., Ferreira J. G. (1997) A model for the simulation of macroalgal population dynamics and productivity. Ecological Modelling 98:199-214

Duarte P., Macedo M., Fonseca L. (2006) The relationship between phytoplankton diversity and community function in a coastal lagoon. Hydrobiologia 555:3-18

Dyer K. (1997) Estuaries. John Wiley & Sons, Chichester. 195 pp

Dyke P. (2001) Coastal and shelf sea modelling. Kluwer. 257 pp

EC (2000) Directive 2000/60/EC of the European Parliament and of the Council of 23 October 2000 establishing a framework for Community action in the field of water policy. Official Journal of the European Communities L327, p 1-73 (22.12.2000)

EEC (1975) Council Directive of 16 June 1975 concerning the quality required of surface water intended for the abstraction of drinking water in the Member States (75/440/EEC). Official Journal of the European Community, p 26-31 (25-07-1975)

EEC (1976) Council Directive of 8 December 1975 concerning the quality of bathing water (76/160/EEC) Official Journal of the European Community. Official Journal of the European Community, p 1-7 (05-02-1976)

Eilers P. H. C., Peeters J. C. H. (1988) A Model for the Relationship between Light-Intensity and the Rate of Photosynthesis in Phytoplankton. Ecological Modelling 42:199-215

Elliott M., McLusky D. S. (2002) The need for definitions in understanding estuaries. Estuarine Coastal and Shelf Science 55:815-827

Eppley R., Renger E., Venrick E., Mullin M. (1973) A study of phytoplankton dynamics and nutrient cycling in the Central Pacific Gyre of the North Pacific Ocean. Limnology and Oceanography 18:534-551

Falconer R. A., Lin B. (1997) Three-dimensional modelling of water quality in the Humber Estuary. Water Research 31:1092-1102

Falkowski P. G. (1981) Light-shade adaptation and assimilation numbers. Journal of Plankton Research 3:203-216

Falkowski P. G., Raven J. A. (1997) Aquatic photosynthesis. Blackwell, London. 373 pp

Falkowski P. G., Wirick C. D. (1981) A Simulation-Model of the Effects of Vertical Mixing on Primary Productivity. Marine Biology 65:69-75

Ferreira M., Antunes P., Gil O., Vale C., Reis-Henriques M. A. (2004) Organochlorine contaminants in flounder (Platichthys flesus) and mullet (Mugil cephalus) from Douro estuary, and their use as sentinel species for environmental monitoring. Aquatic Toxicology 69:347-357

Fisher T., Peele E., Ammermen J., Harding L. (1992) Nutrient limitation of phytoplankton in Chesapeake Bay. Marine Ecology Progress Series 82:51-63

Gallegos C., Jordan T. (1997) Seasonal progression of factors limiting phytoplankton pigment biomass in the Rhode River estuary, Maryland (USA). I. Controls on phytoplankton growth. Marine Ecology Progress Series 161:185-198

Gallegos C. L., Platt T., Harrison W. G., Irwin B. (1983) Photosynthetic Parameters of Arctic Marine-Phytoplankton - Vertical Variations and Time Scales of Adaptation. Limnology and Oceanography 28:698-708

Gameiro C., Cartaxana P., Cabrita M. T., Brotas V. (2004) Variability in chlorophyll and phytoplankton composition in an estuarine system. Hydrobiologia 525:113-124

Gazeau F., Smith S., Gentili B., Frankignoulle M., Gattuso J. (2004) The European coastal zone: characterization and first assessment of ecosystem metabolism. Estuarine, Coastal and Shelf Science 60:673-694

Geider R. J., MacIntyre H. L., Kana T. M. (1996) A dynamic model of photoadaptation in phytoplankton. Limnology and Oceanography 41:1-15

Goosen N. K., Kromkamp J., Peene J., van Rijswik P., van Breugel P. (1999) Bacterial and phytoplankton production in the maximum turbidity zone of three European estuaries: the Elbe, Westerschelde and Gironde. Journal of Marine Systems 22:151-171

Grasshoff K., Ehrhardt M., Kremling K. (1983) Methods of sea-water analysis. Verlag Chemie, Weinheim. 419 pp

Harding L. W., Mallonee M. E., Perry E. S. (2002) Toward a predictive understanding of primary productivity in a temperate, partially stratified estuary. Estuarine Coastal and Shelf Science 55:437-463

Harding L. W., Prezelin B. B., Sweeney B. M., Cox J. L. (1982) Primary Production as Influenced by Diel Peridiocity of Phytoplankton Photosynthesis. Marine Biology 67:179-186

Heip C., Goosen N., Herman P., Kromkamp J., Middelburg J., Soetaert K. (1995) Production and consumption of biological particles in temperate tidal estuaries. Oceanography and Marine Biology - An Annual Review 33:1-149

Hopkinson C., Vallino J. (1995) The relationships among mans activities in watersheds and estuaries - a model of runoff effects on patterns of estuarine community metabolism. Estuaries 18:598-621

Huang W. R., Spaulding M. (2002) Modelling residence-time response to freshwater input in Apalachicola Bay, Florida, USA. Hydrological Processes 16:3051-3064

Huisman J., Sommeijer B. (2002) Maximal sustainable sinking velocity of phytoplankton. Marine Ecology Progress Series 244:39-48

Humborg C. (1997) Primary Productivity Regime and Nutrient Removal in the Danube estuary. Estuarine, Coastal and Shelf Science 45:579-589

Huret M., Dadou I., Dumas F., Lazure P., Garcon V. (2005) Coupling physical and biogeochemical processes in the Rio de la Plata plume. Continental Shelf Research 25:629-653

Ibanez C., Pont D., Prat N. (1997) Characterization of the Ebre and Rhone estuaries: A basis for defining and classifying salt-wedge estuaries. Limnology and Oceanography 42:89-101

ICES (1996) CM /L:3. Biological Oceanography Commitee. Report of the Working Group on Phytoplankton Ecology. Report No. Ref:C+E+Env

James I. D. (2002) Modelling pollution dispersion, the ecosystem and water quality in coastal waters: a review. Environmental Modelling & Software 17:363-385

Jassby A. D., Kimmerer W. J., Monismith S. G., Armor C., Cloern J. E., Powell T. M., Schubel J. R., Vendlinski T. J. (1995) Isohaline Position as a Habitat Indicator for Estuarine Populations. Ecological Applications 5:272-289

Jassby A. D., Platt T. (1976) Mathematical Formulation of Relationship between Photosynthesis and Light for Phytoplankton. Limnology and Oceanography 21:540-547

Ji Z. G., Hu G. D., Shen J. A., Wan Y. S. (2007) Three-dimensional modeling of hydrodynamic processes in the St. Lucie Estuary. Estuarine Coastal and Shelf Science 73:188-200

Joint I. R. (1978) Microbial production of an estuarine mudflat. Estuarine, Coastal and Marine Science 7:185-195

Joint I. R., Pomeroy A. J. (1981) Primary production in a turbid estuary. Estuarine, Coastal and Shelf Science 13:303-316

Jones M. (1984) Nitrate reduction by shaking with cadmium: alternative to cadmium columns. Water Research 18:643-646

Jordan T. E., Correll D. L., Miklas J., Weller D. E. (1991) Long-Term Trends in Estuarine Nutrients and Chlorophyll, and Short-Term Effects of Variation in Watershed Discharge. Marine Ecology Progress Series 75:121-132

Jørgensen S., Bendoricchio G. (2001) Fundamentals of ecological modelling. Elsevier, Amsterdam. 530 pp

Jouenne F., Lefebvre S., Veron B., Lagadeuc Y. (2005) Biological and physicochemical factors controlling short-term variability in phytoplankton primary production and photosynthetic parameters in a macrotidal ecosystem (eastern English Channel). Estuarine Coastal and Shelf Science 65:421-439

Kashefipour S. M., Lin B., Harris E., Falconer R. A. (2002) Hydro-environmental modelling for bathing water compliance of an estuarine basin. Water Research 36:1854-1868

Kimmerer W. (2002a) Effects of freshwater flow on abundance of estuarine organisms: physical effects or trophic linkages? Marine Ecology Progress Series 243:39-55

Kimmerer W. (2002b) Physical, biological, and management responses to variable freshwater flow into the San Francisco estuary. Estuaries 25:1275-1290

Knauss J. A. (1997) Introduction to Physical Oceanography. Prentice Hall, Englewood Cliffs, NJ. 309 pp

Kocum E., Underwood G., Nedwell D. (2002) Simultaneous measurement of phytoplankton primary production, nutrient and light availability along a turbid, eutrophic UK east coast estuary (the Colne Estuary). Marine Ecology Progress Series 231:1-12

Kromkamp J., Peene J., Van Rijswijk P., Sandee A., Goosen N. (1995) Nutrients, light and primary production by phytoplankton and microphytobenthos in the eutrophic, turbid Westerschelde Estuary (The Netherlands). Hydrobiologia 311:9-19

Kurup G. R., Hamilton P., Patterson J. C. (1998) Modelling the effect of seasonal flow variations on the position of salt wedge in a microtidal estuary. Estuarine Coastal and Shelf Science 47:191-208

Lacroix G., Ruddick K., Park Y., Gypens N., Lancelot C. (2007) Validation of the 3D biogeochemical model MIRO&CO with field nutrient and phytoplankton data and MERIS-derived surface chlorophyll a images. Journal of Marine Systems 64:66-88

Landry M., Peterson W., Lorenzen C. (1995) Zooplankton Grazing, Phytoplankton Growth, and Export Flux - Inferences From Chlorophyll Tracer Methods. ICES Journal of Marine Science 52:337-345

Larson M., Bellanca R., Jonsson L., Chen C. Q., Shi P. (2005) A model of the 3D circulation, salinity distribution, and transport pattern in the pearl river estuary, China. Journal of Coastal Research 21:896-908

Lauria M., Purdie D., Sharples J. (1999) Contrasting phytoplankton distributions controlled by tidal turbulence in an estuary. Journal of Marine Systems 21:189-197

Legates D. R., McCabe G. J. (1999) Evaluating the use of "goodness-of-fit" measures in hydrologic and hydroclimatic model validation. Water Resources Research 35:233-241

Levasseur A., Shi L., Wells N. C., Purdie D. A., Kelly-Gerreyn B. A. (2007) A three-dimensional hydrodynamic model of estuarine circulation with an application to Southampton Water, UK. Estuarine Coastal and Shelf Science 73:753-767

Li W. K. W., Harrison W. G. (1982) Carbon Flow into the End-Products of Photosynthesis in Short and Long Incubations of a Natural Phytoplankton Population. Marine Biology 72:175-182

Liu W. C., Chen W. B., Cheng R. T., Hsu M. H., Kuo A. Y. (2007) Modeling the influence of river discharge on salt intrusion and residual circulation in Danshuei River estuary, Taiwan. Continental Shelf Research 27:900-921

Lizon F., Lagadeuc Y., Brunet C., Aelbrecht D., Bentley D. (1995) Primary Production and Photoadaptation of Phytoplankton in Relation with Tidal Mixing in Coastal Waters. Journal of Plankton Research 17:1039-1055

Lohrenz S. E., Fahnenstiel G. L., Redalje D. G. (1994) Spatial and Temporal Variations of Photosynthetic Parameters in Relation to Environmental Conditions in Coastal Waters of the Noethern Gulf of Mexico. Estuaries 17:779-795

MacCaull W. A., Platt T. (1977) Diel Variations in Photosynthetic Parameters of Coastal Marine-Phytoplankton. Limnology and Oceanography 22:723-731

Macedo M. F., Duarte P., Mendes P., Ferreira J. G. (2001) Annual variation of environmental variables, phytoplankton species composition and photosynthetic parameters in a coastal lagoon. Journal of Plankton Research 23:719-732

MacIntyre H. L., Cullen J. J. (1996) Primary production by suspended and benthic microalgae in a turbid estuary: Time-scales of variability in San Antonio Bay, Texas. Marine Ecology Progress Series 145:245-268

Madariaga I. (1995) Photosynthetic characteristics of phytoplankton during the development of a summer bloom in the Urdaibai Estuary, Bay of Biscay Estuarine, Coastal and Shelf Science 40:559-575

Madariaga I. (2002) Short-term variations in the physiological state of phytoplankton in a shallow temperate estuary. Hydrobiologia 475:345-358

Magalhaes C. M., Bordalo A. A., Wiebe W. J. (2003) Intertidal biofilms on rocky substratum can play a major role in estuarine carbon and nutrient dynamics. Marine Ecology Progress Series 258:275-281

Magalhaes C. M., Joye S. B., Moreira R. M., Wiebe W. J., Bordalo A. A. (2005) Effect of salinity and inorganic nitrogen concentrations on nitrification and denitrification rates in intertidal sediments and rocky biofilms of the Douro River estuary, Portugal. Water Research 39:1783-1794

Malej A., Mozetic P., Malacic V., Terzic S., Ahel M. (1995) Phytoplankton responses to freshwater inputs in a small semienclosed gulf (Gulf of Trieste, Adriatic Sea). Marine Ecology Progress Series 120:111-121

Mallin M., Cahoon L., McIver M., Parsons D., Shank G. (1999) Alternation of factors limiting phytoplankton production in the Cape Fear River Estuary. Estuaries 22:825-836

Mallin M., Paerl H., Rudek J., Bates P. (1993) Regulation of estuarine primary production by watershed rainfull and river flow. Marine Ecology Progress Series 93:199-203

Malone T., Conley D., Glibert P., Harding J. L., Sellner K. (1996) Scales of nutrient limited phytoplankton productivity: the Chesapeake Bay example. Estuaries 19:371-385

Malone T., Crocker L., Pike S., Wendler B. (1988) Influences of river flow on the dynamics of phytoplankton production in a partially stratified estuary. Marine Ecology Progress Series 48:235-249

Marra J., Heinemann K., Landriau G. (1985) Observed and Predicted Measurements of Photosynthesis in a Phytoplankton Culture Exposed to Natural Irradiance. Marine Ecology Progress Series 24:43-50

McLusky D., Elliot M. (2004) The estuarine ecosystem: ecology, threats and management. Oxford University Press, New York. 214 pp

Mingelbier M., Klein B., Claereboudt M. R., Legendre L. (1994) Measurement of Daily Primary Production Using 24-H Incubations with the C-14 Method - a Caveat. Marine Ecology-Progress Series 113:301-309

Moisander P. H., McClinton E., Paerl H. W. (2002) Salinity effects on growth, photosynthetic parameters, and nitrogenase activity in estuarine planktonic cyanobacteria. Microbial Ecology 43:432-442

Mortazavi B., Iverson R., Landing W., Lewis G., Huang W. (2000) Control of phytoplankton production and biomass in a river-dominated estuary: Apalachicola Bay, Florida, USA. Marine Ecology Progress Series 198:19-31

Mucha A. P., Vasconcelos M. T. S. D., Bordalo A. A. (2003) Macrobenthic community in the Douro estuary: relations with trace metals and natural sediment characteristics. Environmental Pollution 121:169-180

Mucha A. P., Vasconcelos M. T. S. D., Bordalo A. A. (2004) Vertical distribution of the macrobenthic community and its relationships to trace metals and natural sediment characteristics in the lower Douro estuary, Portugal. Estuarine Coastal and Shelf Science 59:663-673

Mucha A. P., Vasconcelos M. T. S. D., Bordalo A. A. (2005) Spatial and seasonal variations of the macrobenthic community and metal contamination in the Douro estuary (Portugal). Marine Environmental Research 60:531-550

Nash J. E., Sutcliffe J. V. (1970) River flow forecasting through conceptual models part I -- A discussion of principles. Journal of Hydrology 10:282-290

Nichols F. H., Cloern J. E., Luoma S. N., Peterson D. H. (1986) The Modification of an Estuary. Science 231:567-573

Nihoul J. C. J. (1982) Hydrodynamics of semi-enclosed seas In: Nihoul J (ed) Oceanography of semi-enclosed seas. Elsevier, Amsterdam, p 1- 12

Painting S. J., Devlin M. J., Malcolm S. J., Parker E. R., Mills D. K., Mills C., Tett P., Wither A., Burt J., Jones R., Winpenny K. (2007) Assessing the impact of nutrient enrichment in estuaries: Susceptibility to eutrophication. Marine Pollution Bulletin 55:74-90

Parsons T., Maita Y., Lalli C. (1984) A manual of chemical and biological methods for seawater analysis. Pergamon press, Elmsford, NY. 173 pp

Passone S., Das D. B., Nassehil V., Bikangaga J. H. (2003) Design of discharge policies for multiple effluent sources and returning pollutants scenarios in a branching estuary. Estuarine Coastal and Shelf Science 56:227-237

Pastuszak M., Nagel K., Grelowski A., Mohrholz V., Zalewski M. (2003) Nutrient dynamics in the Pomeranian Bay (Southern Baltic): Impact of the Oder River outflow. Estuaries 26:1238-1254

Pennock J. R., Sharp J. H. (1994) Temporal Alternation between Light-Limitation and Nutrient-Limitation of Phytoplankton Production in a Coastal-Plain Estuary. Marine Ecology-Progress Series 111:275-288

Pereira A., Duarte P. (2005) EcoDynamo Ecological Dynamics Model Application University Fernando Pessoa. Available at http://www.dittyproject.org/Reports.asp

Pereira J., Schettini C. A. F., Rorig L., Siegle E. (2001) Intratidal variation and net transport of dissolved inorganic nutrients, POC and chlorophyll a in the Camboriu River Estuary, Brazil. Estuarine Coastal and Shelf Science 53:249-257

Pitcher G. C., Walker D. R., Mitchellinnes B. A. (1989) Phytoplankton Sinking Rate Dynamics in the Southern Benguela Upwelling System. Marine Ecology Progress Series 55:261-269

Platt T., Gallegos C. L., Harrison W. G. (1980) Photoinhibition of photosynthesis in natural assemblages of marine phytoplankton. Journal of Marine Research 38:687-701

Portela L., Neves R. (1994) Modelling temperature distribution in the shallow Tejo estuary. In: Tsakiris G, Santos MA (eds) Advances in Water Resources Technology and Management. Balkema, Rotterdam, p 457-463

Prezelin B. B. (1992) Diel Periodicity in Phytoplankton Productivity. Hydrobiologia 238:1-35

Proctor L. M., Fuhrman J. A. (1991) Roles of Viral-Infection in Organic Particle-Flux. Marine Ecology Progress Series 69:133-142

Ram A. S. P., Nair S., Chandramohan D. (2003) Seasonal shift in net ecosystem production in a tropical estuary. Limnology and Oceanography 48:1601-1607

Ramus J., Eby L., McClellan C., Crowder L. (2003) Phytoplankton forcing by a record freshwater discharge event into a large lagoonal estuary. Estuaries 26:1344-1352

Reis P. (2002) Situação actual dos rios e ribeiros do concelho do Porto. Master thesis, Universidade do Minho, in Portuguese, 123 pp

Robson B. J., Hamilton D. P. (2004) Three-dimensional modelling of a Microcystis bloom event in the Swan River estuary, Western Australia. Ecological Modelling 174:203-222

Rocha C., Galvao H., Barbosa A. (2002) Role of transient silicon limitation in the development of cyanobacteria blooms in the Guadiana estuary, south-western Iberia. Marine Ecology Progress Series 228:35-45

Roegner G. (1998) Hydrodynamic control of the supply of suspended chlorophyll a to infaunal estuarine bivalves. Estuarine, Coastal and Shelf Science 47:369-384

Sakshaug E., Bricaud A., Dandonneau Y., Falkowski P. G., Kiefer D. A., Legendre L., Morel A., Parslow J., Takahashi M. (1997) Parameters of photosynthesis: definitions, theory and interpretation of results. Journal of Plankton Research 19:1637-1670

Santos A. (1995) Modelo hidrodinâmico tridimensional de circulação oceânica estuarina. PhD Thesis. Universidade Técnica de Lisboa. In Portuguese, 272 pp

Saraiva S., Pina P., Martins F., Santos M., Braunschweig F., Neves R. (2007) Modelling the influence of nutrient loads on Portuguese estuaries. Hydrobiologia 587:5-18

Schindler D. (1977) Evolution of phosphorus limitation in lakes. Science 195:260-262

Schroeder W., Dinnel S., Wiseman W. (1990) Salinity stratification in a river-dominated estuary. Estuaries 13:145-154

SCOR-UNESCO (1966) Determination of photosynthetic pigments in seawater. Report of the SCOR-UNESCO working group 17. Monographs on Oceanographic Methodology. UNESCO, Paris, p 11-18

SHOM (1984) Table des marées des grands ports du Monde., Service Hydrographique et Océanographique de la Marine

Silva A. (1996) Implementação de um Modelo Hidromorfológico para a Barra do Douro. Contribuição para a Compreensão do Sistema 3º Congresso da Água, Lisboa, in

Portuguese, available at http://maretec.mohid.com/MaretecManagement/ConferencePapers.asp

Sin Y. S., Wetzel R. L., Anderson I. C. (1999) Spatial and temporal characteristics of nutrient and phytoplankton dynamics in the York River Estuary, Virginia: Analyses of long-term data. Estuaries 22:260-275

Sinclair M. (1978) Summer phytoplankton variability in the lower St. Lawrence Estuary. Journal of Fishery Research Board Canada 35:1171-1185

Sklar F. H., Browder J. A. (1998) Coastal environmental impacts brought about by alterations to freshwater flow in the Gulf of Mexico. Environmental Management 22:547-562

Snow G., Adams J., Bate G. (2000) Effect of river flow on estuarine microalgal biomass and distribution. Estuarine Coastal and Shelf Science 51:255-266

StatSoft I. (2001) STATISTICA (data analysis software system)

Stearns D., Litaker W., Rosenberg G. (1987) Impacts of zooplankton grazing and excretion on short-interval fluctuations in chlorophyll-a and nitrogen concentrations in a well-mixed estuary. Estuarine, Coastal and Shelf Science 24:305-325

Steele J. H. (1962) Environmental control of photosynthesis in the sea. Limnology and Oceanography 7:137-150

Steeman Neilsen E. (1952) The use of radioactive carbon (^{14}C) for measuring organic production in the sea. Journal du Conseil International pour l'Exploration de la Mer 18:117-140

Steeman Nielsen E. (1952) The use of radioactive carbon (^{14}C) for measuring organic production in the sea. Journal du Conseil International pour l'Exploration de la Mer 18:117-140

Struski C., Bacher C. (2006) Preliminary estimate of primary production by phytoplankton in Marennes-Oleron Bay, France. Estuarine Coastal and Shelf Science 66:323-334

Testa J. M., Kemp W. M. (2008) Variability of biogeochemical processes and physical transport in a partially stratified estuary: a box-modeling analysis. Marine Ecology-Progress Series 356:63-79

Thomas W., Simmons E. (1960) Phytoplankton production in the Mississippi Delta. In: Shepard F (ed) Recent sediment, NorthWestern Gulf of Mexico. American Association of Petroleum Geologists, Tulsa, p 103-116

Thompson P. (1998) Spatial and temporal patterns of factors influencing phytoplankton in a salt wedge estuary, the Swan River, Western Australia. Estuaries 21:801-817

Thouvenin B., Gonzalez J. L., Boutier B. (1997) Modelling of pollutant behaviour in estuaries: Application to cadmium in the Loire estuary. Marine Chemistry 58:147-161

Tillmann U., Hesse K. J., Colijn F. (2000) Planktonic primary production in the German Wadden Sea. Journal of Plankton Research 22:1253-1276

Trancoso A. R., Saraiva S., Fernandes L., Pina P., Leitao P., Neves R. (2005) Modelling macroalgae using a 3D hydrodynamic-ecological model in a shallow, temperate estuary. Ecological Modelling 187:232-246

Trigo R. M., Pozo-Vazquez D., Osborn T. J., Castro-Diez Y., Gamiz-Fortis S., Esteban-Parra M. J. (2004) North Atlantic oscillation influence on precipitation, river flow and water resources in the Iberian peninsula. International Journal of Climatology 24:925-944

Ulses C., Grenz C., Marsaleix P., Schaaff E., Estournel C., Meule S., Pinazo C. (2005) Circulation in a semi-enclosed bay under influence of strong freshwater input. Journal of Marine Systems 56:113-132

Uncles R. J., Bloomer N. J., Frickers P. E., Griffiths M. L., Harris C., Howland R. J. M., Morris A. W., Plummer D. H., Tappin A. D. (2000) Seasonal variability of salinity, temperature, turbidity and suspended chlorophyll in the Tweed Estuary. Science of the Total Environment 251:115-124

Uncles R. J., Lewis R. E. (2001) The transport of fresh water from river to coastal zone through a temperate estuary. Journal of Sea Research 46:161-175

Uncles R. J., Smith R. E. (2005) A note on the comparative turbidity of some estuaries of the Americas. Journal of Coastal Research 21:845-852

Uthicke S., Klumpp D. (1998) Microphytobenthos community production at a near-shore coral reef: seasonal variation and response to ammonium recycled by holothurians. Marine Ecology Progress Series 169:1-11

Valiela I., McClelland J., Hauxwell J., Behr P. J., Hersh D., Foreman K. (1997) Macroalgal blooms in shallow estuaries: Controls and ecophysiological and ecosystem consequences. Limnology and Oceanography 42:1105-1118

Van Es F. B. (1977) A preliminary carbon budget for a part of the Ems estuary: the Dollard. Helgolander Wiss Meeresunters 30:283-294

van Spaendonk J. C. M., Kromkamp J. C., de Visscher P. R. M. (1993) Primary production of phytoplankton in a turbid coastal plain estuary, The Westerschelde (The Netherlands). Netherlands Journal of Sea Research 31:267-279

Vieira M., Bordalo A. A. (2000) The Douro estuary (Portugal): a mesotidal salt wedge. Oceanologica Acta 23:585-594

Vreugdenhil C. B. (1989) Computational Hydraulics: an Introduction. Springer-Verlag, New York. 183 pp

Wang C. F., Hsu M. H., Kuo A. Y. (2004) Residence time of the Danshuei River estuary, Taiwan. Estuarine Coastal and Shelf Science 60:381-393

Webb W. L., Newton M., Starr D. (1974) Carbon dioxide exchange of Alnus rubra: A mathematical model. Oecologia 17:281-291

Wetsteyn L., Kromkamp J. C. (1994) Turbidity, nutrients and phytoplankton primary production in the Oosterschelde (The Netherlands) before, during and after a large-scale coastal engineering project (1980-1990). Hydrobiologia 282/283:61-78

Willmott C. J., Ackleson S. G., Davis R. E., Feddema J. J., Klink K. M., Legates D. R., Odonnell J., Rowe C. M. (1985) Statistics for the Evaluation and Comparison of Models. Journal of Geophysical Research-Oceans 90:8995-9005

Xu J. T., Hood R. R. (2006) Modeling biogeochernical cycles in Chesapeake Bay with a coupled physical-biological model. Estuarine Coastal and Shelf Science 69:19-46

Yamamoto T., Hatta G. (2004) Pulsed nutrient supply as a factor inducing phytoplankton diversity. Ecological Modelling 171:247-270

Yin K., Qian P., Wu M., Chen J., Huang L., Song X., Jian W. (2001) Shift from P to N limitation of phytoplankton growth across the Pearl River estuarine plume during summer. Marine Ecology Progress Series 221:17-28

Yuan D., Lin B., Falconer R. A. (2007) A modelling study of residence time in a macro-tidal estuary. Estuarine Coastal and Shelf Science 71:401-411

Zakardjian B., Gratton Y., Vezina A. (2000) Late spring phytoplankton bloom in the Lower St. Lawrence Estuary: the flushing hypothesis revisited. Marine Ecology Progress Series 192:31-48